University of Mississippi

eGrove

2012

Distributed Space-Time Message Relaying for Uncoded/Coded Wireless Cooperative Communications

Peng Huo

Recommended Citation

Distributed Space-Time Message Relaying for Uncoded/Coded Wireless Cooperative Communications

Peng Huo

A dissertation submitted in partial fulfillment
of the requirements for the degree of
Ph.D. of Science in Engineering Science
Electrical Engineering

University of Mississippi

2012

Abstract

During wireless communications, nodes can overhear other transmissions through the wireless medium, suggested by the broadcast nature of plane wave propagation, and may help to provide extra observations of the source signals to the destination. Modern research in wireless communications pays more attention to these extra observations which were formerly neglected within networks. Cooperative communication processes this abundant information existing at the surrounding nodes and retransmits towards the destination in various forms to create spatial and/or coding diversity, thereby to obtain higher throughput and reliability.

The aim of this work is to design cooperative communication systems with distributed space-time block codes (DSTBC) in different relaying protocols and theoretically derive the BER performance for each scenario.

The amplify-and-forward (AF) protocol is one of the most commonly used protocols at the relays. It has a low implementation complexity but with a drawback of amplifying the noise as well. We establish the derivation of the exact one-integral expression of the average BER performance of this system, followed by a novel approximation method based on the series expansion.

An emerging technology, soft decode-and-forward (SDF), has been presented to combine the desired features of AF and DF: soft signal representation in AF and channel coding gain in DF. In the SDF protocol, after decoding, relays transmit the soft-information, which represents the reliability of symbols passed by the decoder, to the destination. Instead of keeping the source node idling when the relays transmit as in the traditional SDF system, we let the source transmit hard information and cooperate with the relays using DSTBC.

By theoretically deriving the detection performance at the destination by either using or not using the DSTBC, we make comparisons among three SDF systems. Interesting results have been shown, together with Monte-Carlo simulations, to illustrate that our proposed one-relay and two-relay SDF & DSTBC systems outperform traditional soft relaying for most of the cases. Finally, these analytic results also provide a way to implement the optimal power allocation between the source and the relay or between relays, which is illustrated in the line model.

Dedication

This work is dedicated to my wife and my parents.

Without their support, I would never be where I am.

Acknowledgments

Table of Contents

List of Figures

List of Tables

Chapter 1
INTRODUCTION

1.1 Cooperative Communications

Traditionally, wireless communications considers the transmission of information between two points that are physically not connected. Current wireless networks goes beyond this point-to-point or point-to-multipoint paradigms of classical networks. One can think of a current wireless system as a virtual antenna array[42,109,21,18], where each antenna in the array corresponds to one node of the entire network. During communication, nodes can overhear other transmissions through the wireless medium and may help to provide extra observations of the source signals to the destination. These observations are usually not considered in current implementations of cellular, wireless LAN or ad hoc systems.

Motivated by the information existence of abundant in wireless networks, modern research in wireless communications pays more attention to this extra observations which were formerly neglected within networks. This information can be utilized by cooperation among nodes in order to improve the performance of communication. Cooperative communications[91,64,40,102,11,68,107,72,33,63] based on relaying nodes have emerged as a promising approach to increase spectral and power efficiency, network coverage, and to reduce outage probability.

Diversity techniques are known as the effective means to cope with fading in wireless channels. The fundamental philosophy behind diversity techniques is to produce independent replicas of the desired signal over fading channels so that the receiver can utilize the multiple faded copies to restore the original signal with higher reliability. For a long time, the concept of diversity has been substantiated in various forms, such as spatial (antenna) diversity[97], temporal diversity and frequency diversity[17].

Antenna diversity, also known as space diversity, is one of several wireless diversity schemes that uses two or more antennas to improve the quality and reliability of a wireless link. In point-to-point communication links, multiple antenna systems have been widely used to achieve spatial (antenna) diversity. When multiple antennas are employed at the receiver, selective combining (SC)[85,84,57,105,106], Equal Gain Combing (EGC)[2,29], or maximum ratio combining (MRC)[93,4,23,43] schemes are usually used to provide antenna diversity gain[65,26].

Unfortunately, nowadays, antenna diversity becomes less competitive since transmission nodes in modern wireless networks are required to be of small size and weight so that it is more likely to use single antenna in each node. In order to overcome this limitation, a new form of spatial diversity, whereby diversity gains are achieved via the cooperation of nodes, has been proposed[25,101,100]. The main idea behind this approach, which is called cooperative diversity[110,101,88], is to use orthogonal relay transmission to achieve diversity gain. In particular, each node has one or several partners. The node and its partner(s) are responsible for transmitting not only their own information, however, also the information of their partner(s). Therefore, a virtual antenna array is obtained through the use of the relays' antennas without complicated signal design or adding more antennas at the nodes[25].

Due to this advantage, cooperative diversity application finds its way into the cellular network and other modern telecommunications framework. The broadcast nature of wireless communications suggests that a source signal transmitted towards the destination can take advantage of neighboring nodes. Cooperative communication processes information at the surrounding nodes and retransmits towards the destination in various forms to create spatial and/or coding diversity, thereby to obtain higher throughput and reliability.

To facilitate study, a classical wireless cooperative communications network is simplified as basic units consists of a source (S), a relay (R), and a destination (D), as shown in Fig. 1.1. The essential form of cooperative cooperation in the physical layer is signal relaying, where the relay augments transmission by forwarding part or all of the signals originated from the source to the destination. The destination receives information both from the source and the
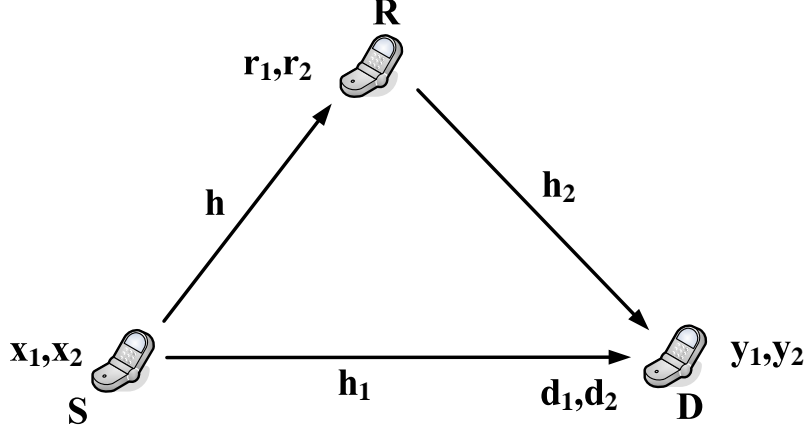
Figure 1.1. The system model of cooperative diversity system.

relay and then decodes the information from the combination of these two signals. Hence, it can be seen that cooperative diversity is an evolution of traditional antenna diversity that uses distributed antennas belonging to each node in a wireless network.

Simplified one-relay system has later been extended to a four-node-network which consists of one source 'S', one destination 'D' and two relays 'R_1' and 'R_2' as shown in Fig. 1.2. The relays demodulate and decode the received data stream and generate the reliability values of the source. These values are forwarded to the destination and combined with signal from the direct link to construct an entire distributed codeword. Turbo decoding is adopted afterwards at the destination to recover the source information.

1.2   Relaying Strategies

Despite the large amount of techniques proposed in wireless cooperative cooperation systems, practical signal relaying strategies have not evolved much out of the three basic forms, namely, Amplify-and-Forward (AF), Decode-and-Forward (DF) and Soft-Decode-and-Forward (SDF).

1.2.1   Amplify-and-Forward (AF)

Amplify-forward lets the relay scale, retransmit or reflect the analog signal waveforms received from the source[92,46,24]. The application of AF is straight-forward, requiring a lower implementation complexity in digital signal processing than its two counterparts.
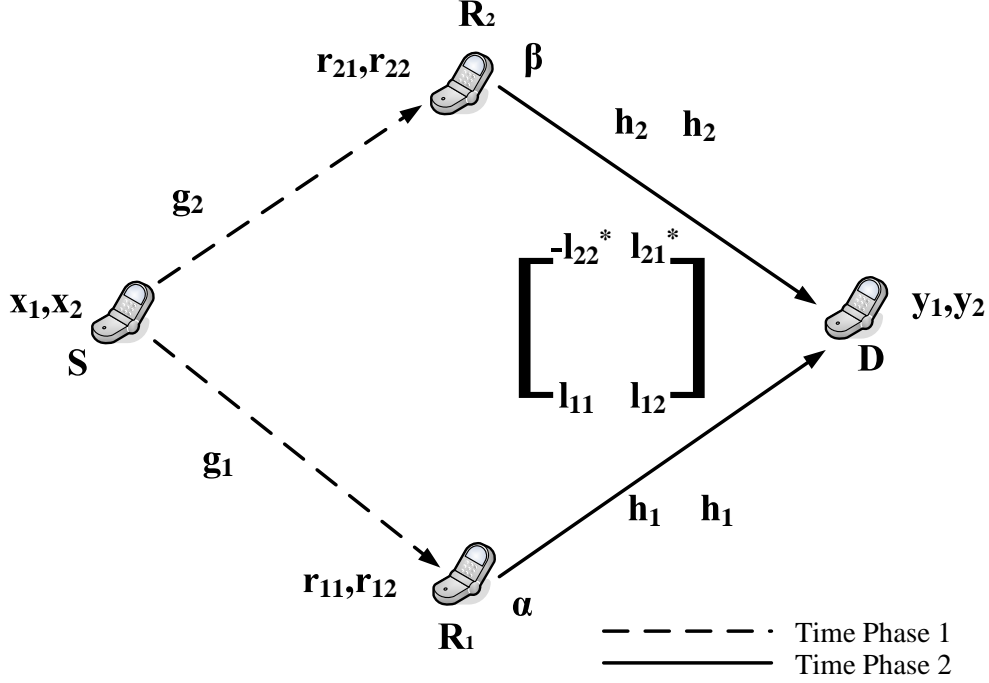
Figure 1.2. The system model of two-relay SDF & DSTBC system.

The prototype of the AF technique is an end-to-end communication system with the assistance of one or multiple relays. The performance of two-hop relayed transmission was first analyzed by Hasna et al. in[38][39], and further in[58], where the moment generating function (MGF) of the Harmonic Mean of two exponential random variables (RV) is used to evaluate the average BER of the end-to-end system over independent Rayleigh fading channels. These works have been extended in[92] where the link between the source and destination is also considered, and the destination combines received signals from both the relay link and the direct link using the Maximum Ratio Combining (MRC) technique. Multiple relays using Amplify-and-Forward (AF) protocol are also considered in the cooperative communications[46][24] and different processing strategies are proposed at the destination. Ikki et al.[46] used the generalized selection combining while Costa et al.[24] considered both equal-gain and maximum ratio combining.

1.2.2 Decode-and-Forward (DF)

Decode-forward performs better than AF in most cases for signal relaying, where the source signals received at the relay are demodulated, decoded and possibly re-encoded using a different code before being forwarded to the destination.

There are a considerable numbers of works[79,80,103,104,34,44,108] published on the general theme of the DF cooperative diversity focusing on the capacity, diversity gain, and outage performance analysis, mainly for the cooperation with single relay.

Examination of the bit error probability (BEP) of DF cooperative systems has been done by many researchers[51]. In[90,78,59], the symbol error probability (SEP) of DF cooperative systems was studied assuming that the relay does not send a signal when the decision at the relay is incorrect. In[71], the SEP for multihop transmission was analyzed assuming that there is no direct link between the source and the destination. In[89], the BEP for DF cooperative systems was analyzed assuming that the channel gain amplitude is real and Gaussian distributed.

Depending on whether and what code is used to re-generate the relay message, decode-forward extends from its basic mode of repetition[54], to more sophisticated modes that exploit space time codes[53,47] and network codes[10].

For multiple nodes joining into the cooperation, opportunistic relaying (OR) technique has been introduced into DF relaying strategy. It has been proposed that only the best relay from a set of available candidate relays is selected to cooperate[12,99,52,13]. The selection strategy is to choose the relay with the best equivalent end-to-end channel gain which is calculated as the minimum of the channel gains of the first and the second hops under the DF protocol.

1.2.3 Soft-Decode-and-Forward (SDF)

As illustrated in the previous two subsections, AF and DF are the two basic strategies in cooperative communications. AF keeps itself from any premature decision and in fact

preserves the soft information content of the received signal. However this scheme fails to benefit from error correction possibility at relay and also amplifies and forwards the front end noise at relay receiver .

On the other hand, the disadvantage of DF is also obvious. When the SNR between the source and the relay is not high enough to ensure almost error-free transmission, the relay will obtain and send wrong information to the destination. This will cause error propagation and degrade the overall decoding performance at the destination.

To deal with this problem, a new relay technique, called Soft-Decode-and-Forward (SDF), is proposed in[86] and[61]. In SDF, instead of making hard decision, the relay first demodulates the received signal from the source, soft-decodes and re-encodes to get the soft-information of the source with a different code. This soft-information is usually *a-posterior* probability from the output of the second encoder and represents the soft reliability for the parity bits of the new code.

1.3   Space-Time Block Code (STBC)

Space-Time Block Code (STBC)[94] uses multiple antennas at both ends of wireless links in order to increase the communication rate and to exploit the diversity[67,20]. It is a combination of modulation and coding across the space and the time dimensions and has been introduced by Alamouti[6] and Tarokh[94,95] et al. A well known example of STBC is the so-called Alamouti code[6] which takes advantage of two transmit antennas over two symbol periods. The Alamouti code, remarkable for having an elegant and simple linear receiver, has become a standard code in STBC. Alamouti's idea for two transmit antennas was based on the orthogonal designs[96,95], which have full diversity and simple linear maximum-likelihood (ML) detectors that decouple the transmitted symbols.

The system model for classical Alamouti's code is shown in Fig. 1.3. Information bits x_1 and x_2 are transmitted cooperatively by two antennas from a source node. Suppose these two antennas have no interferences and the wireless paths between each of them and the
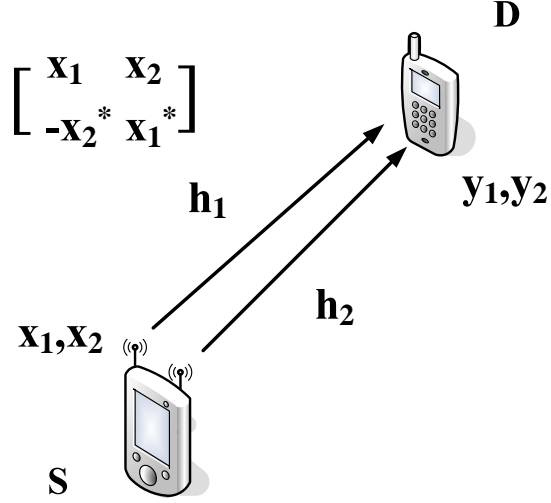
Figure 1.3. System Model for classical Alamouti's code.

destination has Rayleigh fading. Denote h_1 and h_2 as the fading coefficients for these two paths and assume the fading of each path is constant across two consecutive symbols. Two carriers used by two source nodes are with the same frequency. In the first time slot, one antenna transmits x_1 and the other transmits $-x_2^*$. In the second time slot, they forward x_2 and x_1^*, respectively. Suppose that communications synchronization is achieved between the two received signals at the receiver. The destination shown in Fig. 1.3 receives two combined signals as follows:

$$y_1 = \sqrt{E_s} h_1 x_1 - \sqrt{E_s} h_2 x_2^* + v_1 \tag{1}$$

$$y_2 = \sqrt{E_s} h_1 x_2 + \sqrt{E_s} h_2 x_1^* + v_2 \tag{2}$$

where v_1, v_2 are the Gaussian noise at the destination node with $v_i \sim \mathcal{CN}(0, \sigma_v^2)$ for $i = 1, 2$.

By writing it in the matrix form, the received signals are:

$$Y = \sqrt{E_s} HX + V \tag{3}$$

where $Y = [y_1, y_2^*]^T$, $X = [x_1, x_2^*]^T$, $V = [v_1, v_2^*]^T$,

$$H = \begin{bmatrix} h_1 & -h_2 \\ h_2^* & h_1^* \end{bmatrix} .$$

The maximum-likelihood (ML) decoding can be implemented by multiplying the received data with H^+, i.e., decoding with its matched filter. For a general matrix of size $m \times n$, the pseudo-inverse for the matrix H is defined as:

$$H^+ = (H^H H)^{-1} H^H, \tag{4}$$

where H^H represent the Hermitian transpose of the matrix H, which is equal to the conjugate transpose of the matrix. The term

$$H^H H = \begin{bmatrix} |h_1|^2 + |h_2|^2 & 0 \\ 0 & |h_1|^2 + |h_2|^2 \end{bmatrix}, \tag{5}$$

is a diagonal matrix. Therefore, the inverse is just the inverse of the diagonal elements, i.e.:

$$(H^H H)^{-1} = \begin{bmatrix} \frac{1}{|h_1|^2 + |h_2|^2} & 0 \\ 0 & \frac{1}{|h_1|^2 + |h_2|^2} \end{bmatrix} . \tag{6}$$

Therefore, the estimates of the transmitted symbols $[\hat{x}_1, \hat{x}_2^*]^T$ at the destination can be obtained as follows:

$$\begin{bmatrix} \hat{x}_1 \\ \hat{x}_2^* \end{bmatrix} = (H^H H)^{-1} H^H \begin{bmatrix} y_1 \\ y_2^* \end{bmatrix}$$

$$= \sqrt{E_s} \begin{bmatrix} x_1 \\ x_2^* \end{bmatrix} + (H^H H)^{-1} H^H \begin{bmatrix} v_1 \\ v_2^* \end{bmatrix} \tag{7}$$

The result above shows that Space-Time coding combines all the copies of the received signal in an optimal way to extract as much information as possible from each of them. The redundancy from this scheme provides diversity in both space and time domain.

1.4 Distributed Space-Time Block Codes (DSTBC)

Antenna diversity, introduced from STBC, offers significant improvement in link reliability and spectral efficiency through the use of multiple antennas at the transmitter or receiver side[5,69]. The idea of combining the space diversity from STBC with cooperative diversity from cooperative communications has gained broad interest. This new application of Space-time block coding (STBC) in a distributed fashion is termed as Distributed Space-Time Block Code (DSTBC)[53,54,27,82,73,44,70]. There has been a considerable research effort on this new technique over the past few years, especially for single antenna systems, such as wireless sensor networks and ad hoc wireless networks. The classical DSTBC system model is shown in Fig. 1.4 which includes two-time-phase transmissions. In the first time phase, the source radiates to both the relay(s) and the destination, while in the second time phase, the relay and the source cooperatively forward information to the destination by using distributed STBC code.
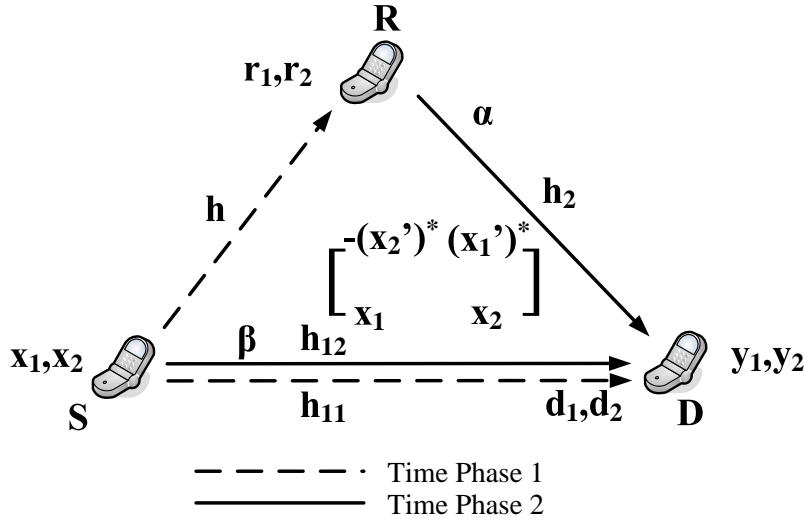
Figure 1.4. System Model for classical Distributed Space-Time Block Code (DSTBC).

Differences between DSTBC and STBC

The differences between DSTBC and classical STBC exist both in infrastructure and transmission symbols. The multiple transmission antennas are deployed on a single source

in classical STBC, while in DSTBC, antennas are put both on source and relay nodes and usually each node has only one antenna. In classical STBC, since all antennas are deployed on the source, each of them transmit error free symbols or its conjugate. For DSTBC, what the relays transmit in the second time phase are a hard/soft copy or conjugate of the source information, and, in most cases, they contain errors which are introduced from the source-to-relay link transmission.

Advantages of DSTBC

DSTBC has wide application in future cellular (as shown in Table 1.1[1]), ad hoc, wireless sensor networks (WSN) and surpasses traditional STBC for several reasons.

Table 1.1. Spacial coding and user cooperation in cellular mobile networks

Generation	3G	Future
Deployment	2003/4	2015~2020
Standard	WCDMA	Beyond IMT-Adv
Total rate	384kbit/s	>10Gbit/s
Bandwidth	5 MHz	>100 MHz
Spatial coding	Spatial diversity coding	Ambient intelligence coding
Examples	**Alamouti coding**	Such as **cooperative MIMO**

The traditional STBC gains are typically realized at the physical layer and require colocated antenna elements at the base station in cellular system. Multiple-antenna techniques are very attractive for deployment in cellular applications at base stations and have already been included in the third-generation wireless standards. Unfortunately, the use of multiple antennas might not be practical at the cellular mobile devices. The same situation is confronted in ad hoc mobile networks due to the size and power constraint in the wireless nodes. This is the dominant reason that DSTBC has been widely studied in one antenna systems and is expected to be widely adopted in the next generation networks.

Wireless environment has its own advantage of broadcasting information during communication between nodes. The signal transmitted by the source nodes is overheard by other nodes, which can be defined as partners. With this "redundant" observation, the source and

its partners can jointly process and transmit their information, creating a virtual antenna array although each of them is equipped with only one antenna.

In distributed relay applications (for example sensor networks) wireless devices often deploy low-speed CPUs and power-constrained batteries. With its simple linear calculation and fast encoding/decoding speed, DSTBC has its advantage in application in wireless sensor networks.

Challenges

Although DSTBC has several advantages beyond classical STBC, the challenge of DSTBC should also be considered. The challenge comes from the infrastructure differences of two protocols. In classical STBC, antennas at the source transmit error-free information symbols, while in DSTBC, the relays do not have the exact same information from the source. Thus, the system performance of DSTBC is usually very complex to analyze.

1.5 Objective of this dissertation

The objective of this dissertation is two-fold: the first is to discuss the DSTBC with AF relaying system, while, the second is to analyze DSTBC with SDF relaying system.

For AF based DSTBC system, we first provide an theoretic model to describe this cooperative system. Then we evaluate the exact average BER performance in a one-integral form and derive a novel approximation method in the form of series expansion. At the end of this paper, various operation scenarios with different channel quality and modulations are used to check the system performance and validate our analytic results.

Soft-Decode-and-Forward system is introduced thereafter. We evaluate the averaged BER after Space-time decoding in SDF system. After that, we discuss the power allocation and optimization of this system based on the line simulation model. The overall system performance after iterative decoding is provided with different channel qualities based on Monte-Carlo simulations.

1.5.1 AF based DSTBC System

Among the most widely used cooperative strategies is amplify-and-forward (AF). The application of DSTBC in AF uses a two-phase 'listen-and-transmit′ protocol. In the first time phase, the source radiates to both the relay and the destination, while, in the second time phase, the relay and the source cooperatively forward information to the destination by using distributed STBC code. The signal sent by the relay in the second phase is a linear function of its received signal and its conjugate.

Related work and Motivation

The AF based DSTBC has been studied for a long time and we enumerate several references both on multiple relays and single relay.

We classify AF as regenerative or non-regenerative by the operation at the relay. For regenerative AF relays, threshold detection is introduced at the relay on the scaled signal[98,81,8]. While, if relays only amplify voltage of the analog signal received from the source and forward it to the destination, they are called non-regenerative AF relays[45,3,7].

Alamouti's code[6] used in two relays which have symmetric attributes are considered in[49,3,48]. Ju et al.[49] have shown a closed-form BER performance with fixed amplifying coefficients at relays. Abouei et al.[3] focused on a non-regenerative dual-hop system where relays remain silent when the inter-user channel gain is less than a predetermined threshold. The pairwise error probability (PEP) for high SNR is considered in[48] where a Chernoff upper bound is developed under Rayleigh fading channels.

The distributed Alamouti's code system with one regenerative relay is treated in[98,81,8]. Tourki et al. considered a scheme in which a regenerative relay chooses to cooperate only if its source-relay channel is of an acceptable quality[98]. They evaluated the usefulness of relaying when the source acts blindly and ignores the decision of the relays whether they may cooperate or not. In[81], Barbarossa et al. considered regenerative relays and derived the optimal maximum-likelihood (ML) detector at the final destination in case of binary phase-

shift keying (BPSK) transmission. The performance of the distributed Alamouti system with one regenerative relay is also analyzed in[8].

Our work treats the problem with one non-regenerative relay. Among all the previous works with one non-regenerative relay, Anghel and Kaveh's work[7] has the same infrastructure as that in our research. In their paper, they have characterized the symbol error rate of DSTBC systems by using bounds based on a few channel approximation in high signal-to-noise ratio (SNR). Nevertheless, to the best of our knowledge, no exact BER performance analysis has been reached for this type of systems. This motivates our interest on the research of one non-regenerative relaying system with Distributed STBC.

Contributions of this work

1. One-integral BER Performance

   Different from Anghel and Kaveh's result[7] with approximate asymptotic bounds at high SNR, our priority is to obtain the exact average BER performance formula which can be numerically calculated. As shown in Chapter 2, we calculate the symbol SNR at the output of the MRC receiver. After that, based on this SNR, a one-integral form of BER is derived when all three channels are assume to have Rayleigh fading. With different channel conditions (SNR of each channel), the exact system performance can be readily obtained from the one-integral form of BER formula numerically, such as through mathematics softwares, like, Mathematica or Matlab.

2. Approximation Method

   Though the BER of this exact one-integral form can be readily obtained from some professional tools, it still involves complicated integration calculations. From this point, we try to find out a series solution to get a satisfying result on the expected system performance. We accomplish this task by proposing a new approximate method for Marcum Q-Function. Based on this method, an approximate BER result in the form of series expansions is derived so that the average BER can be expressed and

tightly up-bounded as a summation of a number of terms that can be readily evaluated.

1.5.2   SDF based DSTBC System

As stated in the previous part of this chapter, Soft-Decode-and-Forward (SDF) combines the best features of soft signal representation in AF and channel coding gain in DF. Therefore, DSTBC could also be applied to SDF systems. Similar to AF based DSTBC, the application of DSTBC in SDF also uses a two-phase protocol. While in the first time phase, the source radiates to both the relay and the destination, in the second time phase, the relay demodulates the received signal from the source, soft-decodes and re-encodes to get the soft-information possibly in a different code. Then the relay and the source cooperatively radiate to the destination by using distributed STBC code.

Related Work and Motivation

Among several papers on applying SDF in different coded cooperative communications systems and analyze their performances, Li et al.[62] study distributed turbo coding two-hop relay system with SDF at the relay. They derived the average upper bound on the bit-error rate (BER) at high SNR by using Harmonic mean and weight enumerating function (WEF). Bao et al.[10] focus on the system with same physical infrastructure as Li et al[62]. They compare the achievable rate for different relaying strategies: AF, DF, SDF, and coded cooperation (CC) on BI-AWGN channels under the definition of Shannon's capacity. Hoshyar et al.[41] extend SDF strategy into higher order MQAM modulation. They prove that the proposed SDF scheme attains the same level of diversity as amplify and forward (AF) scheme while improves the overall system spectrum efficiency through forwarding with higher order modulations.

For SDF based coded cooperative communications systems, in order to fully explore the functionality of the source, instead of keeping it idle as in[9],[41] and in our previous work[75], we proposed a cooperative communications system[76] that the source and the relay can cooperatively send their information to the destination using Space-Time codes[36]. From

Monte-Carlo simulations, our proposed system has better performance than the traditional SDF system without DSTBC. But no analysis work is shown in [76] to verify this performance improvement.

Contributions of this work

To analyze the DSTBC in SDF, we adopt the Gaussian approximation [22] of log likelihood ratio (LLR), which is formerly proposed for the research of message-passing in the sum-product decoder for low-density parity-check (LDPC) codes.

We presented two DSTBC based SDF systems which include one relay and two relays, respectively. They are named as one-relay SDF & STBC system and two-relay SDF & STBC system. We compare the performance of these two systems with classic SDF system without DSTBC, which is called one-relay SDF system. For our proposed one-relay scenario, the signal transmission consists of two time phases and in the first time phase, it does exactly the same work as the classic system with SDF alone: the source radiates to both the relay and the destination. In the second time phase, in our one-relay DSTBC & SDF system, the source and the relay cooperatively transmit parity stream to the destination. The source sends the error-free vertical parity bits (P_v), while the relay amplifies and forwards the LLRs of the vertical parity bits $(\hat{P}_v)$ to the destination in the same carrier frequency.

This one-relay SDF & STBC system has later been extended to a two-relay DSTBC & SDF system. In the first time phase, the source radiates to both relays. The relays demodulate and decode the received data stream and generate the reliability values of the source. In the second time phase, in our two-relay DSTBC & SDF system, relays cooperatively transmit parity stream to the destination.

Based on the Central Limit Theorem, the log-likelihood ratios of the vertical parity bits $\hat{P}_v$ can be approximated as Gaussian distributed random variables. Therefore, the combination of the inter-user channel and the soft-decoder and soft-encoder at the relay (before amplifying/ scaling) can be modeled as a virtual fading channel.

1. BER Performance of DSTBC decoding

   Although relay strategies are considered and Space-time codes are introduced to increase power efficiency and reduce outage probability, it is not clear a priori how much the benefits of cooperative diversity would be, since the nodes are not co-located and are connected via noisy, fading links in wireless networks. The main objective of our work on SDF based DSTBC is to mathematically derive bit error rate (BER) performance of both one-relay and two-relay systems and study how much gain can be obtained with the DSTBC enhancement.

   Regarding the decoders at relays which take the message-passing algorithms, if the channel-LLRs at the input to the decoder are independent and identically Gaussian distributed, then the output log likelihood ratio (LLRs) from the decoder will follow an approximated Gaussian distribution. Even if the inputs are not Gaussian, e.g. for wireless channels experiencing fast Rayleigh fading, by the central limit theorem, the sum would still be a Gaussian if many independent random variables are added. Therefore, the LLR values can be approximated as Gaussian. The exact one-integral form of BER performance at the destination is derived based on the Gaussian approximation on the LLR values for the vertical parity bits at the relays.

2. Power Allocation and Optimization

   A line simulation model is introduced to evaluate the BER performance at the receiver for all three systems: one-relay SDF, one-relay SDF & DSTBC, and two-relay SDF & DSTBC systems. Therefore, the derived one-integral BER is tested against all possible SNR values for all three channels to obtain a fully understanding of the systems' behavior. Furthermore, for the one-relay SDF & DSTBC system, the source transmits in the second time phase may reduce the transmit power of the relay in order to make the total transmission power equal. As a result, a natural question risen in cooperative systems with distributed coding is that how to fully utilize all channels to

achieve better performance. For the proposed two-relay SDF & DSTBC system, there is a tradeoff between relay positions and decoding effects. When relays locate nearer to the destination than to the source, they can hardly provide clean sets of parity LLR messages as the source does though they can deliver this information easily to the destination. Another question risen is that in which position the relays should be located to make the proposed two-relay SDF & DSTBC system outperform our two one-relay systems.

We tried to exploit the performance improvement of our one-relay SDF & DSTBC and two-relay SDF & DSTBC systems stated above by allocating different ratio of power in the second time phase. Numerical results indicate that the proposed two SDF systems with DSTBC are superior to the one-relay system without DSTBC for most of the power ratios. Results also show that in the two-relay SDF & DSTBC system, when two relays cannot provide good LLR messages, the proposed one-relay SDF & DSTBC system may outperform especially when more power are allocated at the source which can transmit error-free parity symbols.

Numerical method on optimization is introduced to look for the value of power allocation ratio where the optimal Space-Time decoded performance is achieved. The numerical results show that the optimal results of power allocation ratio are consistent with the best performance points on the obtained performance curves.

Part I

DISTRIBUTED SPACE-TIME CODE WITH AMPLIFY-AND-FORWARD (AF) RELAYING SYSTEM

Chapter 2
DISTRIBUTED SPACE-TIME CODE WITH AMPLIFY-AND-FORWARD (AF) RELAYING SYSTEM

In this chapter, we consider the distributed Alamouti's code for cooperative diversity networks with Amplify-and-Forward protocol. Based on the conditional expectation, the exact average BER performance is derived in a one-integral form so that the system performance can be numerically calculated. Furthermore, a novel approximation method in the form of series expansion is presented and the BER performance can be tightly bounded with a summation of a number of terms.

The rest of the chapter is organized as follows. In Section 2.1, the model of the distributed Alamouti's code system with one non-regenerative relay is described. In Section 2.2, we establish the derivation of the exact one-integral form of the average BER performance of the system. In addition, we present a novel approximation method for the BER performance based on the series expansion. In Section 2.3, both numerical and simulation results are provided to demonstrate the accuracy of the analysis.

2.1 System Model

The system consists of a source node, a non-regenerative node and a destination node. We denote the link between the source and the destination, the source and the relay, and the relay and the destination, as direct link, inter-user link and relay link, respectively. The transmission of one data frame from the source to the destination is divided into two time phases and, for each time phase, it has two time slots. Let h_{11} and h channel coefficients along the direct link and inter-use link in the 1st time phase, and h_{12} and h_2 be the channel

19
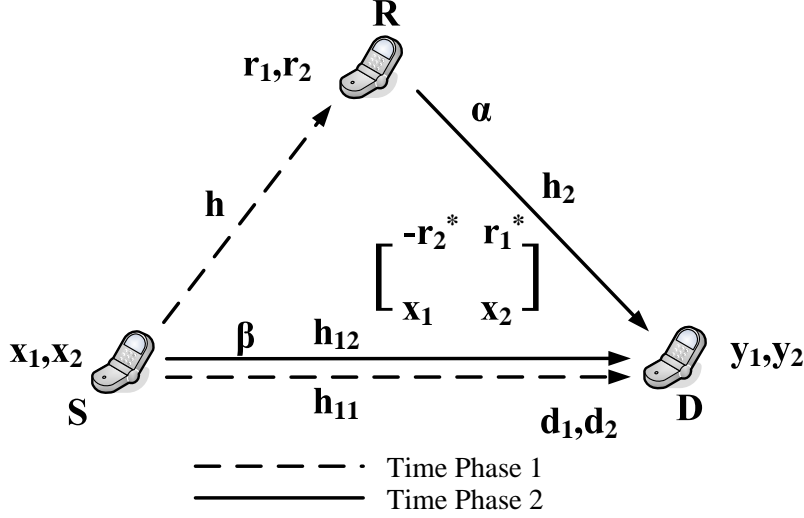
Figure 2.1. The system model of the considered distributed Alamouti's code cooperative diversity system.

fading of the direct link and relay link in the 2nd time phase. All channels are independent, flat Rayleigh fading channels that follow circularly symmetric complex Gaussian distribution with zero mean and different variances. Assume that $E[|h|^2] = \Omega$, $E[|h_{11}|^2] = E[|h_{12}|^2] = \Omega_1$ and $E[|h_2|^2] = \Omega_2$.

The process in the first time phase of the distributed system is shown in Fig. 2.1 with the dash lines. Let $x_i, i = 1, 2$, be the symbols transmitted by the source at the first and second time slots in the first time phase to both the relay and the destination nodes. The signals received at the relay are given by

$$r_i = \sqrt{E_s}hx_i + n_i \quad \text{where} \quad i = 1, 2 \tag{1}$$

where h is the channel gain of the inter-use link with $h \sim \mathcal{CN}(0, \Omega)$. n is the AWGN at the relay node with distribution of the zero-mean circularly symmetric complex Gaussian, i.e., $n_i \sim \mathcal{CN}(0, \sigma_n^2)$, and E_s stands for the average transmission energy per symbol.

In the meantime, the signals received at the destination are:

$$d_i = \sqrt{E_s}h_{11}x_i + w_i \quad \text{where} \quad i = 1, 2 \tag{2}$$

20

where $h_{11} \sim \mathcal{CN}(0, \Omega_1)$ and $w_i \sim \mathcal{CN}(0, \sigma_w^2)$. In the matrix form, we can write (2) as

$$D = \sqrt{E_s} H_{11} X + W$$

where $D = [d_1, d_2^*]^T$, $H_{11} = \begin{bmatrix} h_{11} & 0 \\ 0 & h_{11}^* \end{bmatrix}$, $X = [x_1, x_2^*]^T$ and $W = [w_1, w_2^*]^T$.

The SNR for the direct link in the 1st time phase is therefore $\gamma_1 = \gamma_w |h_{11}|^2$, where $\gamma_w = \frac{E_s}{\sigma_w^2}$.

The difference between the distributed STC system and the conventional AF system exists in the second phase. In the considered system, the relay node cooperates with the source to build up a space-time coding system in a distributed way. It uses the amplify-and-forward (AF) protocol that multiplies a tunable coefficient α to the formerly received signals and then transmits to the destination in the second phase. Due to the use of distributed Alamouti's code, $-\alpha r_2^*$ and αr_1^* are the transmitted symbols at the relay. In the meantime, the source radiates the same information symbols as those transmitted in the first phase by multiplying with another coefficient β, i.e., $\beta \sqrt{E_s} x_1$ and $\beta \sqrt{E_s} x_2$. The model in the second time phase of the proposed system is shown as the solid lines in Fig. 2.1. The receiver observations y_1 and y_2 corresponding to the two symbol periods are given by

$$y_1 = \sqrt{E_s} \beta h_{12} x_1 - \alpha h_2 r_2^* + v_1 \tag{3}$$

$$y_2 = \sqrt{E_s} \beta h_{12} x_2 + \alpha h_2 r_1^* + v_2 \tag{4}$$

where v_1, v_2 are the AWGN at the destination node with $v_i \sim \mathcal{CN}(0, \sigma_v^2)$ for $i = 1, 2$. Substituting r_i and writing in the matrix form, the received signals are:

$$Y = \sqrt{E_s} H X + N + V \tag{5}$$

where $Y = [y_1, y_2^*]^T$, $X = [x_1, x_2^*]^T$, $V = [v_1, v_2^*]^T$,

$$H = \begin{bmatrix} \beta h_{12} & -\alpha h_2 h^* \\ \alpha h_2^* h & \beta h_{12}^* \end{bmatrix} \quad \text{and} \quad N = \begin{bmatrix} -\alpha h_2 n_2^* \\ \alpha h_2^* n_1 \end{bmatrix}.$$

Since $H^H H = ||H||^2 I_2 / 2$ where H^H is the Hermitian of H, the maximum-likelihood (ML) decoding can be implemented by multiplying the received data with H^H, i.e., decoding with its matched filter. We have

$$H^H \begin{bmatrix} y_1 \\ y_2^* \end{bmatrix} = \sqrt{E_s}(\beta^2 |h_{12}|^2 + \alpha^2 |h|^2 |h_2|^2) \begin{bmatrix} 1 & 0 \\ 0 & 1 \end{bmatrix} \begin{bmatrix} x_1 \\ x_2^* \end{bmatrix}$$
$$+ H^H \begin{bmatrix} -\alpha h_2 n_2^* \\ \alpha h_2^* n_1 \end{bmatrix} + H^H \begin{bmatrix} v_1 \\ v_2^* \end{bmatrix} \tag{6}$$

From the above equation, y_1 and y_2 have symmetric form and it can be found that they have the same signal-to-noise ratio as

$$\gamma_2 = \frac{\beta^2 |h_{12}|^2 + \alpha^2 |h|^2 |h_2|^2}{\alpha^2 |h_2|^2 \frac{1}{\gamma_n} + \frac{1}{\gamma_v}} \tag{7}$$

where $\gamma_n = \frac{E_s}{\sigma_n^2}$ and $\gamma_v = \frac{E_s}{\sigma_v^2}$.

The final optimal detection should be conducted based on the maximal ratio combining (MRC) of what have been obtained from both time phases.

It is known that the MRC combining coefficient for each copy of information is the Hermitian matrix of the signal coefficient divided by the noise power. Therefore,

$$C_{MRC}^{(1)} = \frac{\sqrt{E_s} H_{11}^H}{\sigma_w^2} \quad \text{and} \quad C_{MRC}^{(2)} = \frac{\sqrt{E_s} H^H}{\alpha^2 |h_2|^2 \sigma_n^2 + \sigma_v^2} \tag{8}$$

The combined signal then is,

$$
\begin{aligned}
X_{MRC} &= C_{MRC}^{(1)} \cdot D + C_{MRC}^{(2)} \cdot Y = \frac{\sqrt{E_s} H_{11}^H}{\sigma_w^2} \begin{bmatrix} d_1 \\ d_2^* \end{bmatrix} + \frac{\sqrt{E_s} H^H}{\alpha^2 |h_2|^2 \sigma_n^2 + \sigma_v^2} \begin{bmatrix} y_1 \\ y_2^* \end{bmatrix} \\
&= \left(\frac{E_s ||H_{11}||^2 / 2}{\sigma_w^2} + \frac{E_s ||H||^2 / 2}{\alpha^2 |h_2|^2 \sigma_n^2 + \sigma_v^2} \right) X \\
&\quad + \frac{\sqrt{E_s} H_{11}^H}{\sigma_w^2} W + \frac{\sqrt{E_s} H^H}{\alpha^2 |h_2|^2 \sigma_n^2 + \sigma_v^2} (N + V)
\end{aligned}
\tag{9}
$$

In order to estimate $[\hat{x}_1, \hat{x}_2{}^*]^T$ of the transmitted data from X_{MRC}, normalization should be taken as follows before final decisions are made.

$$
\begin{aligned}
\hat{X} &= X_{MRC} / \left(\frac{E_s ||H_{11}||^2 / 2}{\sigma_w^2} + \frac{E_s ||H||^2 / 2}{\alpha^2 |h_2|^2 \sigma_n^2 + \sigma_v^2} \right) \\
&= X + \left[\frac{\sqrt{E_s} H_{11}^H}{\sigma_w^2} W + \frac{\sqrt{E_s} H^H}{\alpha^2 |h_2|^2 \sigma_n^2 + \sigma_v^2} (N + V) \right] \\
&\quad / \left(\frac{E_s ||H_{11}||^2 / 2}{\sigma_w^2} + \frac{E_s ||H||^2 / 2}{\alpha^2 |h_2|^2 \sigma_n^2 + \sigma_v^2} \right).
\end{aligned}
\tag{10}
$$

where $\hat{X} = [\hat{x}_1, \hat{x}_2{}^*]^T$ and $||\cdot||^2$ is the squared Frobenius norm of a certain matrix. Detection can then be directly based on vector $\hat{X}$.

The objective of this work is to analyze the BER of this cooperative communications system with the distributed Alamouti's code. With the fact that the considered distributed system reduces to the conventional AF cooperative system when $\alpha = 1$ and $\beta = 0$, the distributed Alamouti's code system can be considered as a generalization of the conventional cooperative communication system. Therefore, an accurate average BER performance analysis of this system is of high interest.

2.2 BER Performance Analysis

The instantaneous SNR per symbol γ_T at the output of the MRC combiner is given as

$$
\begin{aligned}
\gamma_T &= \sum_{l=1}^{2} \gamma_l = \gamma_1 + \gamma_2 = \frac{E_s}{\sigma_w^2}|h_{11}|^2 + \frac{E_s\beta^2}{\alpha^2|h_2|^2\sigma_n^2 + \sigma_v^2}|h_{12}|^2 + \frac{E_s\alpha^2|h_2|^2}{\alpha^2|h_2|^2\sigma_n^2 + \sigma_v^2}|h|^2 \\
&= \gamma_w|h_{11}|^2 + \mu\beta^2|h_{12}|^2 + \mu\alpha^2|h_2|^2|h|^2
\end{aligned}
\tag{11}
$$

where $\gamma_w = \frac{E_s}{\sigma_w^2}$, $\gamma_n = \frac{E_s}{\sigma_n^2}$, $\gamma_v = \frac{E_s}{\sigma_v^2}$ and $\mu = \frac{1}{\frac{\alpha^2|h_2|^2}{\gamma_n} + \frac{1}{\gamma_v}}$. Average BER is then determined by this γ_T.

2.2.1 The Exact BER expression in One-Integral Form

For a SNR value γ_s (i.e., energy per symbol over noise), the bit error probability P_b for coherent binary signals is given as[31]

$$
P_b(\gamma_s) \approx c_1 Q\left(\sqrt{c_2\gamma_s}\right)
$$

where c_1 is the number of the nearest neighbors to a constellation at the minimum distance, and c_2 is a constant that relates the minimum distance to the average symbol energy. For example, the specific values for coherent BPSK are $c_1 = 1$ and $c_2 = 2$, and in this case $P_b(\gamma_s) = Q\left(\sqrt{2\gamma_s}\right)$ where $Q(\cdot)$ is the Gaussian Q-function. Whereas, for rectangular MQAM, the approximate bit error probability for coherent modulation is [31 p167, Table 6.1]

$$
P_b(\gamma_s) \approx \frac{4(\sqrt{M}-1)}{\sqrt{M}\log_2 M} Q\left(\sqrt{\frac{3\gamma_s}{M-1}}\right).
\tag{12}
$$

The performance for BPSK is exact and that for MQAM is a close approximation based on the nearest neighbor approximation [31 p164]. Since γ_s is often a random variable, in order to evaluate the performance of the system in terms of average BER, the above BER has to be statistically averaged over the density distribution. Two approaches are well known to

solve this problem: the classical PDF-based approach and the MGF-based approach.

PDF-based and MGF-based approaches

The unconditional average probability of error in the considered system can be found as

$$P_b(\mathcal{E}) = \int_0^\infty c_1 Q\left(\sqrt{c_2 \gamma_T}\right) p_{\gamma_T}(\gamma_T) d\gamma_T$$

where γ_T represents the total SNR of the combined signal at the receiver. However, since the PDF of γ_T is usually very difficult to obtain, another method, i.e., the MGF-based method, is more often used.

Using the alternative representation of the Gaussian-Q function

$$Q(x) = \frac{1}{\pi} \int_0^{\pi/2} \exp\left(-\frac{x^2}{2\sin^2\theta}\right) d\theta$$

and assuming $\gamma_T = \sum_{l=1}^L \gamma_l$, where L is the number of diversity paths and the γ_l are independent random variables, we have

$$
\begin{aligned}
P_b(\mathcal{E}) &= \int_0^\infty ... \int_0^\infty c_1 Q(\sqrt{c_2 \gamma_T}) \cdot \prod_{l=1}^L p_{\gamma_l}(\gamma_l) \cdot d\gamma_1 ... d\gamma_L \\
&= \int_0^\infty ... \int_0^\infty \frac{c_1}{\pi} \int_0^{\pi/2} \prod_{l=1}^L \exp\left(-\frac{c_2 \gamma_l}{2\sin^2\theta}\right) \cdot p_{\gamma_l}(\gamma_l) d\theta d\gamma_1 ... d\gamma_L \\
&= \frac{c_1}{\pi} \int_0^{\pi/2} \prod_{l=1}^L \mathcal{M}_{\gamma_l}\left(-\frac{c_2}{2\sin^2\theta}\right) d\theta
\end{aligned}
\tag{13}
$$

where $\mathcal{M}_{\gamma_l}(s) = \int_0^\infty p_{\gamma_l}(\gamma_l) e^{s\gamma_l} d\gamma_l$ is the moment-generating function (MGF) of the SNR per symbol γ_l associate with path l.

To use the MGF method, it is required that γ_T can be expressed as a summation of $\gamma_l, 1 \leq l \leq L$ which must be independent random variables whose MGF can be found explicitly. The final γ_T of our considered system, as shown in (11), is a summation of three

terms. However, the 2nd and 3rd terms are clearly not independent. Furthermore, it is much involved to find either the PDF or the MGF based on the expression of γ_T. As a result, both the PDF-based and the MGF-based approaches cannot be directly applied to our problem. In the following, we solve this BER problem based on the conditional-expectation method.

The Conditional Expectation Approach

Theorem 1. *Let* $Y = f(X_1, X_2, \cdots, X_n)$, *where* $X_i, 1 \leq i \leq n$ *are independent Random variables, then the expectation of* Y *satisfies*

$$E[Y] = E_{X_n}[E_{X_1,\ldots,X_{n-1}}[Y|X_n]].$$

This equation [with minor modification from [77] p106 eqn(3.3)] is known as the theorem of conditional expectation. From (11), it can be found that when h_2 is fixed, γ_T can be represented as a summation of three independent and exponentially distributed terms involving h, h_{11}, h_{12}, and therefore the MGF-based method can be used to find this conditional average BER. The final average BER can further be obtained by averaging over the random variable h_2. That is,

$$
\begin{aligned}
P_b(\mathcal{E}) &= E_{h_{11},h_{12},h,h_2}\left[c_1 Q\left(\sqrt{c_2\gamma_T}\right)\right] = E_{h_{11},h_{12},h,h_2}\left[\frac{c_1}{\pi}\int_0^{\pi/2}\exp\left(-\frac{c_2\gamma_T}{2\sin^2\theta}\right)d\theta\right]\\
&= \frac{c_1}{\pi}\int_0^{\pi/2} E_{h_2}\left[E_{h_{11},h_{12},h}\left[\exp\left(-\frac{c_2}{2\sin^2\theta}\cdot\gamma_T\right)|h_2\right]\right]d\theta\\
&= \frac{c_1}{\pi}\int_0^{\pi/2} E_{h_2}\left[E_{h_{11},h_{12},h}\left[\exp\left(-\frac{c_2}{2\sin^2\theta}\cdot\right.\right.\right.\\
&\qquad\left.\left.\left.\left(\gamma_w|h_{11}|^2 + \mu\beta^2|h_{12}|^2 + \mu\alpha^2|h_2|^2|h|^2\right)\right)|h_2\right]\right]d\theta.
\end{aligned}
\tag{14}
$$

Therefore, the solving process includes two steps. The first is to, for given h_2, average the conditional BER over h, h_{11}, h_{12} respectively. The second is to average the resultant over

h_2. To obtain $E_{h_{11},h_{12},h}[\cdot|h_2]$ in the first step, the following Lemma (with minor modification of [55] Theorem 4.1]) can be employed.

Lemma 1. *Assume a $K \times 1$ vector $\boldsymbol{a} = [a_1, a_2, \cdots, a_k]^T \sim \mathcal{CN}(0_{K\times 1}, \Xi)$. Let $\{\lambda_1, ..., \lambda_r\}$ be the nonzero eigenvalues of Ξ. Then the moment generating function (MGF) of $||\boldsymbol{a}||^2$ is given by*

$$M_{||\boldsymbol{a}||^2}(s) = E_{\boldsymbol{a}}\big[\exp(s||\boldsymbol{a}||^2)\big] = \prod_{i=1}^{r} \frac{1}{1 - s\lambda_i}. \tag{15}$$

In our scenario, we separate γ_T into three parts and have a_i as follows,

$$|a_1|^2 = \gamma_w|h_{11}|^2, \quad |a_2|^2 = \mu\beta^2|h_{12}|^2, \quad \text{and} \quad |a_3|^2 = \mu\alpha^2|h_2|^2|h|^2. \tag{16}$$

Since h_{11}, h_{12}, h are the independent RVs for channel gains in different paths and they follow $h_{11} \sim \mathcal{CN}(0, \Omega_1)$ and $h_{12} \sim \mathcal{CN}(0, \Omega_1)$, $h \sim \mathcal{CN}(0, \Omega)$. All the other parameters (γ_w, μ, α, and, β) are seen as constants. We have,

$$\begin{bmatrix} a_1 \\ a_2 \\ a_3 \end{bmatrix} \sim \mathcal{CN}\left(\begin{bmatrix} 0 \\ 0 \\ 0 \end{bmatrix}, \begin{bmatrix} \gamma_w\Omega_1 & 0 & 0 \\ 0 & \mu\beta^2\Omega_1 & 0 \\ 0 & 0 & \mu\alpha^2|h_2|^2\Omega \end{bmatrix}\right).$$

The nonzero eigenvalues of its covariance matrix are

$$\lambda_1 = \gamma_w\Omega_1, \quad \lambda_2 = \mu\beta^2\Omega_1, \quad \text{and} \quad \lambda_3 = \mu\alpha^2|h_2|^2\Omega. \tag{17}$$

Then, the moment generating function (MGF) of $||\boldsymbol{a}||^2$ given by Lemma 1 is

$$\begin{aligned} E_a\left[\exp\left(-\frac{c_2}{2\sin^2\theta}||a||^2\right)\right] &= \prod_{i=1}^{3} \frac{1}{1 + \frac{c_2}{2\sin^2\theta}\lambda_i} \\ &= \frac{1}{1 + \frac{c_2}{2\sin^2\theta}\gamma_w\Omega_1} \cdot \frac{1}{1 + \frac{c_2}{2\sin^2\theta}\mu\beta^2\Omega_1} \cdot \frac{1}{1 + \frac{c_2}{2\sin^2\theta}\mu\alpha^2|h_2|^2\Omega}. \end{aligned}$$

Therefore,

$$
P_b(\mathcal{E}) = \frac{c_1}{\pi} \int\limits_0^{\pi/2} E_{h_2} \left[\frac{1}{1 + \frac{c_2}{2\sin^2\theta}\gamma_w\Omega_1} \cdot \frac{1}{1 + \frac{c_2}{2\sin^2\theta}\frac{1}{\frac{\alpha^2|h_2|^2}{\gamma_n} + \frac{1}{\gamma_v}}\beta^2\Omega_1} \cdot \right.
$$

$$
\left. \frac{1}{1 + \frac{c_2}{2\sin^2\theta}\frac{1}{\frac{\alpha^2|h_2|^2}{\gamma_n} + \frac{1}{\gamma_v}}\alpha^2|h_2|^2\Omega} \right] d\theta. \tag{18}
$$

By considering the PDF of h_2 in (18), we can derive the unconditional probability $P_b(\mathcal{E})$. The detailed derivation is given in Appendix A which involves parameter substitution, partial fraction and the use of special functions. We state the final average BER formula in the following theorem.

Theorem 2. *The one-integral form of the exact BER performance of the considered distributed Alamouti's code cooperative diversity system, with channel statistics $\boldsymbol{\gamma} = [\gamma_n, \gamma_w, \gamma_v]$, $\boldsymbol{\Omega} = [\Omega, \Omega_1, \Omega_2]$ and the modulation parameters c_1 and c_2, is given as*

$$
P_b(\boldsymbol{\gamma}, \boldsymbol{\Omega}, c_1, c_2)
$$

$$
= \frac{c_1}{2} \int\limits_0^\infty \frac{1}{\Omega_2} \exp\left(-\frac{t}{\Omega_2}\right) \cdot \left[1 - \frac{A^3}{(A-B)(A-C)}\frac{1}{\sqrt{A(A+1)}} \right.
$$

$$
\left. + \frac{B^3}{(A-B)(B-C)}\frac{1}{\sqrt{B(B+1)}} + \frac{C^3}{(A-C)(C-B)}\frac{1}{\sqrt{C(C+1)}} \right] \cdot dt \tag{19}
$$

where $A = Z\beta^2\Omega_1$, $B = Z\alpha^2 t\Omega$, $C = \frac{1}{2}c_2\gamma_w\Omega_1$ and $Z = \frac{c_2/2}{\frac{\alpha^2 t}{\gamma_n} + \frac{1}{\gamma_v}}$.

Proof: See appendix A.

The arguments of this exact one-integral formula are only the channel characteristics of the three links and the type of modulation. This one-integral formula can be calculated numerically, for instance, by using software such as Mathematica or MatLab. Thus, the average BER performance of the distributed Alamouti coding system in any given channel scenario can be readily evaluated.

2.2.2 A Series Expansion of a BER approximation

In this part, we present an approximation method of the Q-function in series expansion based on which we further derive a BER approximation formula for the considered system. With this result, the average BER performance can be very tightly approximated as a summation of a number of easily calculated terms.

Existing Approximations of Marcum Q-Function

The first tight approximation was proposed by Borjesson et al.[14] in the following form,

$$Q(x) \approx \frac{1}{\sqrt{2\pi}} \cdot \frac{1}{(1-a)x + a\sqrt{x^2+b}} \exp\left(-\frac{x^2}{2}\right), x \geqslant 0 \tag{20}$$

where $a = 0.339$ and $b = 5.510$ are used to minimize the maximum absolute relative error.

Karagiannidis and Lioumpas[50] gave another approximation aimed at increasing the tightness in the region of small function's argument values as

$$Q(x) \approx \frac{(1 - \exp(-\frac{Ax}{\sqrt{2}}))\exp(-\frac{x^2}{2})}{B\sqrt{2\pi}x} \tag{21}$$

where $A = 1.98$ and $B = 1.135$. The accuracy with this approximation is remarkable. However, the presence of x in the denominator of the formulas makes it difficult to derive the expression of the final system BER.

In[19], a method of summation of exponential functions was proposed by Chiani et. al as

$$Q(x) \approx \frac{1}{12}\exp(-\frac{x^2}{2}) + \frac{1}{4}\exp(-\frac{2x^2}{3}). \tag{22}$$

In[66], Prony approximations were proposed by Loskot et al. with two equations,

$$Q(x) \approx 0.208 \exp(-0.971x^2) + 0.147 \exp(-0.525x^2), \quad x \geqslant 0 \tag{23}$$

$$Q(x) \approx 0.168 \exp(-0.876x^2) + 0.144 \exp(-0.525x^2)$$
$$+0.002 \exp(-0.603x^2), \quad x \geqslant 0. \tag{24}$$

In order to further reduce the approximation error, Ju et al.[49] modified the Prony method by adjusting the exponents and scalar coefficients, i.e.,

$$Q(x, \rho_1, \rho_2) \approx \frac{1}{12} \exp(-\rho_1 x^2) + \frac{1}{4} \exp(-\rho_2 x^2). \tag{25}$$

In[49], much effort has been conducted to find the most suitable ρ_1 and ρ_2 values in different channel scenarios. Though excellent performance was reported, it might not be expected that the parameters in the approximation of the general Q function depend on specific link quality (SNR values) of a communication system. In the following, we give another method that is similar to the series expansion where accuracy of the approximation increases when more terms are included.

Proposed Marcum Q-Function Approximation

It is well known that the Gaussian-Q function can be represented as

$$Q(x) = \frac{1}{\pi} \int_0^{\pi/2} \exp\left(-\frac{x^2}{2\sin^2\theta}\right) d\theta. \tag{26}$$

From the advanced calculus, one way to numerically calculate this integral is to divide the integral interval into infinite small parts and sum up the integrant values from each tiny part together. We apply this idea to obtain a tight up-bound of Marcum Q-function.

Specifically, for $x \geqslant 0$ we approximate the Q-function as

$$
\begin{aligned}
Q(x) \quad \leqslant \quad & \frac{1}{\pi} \sum_{i=0}^{n-1} \int_{\theta_i}^{\theta_{i+1}} \exp\left(-\frac{x^2}{2\sin^2\theta_{i+1}}\right) d\theta \\
\leqslant \quad & \sum_{i=0}^{n-1} \frac{\theta_{i+1} - \theta_i}{\pi} \exp\left(-\frac{x^2}{2\sin^2\theta_{i+1}}\right).
\end{aligned}
\tag{27}
$$

In order to tighten the bound, we divide the integral interval $[0, 2\pi]$ into n parts. Without the loss of generality, we use the equal interval size. That is,

$$
\theta_i = \frac{\pi}{2n}i, \quad i \in [0, n] \quad \text{and} \quad \theta_{i+1} - \theta_i = \frac{\pi}{2n}, \quad i \in [0, n-1].
\tag{28}
$$

Substituting these equations into (27), we have

$$
Q(x) \leqslant \frac{1}{2n} \sum_{i=0}^{n-1} \exp\left(-\frac{x^2}{2\sin^2(\frac{\pi}{2n}(i+1))}\right), \quad x \geqslant 0.
\tag{29}
$$

We can see that when we increase n which is the number of exponential components, the value of the right part of inequality will tightly bound to the actual curve of Q-function.

Comparison of the proposed method with existing approximations

Fig. 2.2 shows the comparison of some of the approximation methods with the exact Q-Function.

As it can be observed, for a wide range of arguments, especially in the region of high argument value, the Prony approximation is more accurate than Chiani's method. Our proposed approximation has consistent error regarding to all x. When $n = 4$, it is a loose upper bound, while when n reaches to 32, it becomes a very tight bound. Borjesson's method also has very tight approximation result, however, the form of component terms do not have the desired feature for further simplification of the BER formula.

The relative error (RE), as shown in (30), is introduced to give more precise comparison
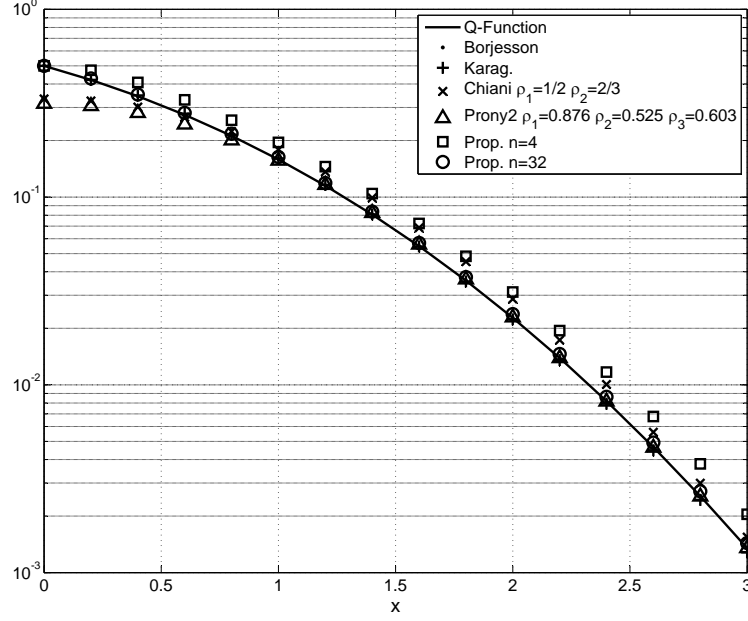
Figure 2.2. Comparison among different Q-Function approximations

for positions where the difference of bounds cannot be identified by eye sight.

$$\bar{e} = \int_0^\infty \frac{F(x) - Q(x)}{Q(x)} dx, \quad (0 < x < \infty) \tag{30}$$

where $F(x)$ is the approximated function.

Table 2.1. The relative error (RE) of different approximations.

Appr.	Borjesson	Karag.	Chiani $\rho_1=1/2$ $\rho_2=2/3$	Prony2 $\rho_1=0.876$ $\rho_2=0.525$ $\rho_3=0.603$
$\bar{e}$	0.1698%	0.8533%	18.1655%	21.4517%

Appr.	Ju $\rho_1=0.47$ $\rho_2=0.82$	Prop. n=4	Prop. n=32	Prop.n=1024
$\bar{e}$	17.5053%	14.4041%	2.0374%	0.0643%

TABLE II shows the RE of different approximations which is consistent with the numerical results in Fig. 2.2. In our proposed method, the RE is asymptotically reduced to 0 by adding more exponential terms to tighten the approximation bound.

Applying Q-function approximations in system performance analysis

It can be observed that the proposed method, together with the Chiani's, Loskot's and Ju's approximation methods in (22), (24) and (25), can be represented as

$$Q(x, \omega, \rho) \approx \sum_{i=1}^{n} \omega_i \exp(-\rho_i x^2), \qquad n \geqslant 2. \tag{31}$$

where $\omega = [\omega_1, ..., \omega_n]$, and $\rho = [\rho_1, ..., \rho_n]$.

Substitute the above equation into the BER representation in (11), we can get

$$
\begin{aligned}
P_b(\mathcal{E}) &= P_b^{appr}(\boldsymbol{\gamma}, \boldsymbol{\Omega}, c_1, c_2, \rho, \omega) \\
&= E_{h_{11}, h_{12}, h, h_2}[c_1 Q\left(\sqrt{c_2 \gamma_T}\right)] \\
&\approx c_1 \sum_{i=1}^{n} \omega_i E_{h_{11}, h_{12}, h, h_2}[\exp(-\rho_i c_2 \gamma_T)] \\
&= \sum_{i=1}^{n} c_1 \omega_i W(\rho_i, c_2, \boldsymbol{\gamma}, \boldsymbol{\Omega}),
\end{aligned}
\tag{32}
$$

where

$$
\begin{aligned}
W(\rho_i, c_2, \boldsymbol{\gamma}, \boldsymbol{\Omega}) &= E_{h_{11}, h_{12}, h, h_2}[\exp(-\rho_i c_2 \gamma_T)] \\
&= E_{h_2}[E_{h_{11}, h_{12}, h}[\exp(-\rho_i c_2 \gamma_T)|h_2]] \\
&= E_{h_2}[E_{h_{11}, h_{12}, h}[\exp(-\rho_i c_2(\gamma_w|h_{11}|^2 + \\
&\quad \mu\beta^2|h_{12}|^2 + \mu\alpha^2|h_2|^2|h|^2))|h_2]].
\end{aligned}
\tag{33}
$$

In appendix B, we have given the derivation of the function $W(\cdot)$. Therefore, the following result can be reached.

Theorem 3. *When the Marcum Q-function is approximated in the form of $Q(x, \omega, \rho) \approx \sum_{i=1}^{n} \omega_i \exp(-\rho_i x^2)$, $n \geq 2$, then the BER performance of the considered cooperative distribut-*

ed system with Alamouti's code can be closely approximated by the following function,

$$P_b^{appr}(\boldsymbol{\gamma}, \boldsymbol{\Omega}, c_1, c_2, \rho, \omega) \approx \sum_{i=1}^{n} c_1 \omega_i W(\rho_i, c_2, \boldsymbol{\gamma}, \boldsymbol{\Omega}),$$

where,

$$
\begin{aligned}
W(\rho_i, c_2, \boldsymbol{\gamma}, \boldsymbol{\Omega}) = & \frac{1}{\Omega_2} \frac{1}{1 + \rho_i c_2 \gamma_w \Omega_1} \frac{1}{1 + \rho_i c_2 \Omega \gamma_n} \cdot \left[\Omega_2 - \frac{(A' - B')^2}{C' - B'} \exp\left(\frac{B'}{\Omega_2}\right) \boldsymbol{Ei}\left(-\frac{B'}{\Omega_2}\right) \right. \\
& \left. - \frac{(A' - C')^2}{B' - C'} \exp\left(\frac{C'}{\Omega_2}\right) \boldsymbol{Ei}\left(-\frac{C'}{\Omega_2}\right) \right]
\end{aligned}
\tag{34}
$$

and,

$$A' = \frac{\gamma_n}{\gamma_v \alpha^2}, \quad B' = \frac{\gamma_n}{\gamma_v \alpha^2} + \rho_i c_2 \beta^2 \Omega_1 \frac{\gamma_n}{\alpha^2}, \quad \text{and} \quad C' = \frac{1}{\gamma_v(\frac{\alpha^2}{\gamma_n} + \rho_i c_2 \alpha^2 \Omega)}. \tag{35}$$

Proof: See appendix B.

By applying the proposed Q-Function Approximation in inequality (29), we have

$$\omega_i = \frac{1}{2n}, \quad n \geqslant 2, \quad \text{and} \quad \rho_i = \frac{1}{2\sin^2(\frac{\pi}{2n}i)}, \quad i \in [1, n]. \tag{36}$$

For a given n, substituting the parameters in Theorem 3, the approximate BER performance of the system can be obtained as an upper bound. This formula expressed in a summation of simple functions provides a very easy way to evaluation the system performance in various channel conditions. It will be shown that with the increase of n value, this approximate BER performance indeed goes to the exact solution shown in Theorem 3 very quickly.

2.3   Numerical results for Amplify-and-Forward relaying

In this section, we use simulation results to validate the analytic results in Theorem 2 and 3. Since the purpose here is to evaluate the accuracy of the theoretic results, we pick

Table 2.2. The error rate in different models and in different SNR regions calculated by (37).

	[0, 10dB]	[10dB, 20dB]	[20dB, 30dB]	[0dB, 30dB]
Chiani $\rho_1=1/2$ $\rho_2=2/3$	27.5669%	52.5206%	64.5079%	47.42%
Prony1 $\rho_1=0.971$ $\rho_2=0.525$	5.31782%	24.8707%	34.6103%	21.00%
Prony2 $\rho_1=0.876$ $\rho_2=0.525$ $\rho_3=0.603$	5.38093%	25.8425%	35.8132%	21.67%
Ju $\rho_1=0.47$ $\rho_2=0.82$	4.8265%	25.0092%	34.9938%	20.96
prop n=2	66.00%	69.17%	68.81%	67.99%
prop n=4	33.29%	34.97%	34.75%	34.34%
prop n=8	16.65%	17.49%	17.38%	17.17%
prop n=16	8.33%	8.74%	8.69%	8.59%
prop n=32	4.16%	4.37%	4.34%	4.29%

the parameters rather arbitrary. The parameters used in the reported experimental results are as follows,

$$\Omega_1 = \Omega_2 = \Omega = 1 \quad \text{and} \quad \alpha = \beta = \frac{1}{\sqrt{2}}.$$

2.3.1 The exact One integral Theoretical BER performance

We compare and analyze the Mote-Carlo simulation results with the exact BER expression in one-integral results when $\gamma_n = 1000dB$ and $\gamma_w = 10dB$. This is an extreme condition where the inter-user link is assumed to be ideal. We change the channel condition of the relay link γ_v from 0dB to 30dB to evaluate the correctness of our one-integral result. In the figure, "BER-v" (curves with circle and X-marks) and "BER-MRC" (curves with square and cross marks) stand for the BER results of the space-time decoding for the 2nd time phase only and the BER results of the final MRC considering both time phases, respectively. As shown in Fig. 2.3, we can clearly find that for both BER-v and BER-MRC, the one-integral theoretical performances and the simulation results match accurately

The classical Alamouti's code (2×1) performance, represented as "Theory-Alamouti-Tx2-Rx1" in dotted-curve with triangle marks, is also plotted. However, it should be noted that even though without noise at the relay receiver, the performance of the considered system in the 2nd time phase alone after ST decoding is not the same as the conventional
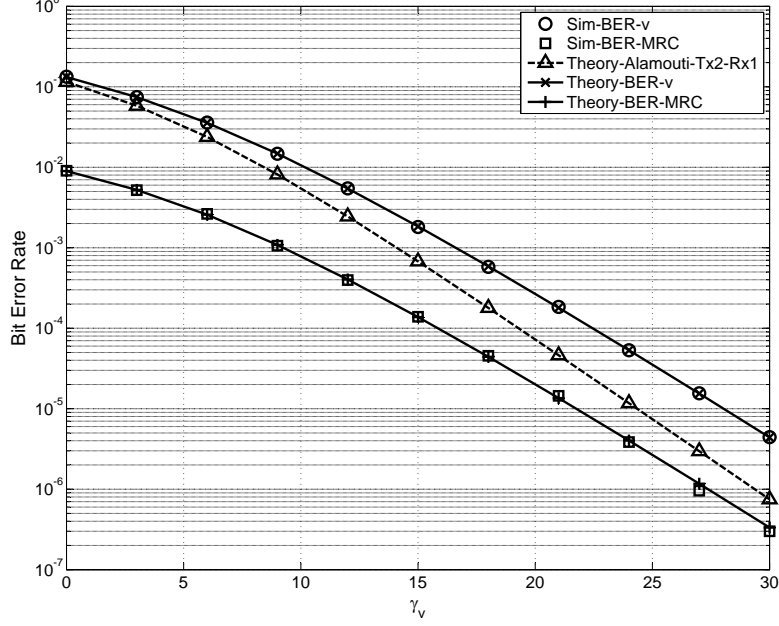
Figure 2.3. Comparison between the analytic and simulation results of the exact One-Integral BER, where $\gamma_n = 1000dB$ and $\gamma_w = 10dB$.

Alamouti's code system. This is because the data from the source to the relay still experience fading. Without noise at the Relay, the overall fading along the path of S-R-D is the multiplication of two independent Rayleigh variables.

In addition to BPSK, different modulation techniques have been considered in simulations. Fig. 2.4 shows the results in another channel condition when both BPSK and 16QAM modulation are tested. We set $\gamma_n = 15dB$, $\gamma_w = 15dB$ and vary γ_v. It needs to be noted that γ_n, γ_w and γ_v in the derivation are signal-to-noise ratios in the symbol level. However, in order to presented both modulation results in one figure, we converted all the SNR in Fig. 2.4 into SNR in the bit level (i.e., E_b/N_o). It can be noted that in terms of BER, the performance of 16QAM is worse than BPSK. However, it uses less bandwidth in communications. In this experiment, again, the simulation and analytic results match to each other perfectly. This exactly match has been observed in all our simulation scenarios with many other results not being presented here due to the space limit. These results have validated the correctness of our one-integral formula given in (19).
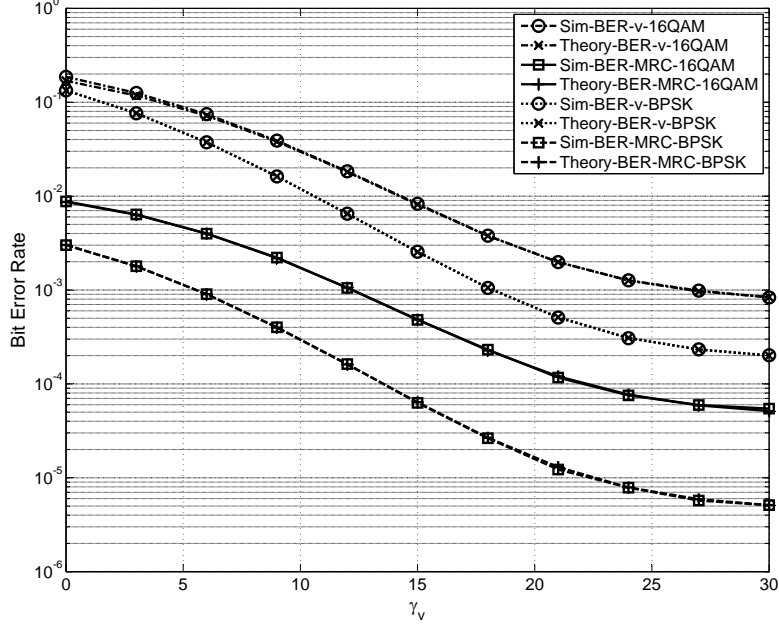
Figure 2.4. The analytic and simulation results for BPSK and 16QAM of the exact One-Integral BER, where $\gamma_n = 15dB$ and $\gamma_w = 15dB$. All SNRs are in E_b/N_o in this case.

2.3.2 The performance of series expansions of BER approximations

In this part, we evaluate the system BER performance based on some of the existing approximation methods and our proposed method. We define the approximation error function as

$$\Phi(\gamma_x) = \frac{|P_b^{appr}(\gamma_x) - P_b^{exact}(\gamma_x)|}{P_b^{exact}(\gamma_x)} \quad \text{and} \quad \overline{\Phi}(\gamma_x) = \frac{1}{\Gamma_2 - \Gamma_1} \int_{\Gamma 1}^{\Gamma_2} \Phi(\gamma_x)d\gamma_x \times 100\%. \quad (37)$$

There are three links in the considered system which are S-R, S-D, R-D. SNRs of two links will be fixed and the SNR of the third link will be changed to measure the errors. Therefore, γ_x can be either γ_n, or γ_w, or γ_v. In this test, we set $\gamma_x = \gamma_n$ and in the meantime set γ_w to 0 dB and γ_v to 15 dB. For different approximation models, (32) is used to calculate $P_b^{appr}(\gamma_x)$. $P_b^{exact}(\gamma_x)$ is obtained from the one-integral exact BER expression in (19). Γ_2 and Γ_1 are the upper and lower interval of γ_x in which we are interested in. BPSK modulation is used in this test.

Fig. 2.5 shows the BER approximation for Chiani's, Prony, and Ju's models. We can

see that Chiani's curve is farthest from the exact result of one-integral curve. Prony and Ju's models give very tight bounds at a low SNR field ($\gamma_n <= 6dB$), however, a loose bound when the channel condition becomes increasing ($\gamma_n > 6dB$).
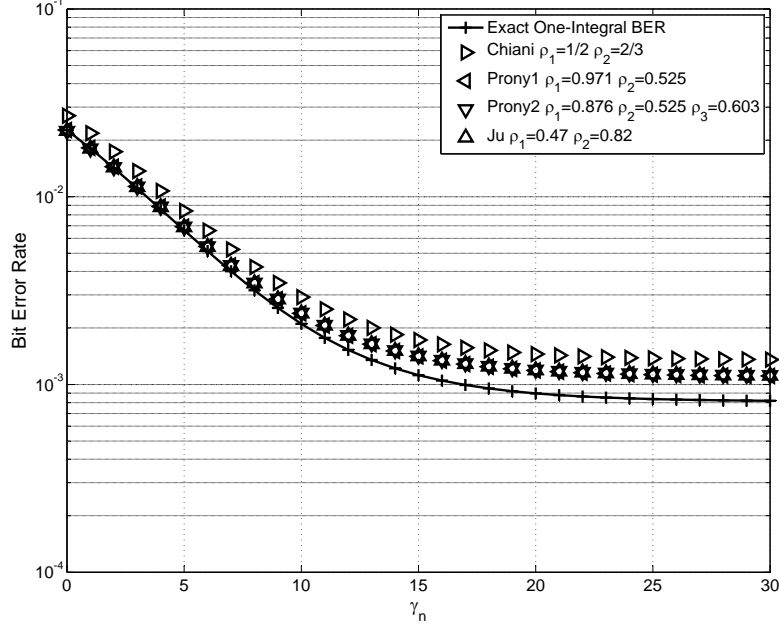
Figure 2.5. The performance of series expansions of BER approximation for Chiani,Prony, and Ju's models when γ_w=0dB and γ_v=15dB

Fig. 2.6 shows the BER of the proposed Q-function approximation. Different from the performance of Prony and Ju's methods, our proposed approximation has errors in both low and high SNR region. However, the larger the n value is used, the smaller the error compared to the actual result is obtained. In order to compare the closeness of approximation shown in the figures, the results of the error function is shown in TABLE 2.2. We divide the interested SNR range into three intervals, [0, 10dB], [10dB, 20dB] and [20dB, 30dB] and collect the cumulative error rate in each part. From this table, it can be found that Chiani's method has the overall weakest performance among existing approximations. Prony and Ju's methods have nice approximation in low SNR realm ($SNR < 6dB$). Our proposed method, when when n is increased to 32, has the best approximate in all SNR intervals among all approximation methods. It should be noted that providing BER approximation
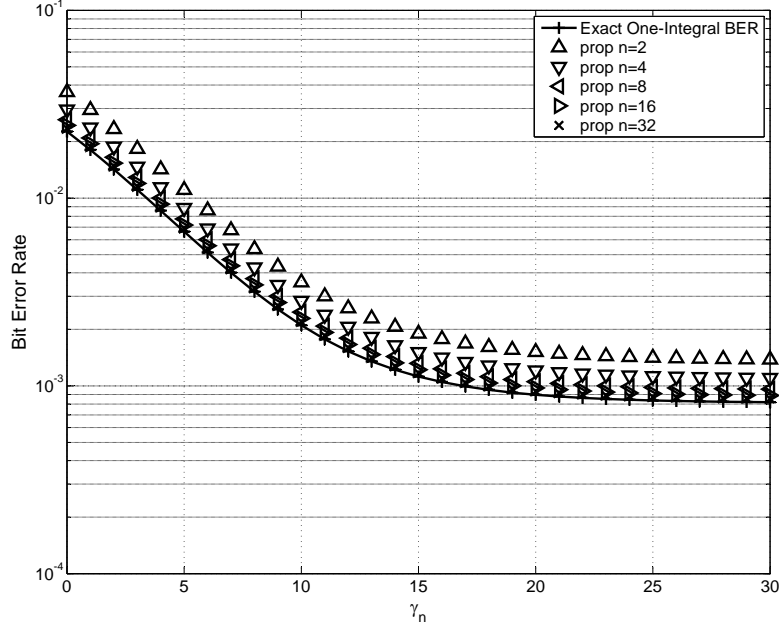
Figure 2.6. The performance of series expansions of BER approximation for proposed models when $\gamma_w=0$dB and $\gamma_v=15$dB

with small and even error in the entire SNR range is a desired feature in the performance analysis because the actual channel condition in a practical communication system may vary considerably from time to time.

Part II

DISTRIBUTED SPACE-TIME CODE WITH SOFT DECODE-AND-FORWARD (SDF) RELAYING SYSTEM

Chapter 3
BCH CODES AND TURBO BCH DECODING

3.1 BCH Codes

The Bose, Chaudhuri, and Hocquenghem (BCH) codes form a large class of powerful random error-correcting cyclic codes. This class of codes is a remarkable generalization of the Hamming codes for multiple-error correction. Binary BCH codes were discovered by Hocquenghem in 1959 and independently by Bose and Chaudhuri in 1960. For any positive integers m($m \geqslant 3$) and t ($t \leq 2^{m-1}$), there exists a binary BCH code with the following parameters:

1. Block length: $n = 2^m - 1$

2. Number of parity-check digits: $n - k \leq mt$

3. Minimum distance: $d_{min} \geq 2t + 1$.

Clearly, this code is capable of correcting any combination of t or fewer errors in a block of $n = 2^m - 1$ digits. We call this code a t-error-correcting BCH code.

In our work, each data packet is encoded with a (n,k,d) EBCH code. The EBCH code is obtained by adding the overall parity check to the conventional BCH codeword to increase the minimum Hamming distance by 1.

3.2 Chase Decoding

Since the discovery of BCH codes in 1960, numerous algorithms have been suggested for their decoding. In 1972, Chase invented a class of decoding algorithms that utilize the soft

outputs provided by the demodulator. At the receiver the demodulator provides the received signal value y_k, given that the corresponding data bit u_k was either 1 or 0, indicating two different features:

1. Its polarity shows whether u_k is likely to be 1 (positive y_k) or 0 (negative y_k)

2. Its magnitude $|y_k|$ indicates the confidence measure provided by the demodulator.

The error correcting capability t of the BCH (n, k, d_{min}) code is related to the minimum Hamming distance d_{min} between the codewords. In general, the error correcting capability, t, of the BCH code is defined as the maximum number of guaranteed correctable errors per codeword, given by:

$$t = \lfloor \frac{d_{min} - 1}{2} \rfloor,$$ (1)

where $\lfloor i \rfloor$ means the largest integer not exceeding i.
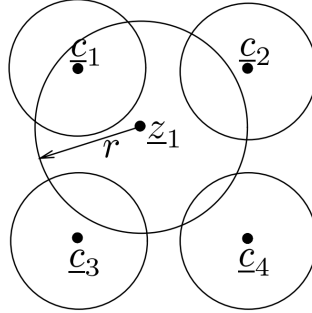
Figure 3.1. Illustration of the Chase algorithm

Figure 3.1 shows the geometric sketch of the decoding process aided by channel measurement information. Accordingly, the received binary n-tuple $\underline{z_1}$ is perturbed with the aid of a set of test patterns TP, which is a binary sequence that contains 1s in the location of the bit positions that are to be tentatively inverted. By adding this test pattern, modulo 2, to the received binary sequence, a new binary sequence $\underline{z}_1'$ is obtained:

$$\underline{z}_1' = \underline{z} \bigoplus TP.$$ (2)

As shown in Figure 3.1, r represents the maximum Hamming distance of the perturbed binary received sequence $\underline{z}_1'$ from the original binary received sequence $\underline{z}_1$. By using a number of test patterns, the perturbed received binary sequence $\underline{z}_1'$ may fall within the decoding sphere of a number of valid BCH codewords. If we increase r, the perturbed received sequence $\underline{z}_1'$ will fall within the decoding sphere of more valid BCH codewords. If the perturbed received binary sequence $\underline{z}_1'$ falls within the decoding sphere of a valid BCH codeword c_1, by invoking algebraic decoding a new error pattern e' is obtained, which may be an all-zero or a non-zero tuple. The actual error pattern $\underline{e}$ associated with the binary received sequence $\underline{z}_1$ is given by:

$$\underline{e} = \underline{e}_1' \bigoplus TP, \tag{3}$$

which may or may not be different from the original test pattern TP, depending on whether the perturbed received binary sequence $\underline{z}_1'$ falls into the decoding sphere of a valid codeword. However, only those perturbed received binary sequences $\underline{z}_1'$ that fall into the decoding sphere of a valid codeword are considered. A maximum likelihood decoder is capable of finding the codeword that satisfies:

$$minweight(\underline{z} \bigoplus c_m), \tag{4}$$

where the range of m is over all possible codewords. Based on similar principles, Chase defined a new channel decoder. However, for the sake of low complexity only a certain limited set of valid codewords is considered by Chase's technique, namely those surrounded by the decoding spheres that the perturbed received binary sequence $\underline{z}_1'$ may fall into. In this case, we are concerned with finding the error pattern $\underline{e}$ of minimum analogue weight, where the analogue weight of an error sequence $\underline{e}$ is defined as:

$$W(\underline{e}) = \sum_{i=1}^{n} e_i |y_i|, \tag{5}$$

43

The Chase algorithm can be summarized in the flowchart shown in Figure 3.2. Each time, the algorithm considers an n-tuple codeword of the BCH code, which is constituted by n number of the received bits $\underline{z}$ and their soft metrics $\underline{y}$. The received bits $\underline{z}$ and their confidence values $\underline{y}$ are assembled, which is the first step shown in Figure 3.2. Then, a set of test patterns TP is generated. For each test pattern, a new sequence $\underline{z}'$ is obtained by modulo-2 addition of the particular test pattern TP and the received sequence $\underline{z}$. The conventional algebraic decoder is invoked to decode the new sequence $\underline{z}'$. If the conventional algebraic decoder found a non-zero error pattern $\underline{e}'$, we are able to find the actual error pattern $\underline{e}$, using Equation (3), associated with the received binary sequence $\underline{z}$. Using Equation (5), the analogue weight W of the actual error pattern $\underline{e}$ can be calculated. The generated test pattern TP will be stored in the memory, if the associated analogue weight W is found to be the lowest. The above procedure will be repeated for every test pattern generated. Upon completing the loop in Figure 3.2, the memory is checked. If there is an error pattern stored, the binary decoded sequence will be $\underline{z} \bigoplus \underline{e}$. Otherwise, the binary decoded sequence is the same as the received sequence $\underline{z}$.

3.3   Product Code and Parallel Concatenated Code

Parallel concatenated codes constitute specific product codes. In general, product codes consist of two linear block codes C_1 and C_2 where C_1 and C_2 have parameters (n_1, k_1, d_{min1}) and (n_2, k_2, d_{min2}), respectively. Typically, $C_1 = C_2$. As shown in Figure 3.3, product codes are obtained by placing the $k_1 \times k_2$ information data bits in an array of k_1 columns and k_2 rows. The k_1 columns and k_2 rows of the information data bits are encoded using C_1 and C_2, respectively. It is shown that the $(n_1 - k_1)$ last columns of Figure 3.3 are codewords of C_2, exactly as the $(n_2 - k_2)$ last rows are codewords of C_1 by construction. Furthermore, the parameters of the resulting product codes are given by $n = n_1 \times n_2$, $k = k_1 \times k_2$ and $d_{min} = d_{min1} \times d_{min2}$, while the code rate is given by $\frac{k_1}{n_1} \times \frac{k_2}{n_2}$. The structure of parallel concatenated codes is the same as that of product codes, except that the redundancy part
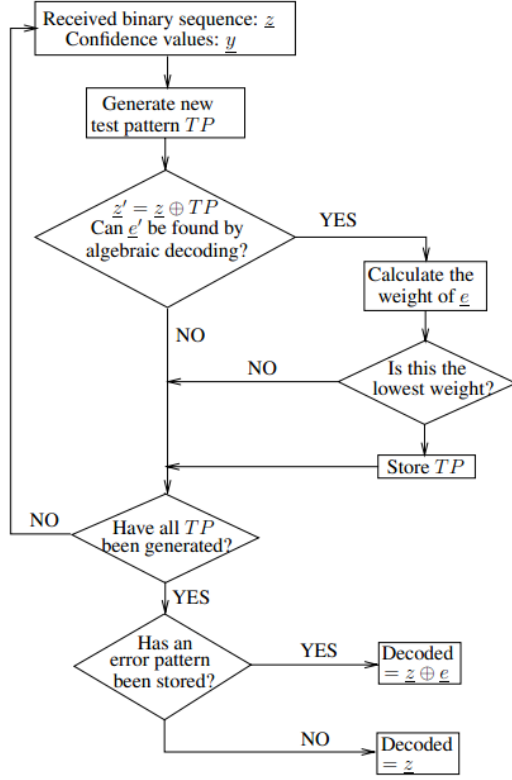
Figure 3.2. Flow chart of the Chase algorithm

arising from checking the parity of the parity part of both codes C_1 and C_2 is omitted. The major disadvantage of parallel concatenated codes is the loss in minimum free distance, which is only $d_{min1} + d_{min2} - 1$, compared to $d_{min1} \times d_{min2}$ in product codes[37].

3.4 Turbo Decoding

The turbo decoding process of BCH codes is shown in Fig. 3.4. The decoder uses the soft channel output $L_c y$ and the intrinsic information $L(u_k)$ to provide the *a-posteriori* information $L(u_k|y)$ at its output, as shown in Fig. 3.4. The extrinsic information, $L_e(u_k)$ is given by subtracting the soft channel output $L_c y$ and the intrinsic information $L(u_k)$ from the *a-posteriori* information $L(u_k|y)$. After being interleaved or de-interleaved, as seen in the figure, the extrinsic information $L_e(u_k)$ becomes the intrinsic information $L(u_k)$ of the second decoder. Similarly, the extrinsic information gained by the second decoder is passed

45

(a) Product Code   (b) Parallel Concatenated Code
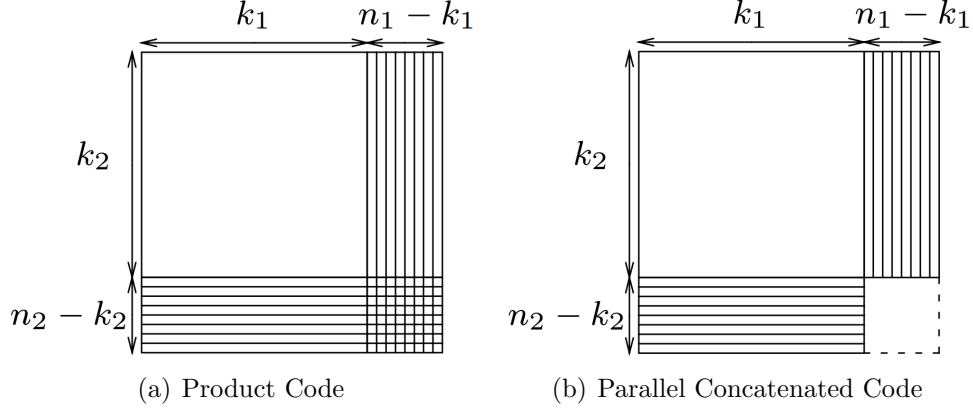
Figure 3.3. Construction of product codes and parallel concatenated codes.

back to the first decoder as its intrinsic information. Basically, both decoders assist each other by exchanging their information related to the data bits and this results in the iterative decoding process. However, there is no intrinsic information for the first decoder in the first iteration, since the extrinsic information of the other decoder is unavailable at this stage.

z :Received samples
u_k :Decoded Databits
$L_c y_k$:Demodulator's soft output
$L(u_k)$:Intrinsic Information
$L_e(u_k)$:Extrinsic Information
$L(u_k|y)$:A Posteriori Information
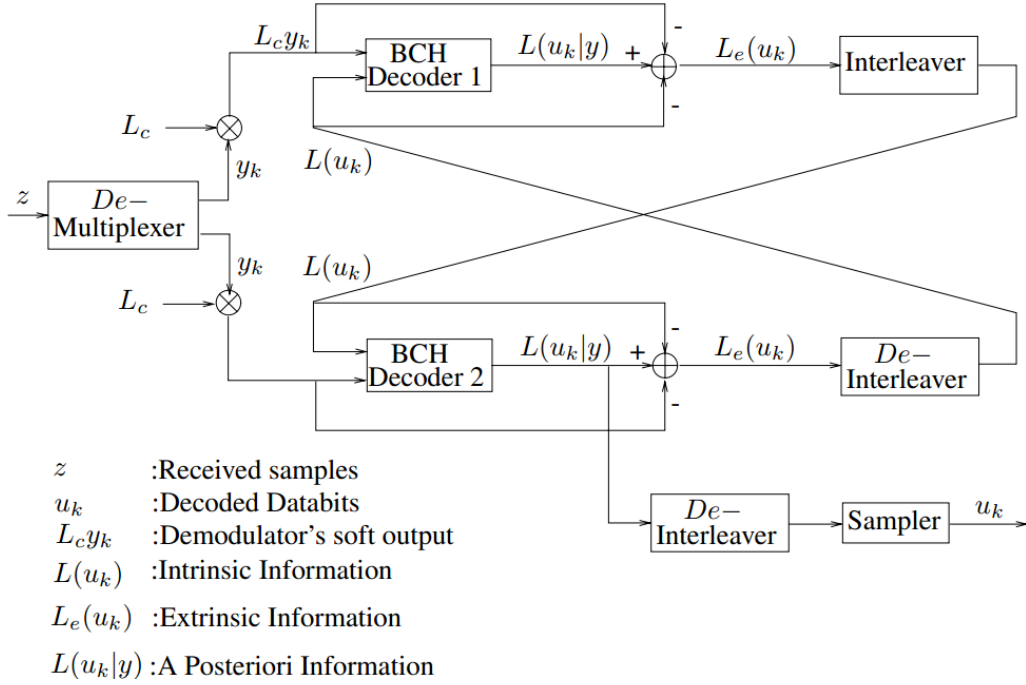
Figure 3.4. Turbo decoder schematic

46

Chapter 4

SOFT DECODE-AND-FORWARD (SDF) RELAYING STRATEGY

4.1 Comparison between AF, DF and SDF

User cooperation involves the introduction of one or multiple cooperating nodes, known as the relays, into the classic point-to-point communication scheme. This technique improves a better communication efficiency as well as the performance of a whole wireless communications system. Despite numerous advances in wireless cooperative cooperation systems, signal relaying strategies widely applied have not evolved much out of the amplify-and-forward (AF) and decode-and-forward (DF).

The amplify-and-forward lets relays scale, retransmit the analog signal waveforms received from the source[92,46,24]. It has a low implementation complexity but with a drawback of amplifying the noise as well. Based on whether the threshold detection is used at relays or not, AF can be further classified as the regenerative[98,81,8] or the non-regenerative[45,3,7]. The application of AF is straight-forward, requiring a lower implementation complexity in signal processing than the other two strategies.

The decode-and-forward constitutes another celebrated practice of signal relaying, where the coded source signals received at the relay are demodulated, decoded and possibly re-encoded using a different code before being forwarded to the destination. Depending on the type of codes used to re-generate the relay message, the DF extends from its basic mode

of repetition[54], to more sophisticated modes that exploit space time codes[53,47] and network codes[10].

In general, AF can operate even when the soure-relay channel experiences outage where the signals are corrupted by the channel fading and other impairments to a level that prohibits the relay from correctly deducing all the data. In DF, however, the erroneous bits, if re-encoded and forwarded to the destination, can mislead the destination and cause severe error propagation. When the source-relay channel quality is sufficient for a clean extraction of the data, DF clearly performs better since it regenerates and passes on a clean set of signals[9]. This protocol may eliminate the noise effect between the source and the relays if the data can be correctly decoded. However, when perfect decoding cannot be guaranteed, relaying erroneously decoded data would cause a severe error propagation at the receiver.

Another signal forwarding strategy, soft-decode-and-forward (SDF), was also proposed[87]. SDF aims to combine the best features of AF and DF: soft signal representation in AF and channel coding gain in DF. In the SDF protocol, the relays demodulate the received signal from the source, soft-decode and re-encode to obtain the soft-information possibly with a different code and then relay this information to the destination. This soft-information represents the reliability for the coded data at the relay and can be transmitted either via direct analog modulation or via digital modulation over the quantized values.

Comparing with AF and DF, SDF has its own advantages. On the first hand, when channel quality is insufficient, the soft-information is weak and the system has a similar performance as AF which can be treated as forwarding the signals in their soft reliability form. On the other hand, when the relays correctly decode the received information, the normalized soft information which is the output of SDF based relay approaches a clean set of signals which is the same as the output of DF based relays. Due to these advantages, SDF has a best performance among these three relaying strategies.

Hoshyar et al.[41] applies SDF strategy to higher order MQAM modulation and showed the improvement of the overall system spectrum efficiency. Li et al.[62] studied the distributed

turbo coding in a two-hop relay system with SDF at the relay. They derived the average upper bound on the bit-error rate (BER) at high SNR by using Harmonic mean and weight enumerating function (WEF). Bao et. al.[9] compared different relaying strategies of AF, DF and SDF over BI-AWGN channels. They gave formulas in the information-theoretic achievable rate for each scheme and made a conclusion that the SDF system combined with coded cooperation are capable of considerably better performances than the existing schemes by both analysis and simulations.

Despite many interesting results in SDF, existing schemes consider the transmission in two time phases where in the second time phase, the relay sends the soft information while the source is idling. In fact, the source can actually send the hard information in the second time phase to cooperate with the soft information sent by the relay, which provides diversity in fading environment. To the best of our knowledge, the integration of the SDF protocol with the distributed space-time block codes (DSTBC) to improve the system performance has not been considered previously, which is a common missing part in SDF-based cooperative systems.

In our recent work[76], we have initiated the study of the use of DSTBC with SDF. We have demonstrated via the Monte-Carlo simulations that one-relay SDF & DSTBC system has better performance compared with the traditional SDF systems where DSTBC is not used. However, there is not any analysis work and insights of the performance improvement having been provided in[76]. It can be envisioned that in the 2nd time phase, the source and the relay can coordinately send their information to the destination using DSTBC. The source forwards the error free information of some parity bits while, in the meantime, the relay transmits the soft information to the destination. This is different from the classic space-time codes where both transmit nodes send error-free information of the same symbol sequence. Although transmit diversity can be explored in DSTBC, the source-destination channel is usually much worse than the relay channel. Therefore, one natural question is whether and to what extent the distributed Space-Time codes can enhance the SDF

49

communications. In addition, the overall transmit power in general should be fixed, another question then is how the power will be allocated between the source and the relay nodes to achieve the best enhancement. The contribution of this dissertation is the answers to these questions. Specifically, we give a theoretic result of the DSTBC performance in the second time phase based on the Gaussian approximation of the soft information at the relay. Although this one-relay SDF system with DSTBC enhancement could be applied to any coded cooperative system, we adopt the DTPC with EBCH component codes in this research as an example.

Furthermore, we propose a system with two relays which adopts SDF with DSTBC as well. We have theoretically derived the DSTBC performance in the second time phase based on the Gaussian approximation of the soft information at the relay. We also compared this two-relay SDF & DSTBC system with one-relay SDF & DSTBC cooperative system and one-relay system with SDF relaying alone. All systems adopt Distributed Turbo Product Codes and Space-Time block codes, where the Extended Bose Chaudhuri Hochquenghem (EBCH) codes are used as component codes.

- **1. One-relay SDF system**

    We have one source, one relay and one destination in this system. This reference system uses traditional SDF at relay. The source keeps idle when the relay transmits LLR in the second time phase.

- **2. One-relay SDF & DSTBC system**

    This system has one source, one relay and one destination as well. The source and the relay can cooperatively send their information to the destination using Space-Time codes. It fully explores the functionality of the source, instead of keeping it idle as in the one-relay SDF system. We approximate the soft information transmitted by relay using Gaussian approximation and evaluate the averaged BER after the Space-time decoding.

- **3. Two-relay SDF & DSTBC system**

  The two-relay SDF & DSTBC system considers a scenario where the source node transmits information to the destination via two relay nodes. SDF is used in the relays, however, assuming the availability of synchronization between relays. The soft information from different relays will be transmitted cooperatively with Alamouti's code to the destination. We assume that the soft information, i.e., the log-likelihood ratio (LLR) values after a channel decoder at each relay, follows an approximated Gaussian distribution.

4.2 Soft Decoding/Re-encoding at the Relay

In general, block encoding takes a k-bits information word, and generates a n-bits codeword. Furthermore, systematic block codes are constructed by appending the $n - k$ parity bits to the end of the k-bits input information word. The complete product codes are formed by serial concatenating the two systematic linear block codes $\mathcal{C}^1$ and $\mathcal{C}^2$ and having an intermediate matrix interleaver. The two component codes $\mathcal{C}^1$ and $\mathcal{C}^2$ are assumed to be identical and have parameters (n, k, δ), where n, k, and δ stand for code length, code dimension and minimum Hamming distance of the code, respectively.

The operation at the relay is carried out in three steps: First, the relay soft-decodes the received sequences and generate the LLR output for the decision bits. Then the LLR values are used to infer the LLR values of the vertical parity bits. Finally, the soft output for the parity bits is obtained and ready to forward cooperatively with the source to the destination in the second time slot.

Let the transmitted $k \times n$ matrix of BPSK modulated symbols from the source be expressed as:

$$\mathbf{X} = [\overline{\mathbf{x}}_1, \overline{\mathbf{x}}_2, \overline{\mathbf{x}}_3, \cdots, \overline{\mathbf{x}}_k]^T, \tag{1}$$

where $\overline{\mathbf{x}}_i = [x_i^1, x_i^2, x_i^3, \cdots, x_i^n]$ is a codeword of n bits. The superscript 'T' stands for the

vector's transpose. Also, let the output of the inter-user channel at the relay be written as:

$$\mathbf{Y} = [\overline{\mathbf{y}}_1, \overline{\mathbf{y}}_2, \overline{\mathbf{y}}_3, \cdots, \overline{\mathbf{y}}_k]^T,$$

where $\overline{\mathbf{y}}_i = [y_i^1, y_i^2, y_i^3, \cdots, y_i^n]$, $y_i^j = h\dot{x}_i^j + z_i^j$, $1 \leq i \leq k$, $1 \leq j \leq n$. $z_i^j \sim \mathcal{CN}(0, \sigma_z^2)$ and $h \sim \mathcal{CN}(0, \Omega)$ are the noise and fading of the inter-user channel.

Upon the receiving of sources transmission at the relay, Chase II decoding algorithm is used to decode the received matrix $\mathbf{Y}$ to get the ML decision $\mathbf{D}$ (matrix of dimension $n \times k$), where

$$\mathbf{D} = [\overline{\mathbf{d}}_1, \overline{\mathbf{d}}_2, \overline{\mathbf{d}}_3, \cdots, \overline{\mathbf{d}}_k]^T,$$

and $\overline{\mathbf{d}}_i = [d_i^1, d_i^2, d_i^3, \cdots, d_i^n]$, with $d_i^j \in \{-1, +1\}$. Chase II algorithm searches for the decision codeword $\overline{\mathbf{d}}_i$ with the minimum Euclidean distance from the received vector $\overline{\mathbf{y}}_i$.

The first step in obtaining the soft parity bits is to find the LLR of the decoded bits in the matrix $\mathbf{D}$. The normalized extrinsic output of the decoder for jth bit in the ith input vector can be expressed in terms of LLR of the decision as:

$$w_i^j = \frac{\sigma^2}{2} L(d_i^j) - y_i^j, \tag{2}$$

where

$$L(d_i^j) = \ln \left(\frac{P(x_i^j = +1 | \overline{\mathbf{y}}_i)}{P(x_i^j = -1 | \overline{\mathbf{y}}_i)} \right),$$

is the LLR of transmitted bit x_i^j given the received sequence $\overline{\mathbf{y}}_i$, d_i^j is the decoder decision.

Once a decision codeword $\overline{\mathbf{d}}_i$ is found, the decision confidence value ϕ_i will be evaluated. The confidence value is defined as the probability that the decoder makes a correct decision given the received sequence $\overline{\mathbf{y}}_i$. The value ϕ_i is defined in 3 as a function of destructive

Euclidean distance between the received vector and the decision codeword[56]:

$$\phi_i = f\left(\sum_{j\in\{j|(y_i^j-d_i^j).d_i^j<0\}}(y_i^j-d_i^j)^2\right), 1\le i\le k. \tag{3}$$

where the function $f(\cdot)$ is pre-defined by a lookup table to reduce the computational complexity of the implementation.

Using the DBD soft-decoding method proposed in[56] and rewriting the LLR in terms of the normalized extrinsic information and channel output, the LLR of decoder output bit d_i^j is:

$$L(d_i^j) = d_i^j \ln\left(\frac{\phi_i + \exp(2y_i^j d_i^j/\sigma^2)}{1-\phi_i}\right). \tag{4}$$

It was found in[35] that the LLR of a parity bit for two statically independent random bits u_1 and u_2 can be obtained as:

$$L(u_1 \oplus u_2) = \log\frac{1 + e^{L(u_1)}e^{L(u_2)}}{e^{L(u_1)} + e^{L(u_2)}}$$
$$\approx \text{sign}(L(u_1)\cdot L(u_2))\cdot\min(|L(u_1)|,|L(u_2)|). \tag{5}$$

Using induction, this relation can be generalized to k bits. Assuming that $u_{\mathcal{X}}$ is the parity bit for a set of bits $\mathcal{X}\in\{u_1,u_2,\cdots,u_k\}$, which can be expressed as:

$$u_{\mathcal{X}} = \sum_{u_i\in\mathcal{X}}^{\oplus} u_i,$$

then the LLR of bit $u_\mathcal{X}$ given the LLR of set $\mathcal{X}$ is obtained as:

$$
\begin{aligned}
L(u_\mathcal{X}) &= L\left(\sum_{u_i \in \mathcal{X}} \oplus\, u_i\right) \\
&= \log \frac{\prod\limits_{u_i \in \mathcal{X}} \left(e^{L(u_i)} + 1\right) + \prod\limits_{u_i \in \mathcal{X}} \left(e^{L(u_i)} - 1\right)}{\prod\limits_{u_i \in \mathcal{X}} \left(e^{L(u_i)} + 1\right) - \prod\limits_{u_i \in \mathcal{X}} \left(e^{L(u_i)} - 1\right)} \\
&= 2 \cdot \tanh^{-1}\left(\prod_{u_i \in \mathcal{X}} \tanh(L(u_i)/2)\right) \\
&\approx \operatorname{sign}\left(\prod_{u_i \in \mathcal{X}} L(u_i)\right) \cdot \min_{u_i \in \mathcal{X}} |L(u_i)|.
\end{aligned}
\tag{6}
$$

where the third equality follows from using the two following relations:

$$
\tanh(u/2) = \frac{e^u - 1}{e^u + 1}, \qquad 2\tanh^{-1}(u) = \log \frac{1+u}{1-u}.
$$

Parity bits for a linear block code can be obtained using the generator matrix for this code. A linear code generator matrix is any matrix whose rows are the bases of the code space. The relay uses a EBCH code generator matrix in systematic form as $\mathbf{G} = [\mathbf{I}_k | \mathbf{P}]$ to generate the vertical parity P_v, where $\mathbf{I}_k$ is the identity matrix of rank k, $\mathbf{P} = [\bar{\mathbf{p}}_{k+1}, \bar{\mathbf{p}}_{k+2}, \cdots, \bar{\mathbf{p}}_{n-1}]$ is a $k \times (n-k-1)$ matrix responsible for generating the $n-k-1$ parity bits for the information bits, where $\bar{\mathbf{p}}_i$ is a k-bits vector in GF(2). The n-th parity bit in the EBCH codeword (the overall parity bit) is generated such that the overall number of 1's in the codeword is odd.

At the relay we are only interested in generating the vertical parity bits P_v for the decoded matrix from the received matrix over the inter-user channel. The decoded matrix $\mathbf{D}$, which is composed of estimates of S and P_h, is considered as systematic information at the relay. Therefore, P_v can be obtained by performing the matrix multiplication $\mathbf{DG}$. Let $\mathbf{E}$ $(n \times n)$

be the result from EBCH encoding of the decoded matrix $\mathbf{D}$:

$$
\begin{aligned}
\mathbf{E} &= [\mathbf{DG}|\ \bar{\mathbf{e}}_n] \\
&= [\mathbf{DI}_k|\mathbf{DP}|\ \bar{\mathbf{e}}_n] \\
&= [\mathbf{D}\ \ |\mathbf{DP}|\ \bar{\mathbf{e}}_n] \\
&= [\bar{\mathbf{e}}_1, \bar{\mathbf{e}}_2, \bar{\mathbf{e}}_3, \cdots, \bar{\mathbf{e}}_k, \bar{\mathbf{e}}_{k+1}, \cdots, \bar{\mathbf{e}}_{n-1}, \bar{\mathbf{e}}_n].
\end{aligned}
\tag{7}
$$

where the last column $\bar{\mathbf{e}}_{\mathbf{n}}$ contains the overall parity bits.

The resulting matrix $\mathbf{E}$ is composed of two parts, the systematic and the parity parts, $\mathbf{E_s} = [\bar{\mathbf{e}}_1, \bar{\mathbf{e}}_2, \bar{\mathbf{e}}_3, \cdots, \bar{\mathbf{e}}_k] = [\overline{\mathbf{d}}_1, \overline{\mathbf{d}}_2, \overline{\mathbf{d}}_3, \cdots, \overline{\mathbf{d}}_k] = \mathbf{D}$ and $\mathbf{E_p} = [\bar{\mathbf{e}}_{k+1}, \cdots, \bar{\mathbf{e}}_{n-1}, , \bar{\mathbf{e}}_n]$ respectively, where $\bar{\mathbf{e}}_i = [e_i^1, e_i^2, \cdots, e_i^n]^T$ is n-bits vector. The latter, which we refer to as the estimate of the vertical parity $(\hat{P}_v)$, is transmitted as soft information to the destination. To obtain the soft information for the generated parity $\mathbf{E_p}$ we use the result in[36]. The LLR for the parity bit e_i^j, $k + 1 \leq i \leq n - 1, 1 \leq j \leq n$ is given by:

$$
\begin{aligned}
L(e_i^j) &= L\left(\bar{\mathbf{p}}_i^T \overline{\mathbf{d}}^j\right) \\
&= L\left(\sum_{l \in \mathcal{X}_i} \oplus\ d_l^j\right), \mathcal{X}_i = \{l | p_i^l = 1\} \\
&\approx \operatorname{sign}\left(\prod_{l \in \mathcal{X}_i} L(d_l^j)\right) \cdot \min_{l \in \mathcal{X}_i} \left|L(d_l^j)\right|,
\end{aligned}
\tag{8}
$$

where $\overline{\mathbf{d}}^j$ is the jth row in $\mathbf{D}$, $\mathcal{X}_i$ refers to the set of indices in which the vector $\bar{\mathbf{p}}_i$ has 1's. The values of $L(d_l^j), l \in \mathcal{X}_i$ are found from[74]. The LLR of the last column of $\mathbf{E}$, i.e. $\bar{\mathbf{e}}_n$, that is composed of rows' overall parity bits, is obtained by setting $\mathcal{X}_n = \{1, 2, 3, \cdots, n - 1\}$ in eqn. (8).

Chapter 5
GAUSSIAN APPROXIMATION ON LLR MESSAGES

In Chapter 4, we have illustrated the way from which relays get the LLR values. It soft decodes the received sequences and obtain the LLR values from the Chase-II decoder. The relay then re-encodes the obtained outputs in another (vertical) direction, and gets the log-likelihood ratios of the vertical parity bits (P_v). Instead of making binary hard decisions based on soft values, the relay amplifies and forwards the LLR values directly to the destination using Amplitude Modulation techniques. With this simple extension, i.e., forwarding soft LLRs in lieu of hard encoder decisions, SDF combines the best feature of AF: forwarding the signals in their soft reliability forms, with the advantage of DF: exploiting the coding gain in the entire source-relay SNR region.

To better understand SDF, let us take a closer examination of the LLR values by using the Gaussian approximation[22]. The Gaussian assumption states that, for an infinite length or very long code with a soft message-passing decoder, if the channel-LLRs at the input to the decoder are independent and identically Gaussian distributed, then the output LLRs from the decoder will follow an approximated Gaussian distribution[9].

The Gaussian Approximation (GA) approach was proposed by Richardson et. al.[22] to analyze the LLR values for iterative decoding in low-density parity-check (LDPC) codes. They presented a simple method to estimate the threshold for irregular LDPC codes on memoryless binary-input continuous-output AWGN channels with sum-product decoding. They adopted density evolution to calculate the thresholds of message-passing decoding and this method is based on approximating message densities as Gaussians (for regular LDPC codes) or Gaussian mixtures (for irregular LDPC codes).

They stated that the LLR message from the channel is Gaussian with mean $2/\sigma_n^2$ and variance $4/\sigma_n^2$, where σ_n^2 is the variance of the channel noise. Thus, if all inputs (which are independent and identically distributed (i.i.d.)) are Gaussian, then the resulting sum is also Gaussian because it is the sum of independent Gaussian random variables.

They also illustrated that even if the inputs are not Gaussian, by the central limit theorem, the sum would look like a Gaussian if many independent random variables are added.

Based on Richardson's work, a LDPC-coded miltiple-input-multiple-output (MIMO) system with STBC was studied by Tan et. al.[93]. They approximated the pdfs of incoming LLR at bit nodes in the decoder by GA which were used to calculate the output LLR afterwards.

Later, the GA approach was applied in turbo decoder by Gamal and Hammons[28], because the extrinsic information from constituent maximum a posteriori (MAP) decoders can be well approximated as Gaussian random variables as well.

5.1   Gaussian Approximation on LLRs of Turbo codes

The modern decoding algorithms for channel codes, including the sum-product algorithm for low-density parity-check (LDPC) codes and the maximum *a-posteriori* probability (MAP) algorithm for turbo codes, all use the belief propagation and can be collectively called the message-passing algorithms. The soft output of the decoder, represented as the LLR values, can be seen as the result of the sum effect of independent random variables. By GA stated above, these values approach to a Gaussian distribution.

The Gaussian approximation also applies to the situation of fading channels. It has been stated by Richardson[22] that even if the inputs are not Gaussian, by the central limit theorem, the sum would look like a Gaussian if many independent random variables are added. It also has been shown in Eqn. (16) of[93] that, for wireless channels which experience fading, the LLR messages can be approximated to be Gaussian distributed.

To illustrate, we transmit the source information coded by a turbo code with the generator $[7, 5]_{oct}$ to the relays through a fast Rayleigh fading channel and then obtain the LLR

values with the MAP decoding. Monte-Carlo simulations have been taken by changing the source to relay channel condition from 2 dB, 6 dB to 10 dB. Then the LLR histograms are shown in Fig. 5.1 with the dot, "x" and "+" marks, respectively. It can be noted that these histograms match very well with the three solid curves drawn from the Gaussian distribution with the mean and variance calculated directly from the LLR values.
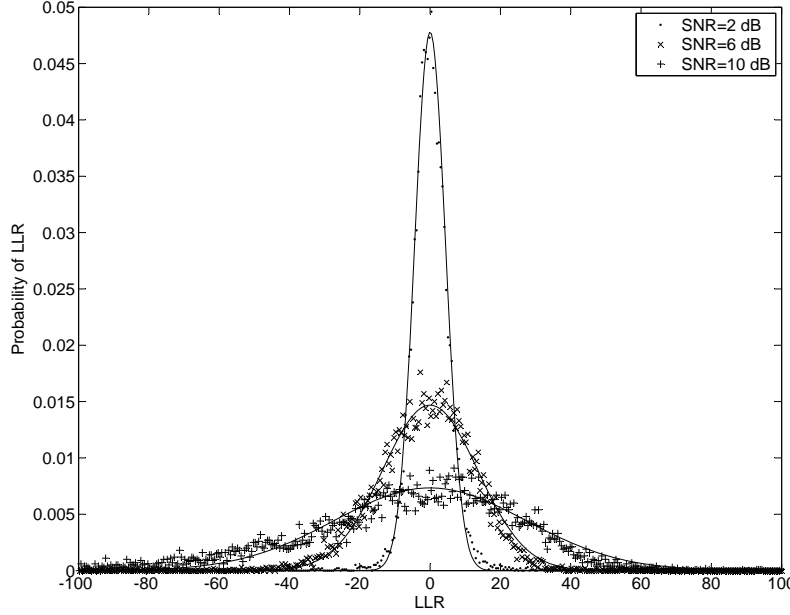
Figure 5.1. The distribution of LLR in turbo codes after MAP decoding through fast Rayleigh fading channel.

A second experiment is shown as in Fig. 5.2 for a verification of LLRs distribution when CSI information is available and not at the receiver. The wireless channels also experience fast Rayleigh fading as in the previous experiment and turbo codes $[7, 5]_{oct}$ is used as well. We transmit coded frames via a wireless channel with $SNR = 6$dB. The sequences are obtained at the receiver and it will then be passed through a MAP decoder and we analyze the distribution of LLRs at the output. The LLRs are normalized to the mean value and the "+" and "x" marks show the LLR histograms when the channel state information (CSI) are either available or unavailable at the receiver respectively. It can be noted that these histograms match very well too with the solid and dash curves drawn from the Gaussian

distribution with the mean and variance calculated directly from the LLR values.
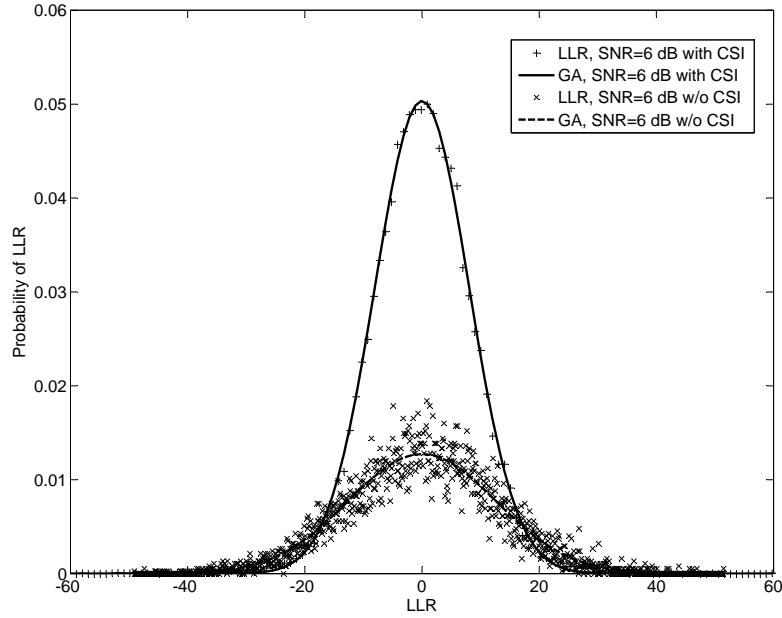
Figure 5.2. The distribution of LLR in turbo codes after MAP decoding through fast Rayleigh fading channel when CSI is either available or unavailable.

5.2 Gaussian Approximation on LLRs of EBCH codes

We adopt EBCH code (as stated in Section 3.1) as the component code to transmit information from the source to relay(s). After having received the coded frame, the relay(s) pass(es) it through a Chase decoder to infer the LLR messages. The Chase decoding algorithm can be seen as a message-passing algorithms as well since the *a posteriori* information is calculated by the received symbol of certain time slot combined with symbols of other time slots within the same coded frame. Therefore, the soft output of the Chase decoder, represented as the LLR values, can be seen as the result of the sum effect of independent random variables. By GA stated above, these values approach to a Gaussian distribution.

We verify the output of the Chase decoder by using two Monte-Carlo simulations. In our first experiment, we transmit the source information coded by a EBCH code with ($n = 64, k = 51, \delta = 6$) where the k, n and δ represent the source bit length, codeword length and the free distance of the code, respectively. The wireless channel is a theoretic AWGN

channel and we obtain the LLR values after the Chase II decoding. Fig. 5.3 shows the LLR distribution when the wireless channel SNR is 3dB. The histogram overlap with the solid curve drawn from the Gaussian distribution with the mean and variance calculated directly from the LLR values. This indicates that the LLR values can be accurately approximated by Gaussian distributed random variables.
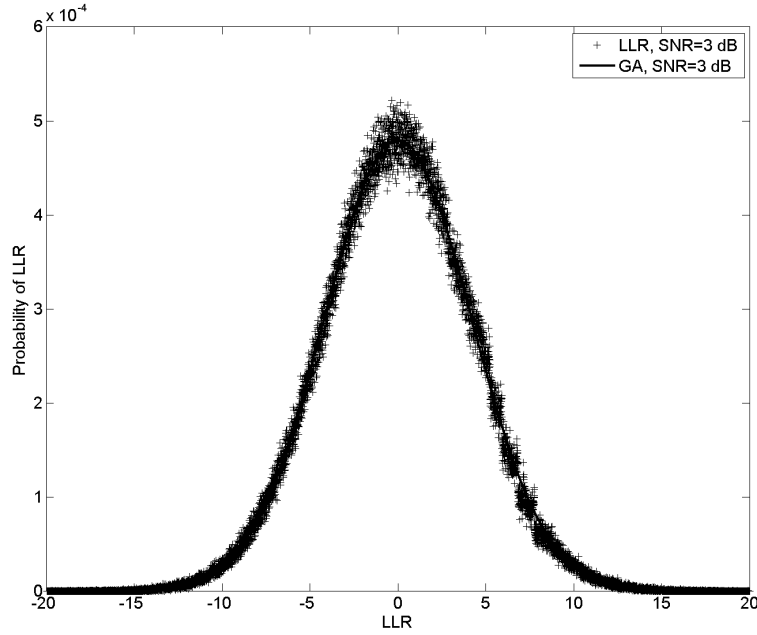
Figure 5.3. The distribution of LLR in EBCH codes after Chase II decoding through AWGN channel.

When the wireless channel experiences Rayleigh fading, the symbols received at the relay are not Gaussian. However, since the LLR value for each symbol can be seen as the sum of information symbols, from the central limit theorem, the distribution of output values would look like Gaussian as well. The second experiment is shown under the Rayleigh fading channel when the wireless channel SNR is 3dB as well. Fig. 5.4 shows the LLR distribution and it is near Gaussian. For the convenience of calculation, we check the confidence value ϕ by look-up table. Due to this approximation, our result in Fig. 5.4 approaches Gaussian approximation curve only when LLR value is bigger than -2.
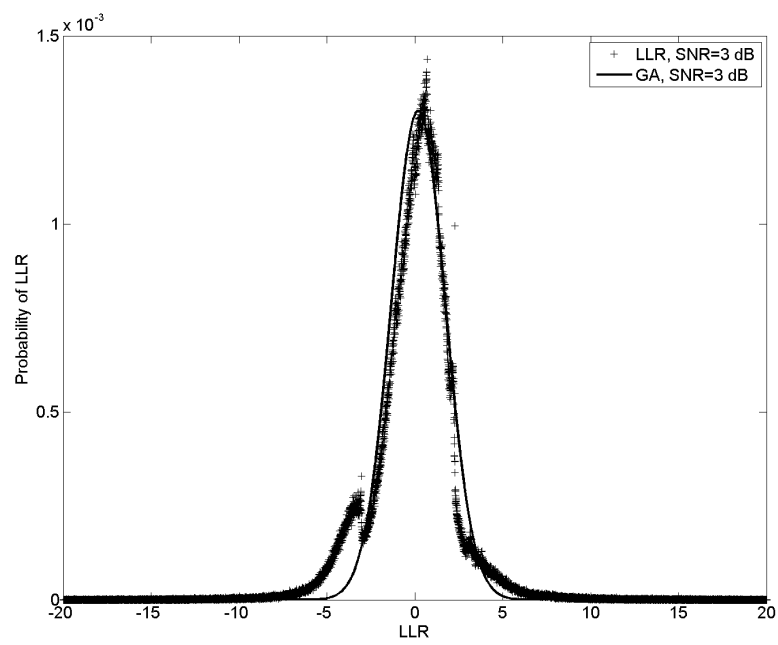
Figure 5.4. The distribution of LLR in EBCH codes after Chase II decoding through fast Rayleigh fading channel.

Chapter 6
DISTRIBUTED SPACE-TIME CODE ENHANCED SOFT DECODE-AND-FORWARD (SDF) RELAYING SYSTEM WITH ONE RELAY

6.1 System Model

We consider a three-node-network consisting of one source 's', one destination 'd' and one relay 'r'. Any transmission from the source to the destination requires two time phases. The channels between the three nodes are assumed to be mutually independent with Rayleigh fading coefficients. We denote the link between the source and the relay, the source and the destination, and the relay and the destination, as inter-user link, direct link and relay link, respectively. We use h, h_1, and h_2 to represent the channel attenuations for each channel and they follow $h \sim \mathcal{CN}(0, \Omega)$, $h_1 \sim \mathcal{CN}(0, \Omega_1)$ and $h_2 \sim \mathcal{CN}(0, \Omega_2)$. Assume all noises at the receivers are white Gaussian noises and we denote σ_z^2 and σ_w^2 to be the noise variances at the relay and destination in the first time phase and σ_v^2 to be the noise variance at the destination in the second time phase.

As shown in Fig. 6.1, the information bits are formed into a $k_1 \times k_2$ matrix S. The complete product codes are formed by serial concatenating two systematic linear block codes $\mathcal{C}^1$ and $\mathcal{C}^2$ with a block interleaver. The two component codes $\mathcal{C}^1$ and $\mathcal{C}^2$ are assumed to be identical here. Each data packet is encoded with a (n, k, δ) EBCH code to produce rows parity P_h. The EBCH code is obtained by adding the overall parity check to the conventional BCH codeword to increase the minimum Hamming distance by 1. The output $k \times n$ matrix of bits are broadcasted from the source to the relay and the destination in the first time phase. The relay uses a SISO decoder with Chase-II algorithm to obtain the LLR values
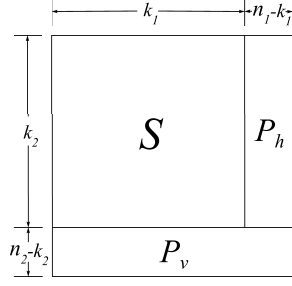
Figure 6.1. Structure of a complete Turbo Product Code as received at the destination

of the decoded codewords for the received sequences. The LLR values are further used to obtain the soft information for the vertical parity bits P_v through the other EBCH encode.

This soft information at the relay can be seen as a soft copy of parity bits P_v that can be generated at the source. Since both the source and the relay have the information for the same parity bits, we can use Alamouti's code[6] to coordinately send the information in the second time phase. It should be noted that the information radiated from the source and relay is not exactly same, which is different from the classical Alamouti's codes. After the destination has received the space-time coded information in the second time phase, it decodes them using space-time decoding algorithm. At this time, the destination has had two data set. One is the information of source and the row parity P_h in the first time phase and the other is the information about the vertical parity P_v after STBC decoding. Therefore, it can combine them together to form a complete TPC and then conducts turbo decoding to recover the original source data.

6.2 Space-Time Cooperative Communications

The solid lines in Fig. 6.2 shows DSTBC in the 2nd time phase in the one-relay SDF & DSTBC system The source sends the error-free parity matrix P_v while the relay transmits the LLR for the parity bits $\hat{P}_v$ using the amplifying and forwarding. We can reorganize these two $(n-k) \times n$ parity matrices serially and denote the column parity bits at source as $[x_1, x_2, x_3, x_4, ...x_{(n-k)\times n}]$ while the soft information at relay as $[l_1, l_2, l_3, l_4, ...l_{(n-k)\times n}]$.
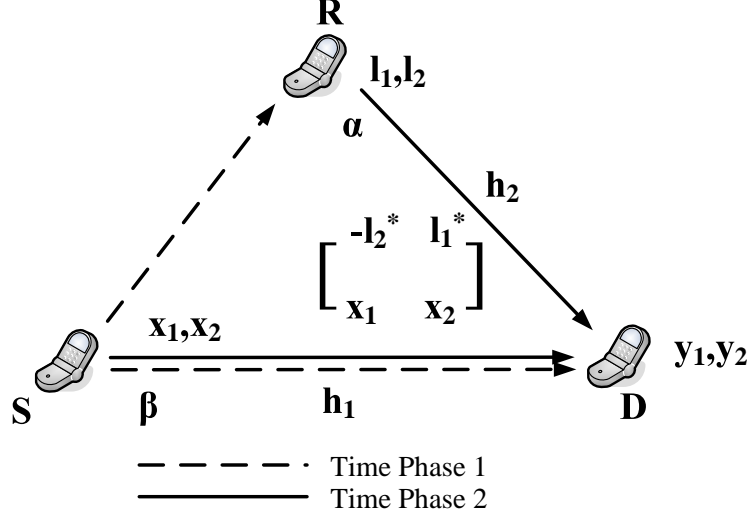
Figure 6.2. System Model for proposed one-relay SDF & DSTBC system

In order to understand the performance of DSTBC, we start with the distribution of the LLR values by using the Gaussian approximation. Rooted at Central Limit Theorem (CLT), the Gaussian assumption states that, for a code with a soft message-passing decoder, the output LLRs from the decoder follow an approximated Gaussian distribution[22],[9].[30] provided solid statistical justification for the Gaussian approximation in turbo codes on why and how well the assumption holds.

After horizontal decoding, the LLRs of vertical parity bits are obtained by an EBCH encoder based on (8). Each bit of matrix $\hat{P}_v$ can be seen as a decision of arithmetic summation of *a-posteriori* probabilities (APPs) which are the output of Chase-II decoder calculated from (4). From CLT, $\hat{P}_v$ can be approximated as Gaussian distributed random variables. Let μ_l be the mean and σ_l^2 be the variance of $\hat{P}_v$. Then the LLR value of a particular transmitted information bit x_i can be represented as

$$l_i = \sqrt{E_s}\mu_l x_i + n_i, \tag{1}$$

where $n_i \sim \mathcal{CN}(0, \sigma_l^2)$ and $i = 1, ..., (n-k) \times n$. With pre-normalization before the signals

retransmit at the relay to the destination, the signal can be represented as

$$\hat{l}_i = \sqrt{E_s}x_i + \hat{n}_i, \tag{2}$$

where $\hat{n}_i \sim \mathcal{CN}(0, \sigma_l^2/\mu_l^2)$ and $i = 1, ..., (n-k) \times k$.

From (2), the estimated signal $\hat{l}$ at the relay before retransmission can be considered as the information stream transmitted from the source plus a white Gaussian noise $\hat{n}$. In other words, it lets us to model the combination of the inter-user channel and the signal processing at the relay as a virtual Gaussian channel with effective SNR as

$$\gamma_{\hat{l}} = \frac{E_s\mu_l^2}{\sigma_l^2}. \tag{3}$$

We denote $\hat{l}$ as l and $\hat{n}$ as n for the rest of this paper.

This well received Gaussian approximation in soft decoding (3) is also verified by simulations using TPC. Table 6.1 shows the estimated LLR means and variances under different conditions of the inter-user channel with $\Omega = 1$(assume $x_i^j = -1$ is transmitted and x_i^j is stated in (1) where $1 \leq i \leq k$, $1 \leq j \leq n$).

Table 6.1. LLR message distribution under different inter-user channel conditions.

γ_z(dB)	γ_z	$\hat{\mu}_l$	$\hat{\sigma}_l^2$	γ_l
0	1	0.0035	1.0000	1.225×10^{-5}
6.02	4	-0.8469	0.2828	2.5362
7.13	5.1653	-0.9547	0.0886	10.2883
20	100	-0.9981	0.0038	2.6216×10^2

6.2.1 Space-Time Encoding

We rearrange P_v and $\hat{P}_v$ into two series of signals as shown in Table 7.1 and radiated from the source and relay, respectively. α and β are amplification factors in the relay and source, which can be used to adjust the total transmission power and the power allocation.

After distributed space-time coding, the receiver observations y_1^{prop} and y_2^{prop} are given by

$$y_1^{prop} = \sqrt{E_s}\beta h_1 x_1 - \alpha h_2 l_2^* + v_1 \tag{4}$$

$$y_2^{prop} = \sqrt{E_s}\beta h_1 x_2 + \alpha h_2 l_1^* + v_2 \tag{5}$$

where v_1, v_2 are the Gaussian noise at the destination node with $v_i \sim \mathcal{CN}(0, \sigma_v^2)$ for $i = 1, 2$.

Substituting l_i and writing in the matrix form, the received signals are:

$$Y = \sqrt{E_s}HX + N + V \tag{6}$$

where $Y = [y_1^{prop}, (y_2^{prop})^*]^T$, $X = [x_1, x_2^*]^T$, $V = [v_1, v_2^*]^T$,

$$H = \begin{bmatrix} \beta h_1 & -\alpha h_2 \\ \alpha h_2^* & \beta h_1^* \end{bmatrix} \quad \text{and} \quad N = \begin{bmatrix} -\alpha h_2 n_2^* \\ \alpha h_2^* n_1 \end{bmatrix}.$$

6.2.2   Space-Time Decoding

When the destination has received the mixed signal from both the source and relay, the classical space-time decoding algorithm is adopted to estimate the transmitted symbols, which is implemented by multiplying the received data with H^+, i.e., decoding with its matched filter. For a general matrix of size $m \times n$, the pseudo-inverse for the matrix H is defined as:

$$H^+ = (H^H H)^{-1} H^H, \tag{7}$$

Table 6.2. Symbols transmitted at antennas

	Bit_1	Bit_2	Bit_3	Bit_4	...
Antenna at Relay	$-\alpha l_2^*$	αl_1^*	$-\alpha l_4^*$	αl_3^*	...
Antenna at Source	βx_1	βx_2	βx_3	βx_4	...

66

where H^H represents the Hermitian of the matrix H, which is equal to the conjugate transpose of the matrix. The term:

$$H^H H = \begin{bmatrix} \beta^2|h_1|^2 + \alpha^2|h_2|^2 & 0 \\ 0 & \beta^2|h_1|^2 + \alpha^2|h_2|^2 \end{bmatrix},$$

(8)

is a diagonal matrix. The estimates of the transmitted symbols $[\hat{x}_1, \hat{x}_2^*]^T$ at the destination can be obtained as follows:

$$\begin{bmatrix} \hat{x}_1 \\ \hat{x}_2^* \end{bmatrix} = H^+ \begin{bmatrix} y_1^{prop} \\ (y_2^{prop})^* \end{bmatrix}$$

$$= \sqrt{E_s} \begin{bmatrix} x_1 \\ x_2^* \end{bmatrix} + H^+ \begin{bmatrix} -\alpha h_2 n_2^* \\ \alpha h_2^* n_1 \end{bmatrix} + H^+ \begin{bmatrix} v_1 \\ v_2^* \end{bmatrix}$$

From the above equation, y_1^{prop} and $(y_2^{prop})^*$ have the same signal-to-noise ratio as

$$\gamma_T = \frac{\beta^2|h_1|^2 + \alpha^2|h_2|^2}{\alpha^2|h_2|^2 \frac{1}{\gamma_l} + \frac{1}{\gamma_v}}$$

(9)

where γ_l is from (3) and $\gamma_v = \frac{E_s}{\sigma_v^2}$.

6.3 Performance of DSTBC Decoding

In this part, we investigate the performance of using DSTBC and that use of soft relaying alone without STBC. In order to justify the use of DSTBC, a basic assumption adopted here directly without proof is that if the decoding of DSTBC outperforms the use of SDF alone in the 2nd time phase, the overall performance of the system using DSTBC also outperforms the system without DSTBC. This assumption holds intuitively as the system performance cannot be degraded when one component of the system is improved.

For a SNR value γ_s (i.e., energy per symbol over noise), the bit error probability P_b for

coherent binary signals is given as[31]

$$P_b(\gamma_s) \approx c_1 Q\left(\sqrt{c_2 \gamma_s}\right) \tag{10}$$

where c_1 is the number of the nearest neighbors to a constellation at the minimum distance, and c_2 is a constant that relates the minimum distance to the average symbol energy. c_1, c_2 are determined by the type of modulation used.

6.3.1 Averaged BER for Decoding of DSTBC

The averaged BER can be obtained by averaging over the random variable h_1 and h_2, Using the conditional expectation, we have

$$
\begin{aligned}
& P_b(\mathcal{E}) \\
=\ & E_{h_1,h_2}\left[c_1 Q\left(\sqrt{c_2 \gamma_T}\right)\right] \\
=\ & E_{h_1,h_2}\left[\frac{c_1}{\pi}\int_0^{\pi/2}\exp\left(-\frac{c_2 \gamma_T}{2\sin^2\theta}\right)d\theta\right] \\
=\ & \frac{c_1}{\pi}\int_0^{\pi/2} E_{h_2}\left[E_{h_1}\left[\exp\left(-\frac{c_2}{2\sin^2\theta}\cdot\gamma_T\right)|h_2|\right]\right]d\theta \\
=\ & \frac{c_1}{\pi}\int_0^{\pi/2} E_{h_2}\left[E_{h_1}\left[\exp\left(-\frac{c_2}{2\sin^2\theta}\cdot\left(\frac{\beta^2|h_1|^2 + \alpha^2|h_2|^2}{\alpha^2|h_2|^2\frac{1}{\gamma_l} + \frac{1}{\gamma_v}}\right)\right)|h_2|\right]\right]d\theta.
\end{aligned} \tag{11}
$$

Therefore, the solving process includes two steps. The first is to average the conditional BER over h_1 given h_2 and the second is to average the result over h_2.

Step 1. Let

$$
\begin{aligned}
\psi(\tilde{h}) &= \exp\left[-\frac{c_2}{2\sin^2\theta}\cdot\gamma_T\right] \\
&= \exp\left[-\frac{c_2}{2\sin^2\theta}\cdot\left(\frac{\beta^2|h_1|^2 + \alpha^2|h_2|^2}{\alpha^2|h_2|^2\frac{1}{\gamma_l} + \frac{1}{\gamma_v}}\right)\right].
\end{aligned} \tag{12}
$$

Set $\rho = \frac{1}{\alpha^2 |h_2|^2 \frac{1}{\gamma_l} + \frac{1}{\gamma_v}}$. For a given h_2, averaging over h_1,

$$
\begin{aligned}
& E_{h_1}[\psi(\tilde{\boldsymbol{h}})] \\
= {} & \int_0^\infty \exp\left[-\frac{c_2}{2\sin^2\theta} \cdot (\rho\beta^2 t_1 + \rho\alpha^2 |h_2|^2) \right] \cdot \frac{1}{\Omega_1} e^{-\frac{t_1}{\Omega_1}} \cdot dt_1 \\
= {} & \frac{1}{\Omega_1} \exp\left(-\frac{c_2}{2\sin^2\theta} \cdot \rho\alpha^2 |h_2|^2 \right) \\
& \int_0^\infty \exp\left[-\left(\frac{c_2}{2\sin^2\theta} \cdot \rho\beta^2 + \frac{1}{\Omega_1}\right) t_1 \right] \cdot dt_1 \\
= {} & \frac{1}{\Omega_1} \exp\left(-\frac{c_2}{2\sin^2\theta} \cdot \rho\alpha^2 |h_2|^2 \right) \frac{1}{\frac{c_2}{2\sin^2\theta} \cdot \rho\beta^2 + \frac{1}{\Omega_1}}.
\end{aligned}
\tag{13}
$$

Step 2. By substituting the above equation into (11), we obtain

$$
\begin{aligned}
P_b(\mathcal{E}) = {} & \frac{1}{\Omega_1} \frac{c_1}{\pi} \int_0^{\pi/2} E_{h_2}\left[\exp\left(-\frac{c_2}{2\sin^2\theta} \cdot \frac{\alpha^2 |h_2|^2}{\alpha^2 |h_2|^2 \frac{1}{\gamma_l} + \frac{1}{\gamma_v}} \right) \right. \\
& \left. \frac{1}{\frac{c_2}{2\sin^2\theta} \cdot \frac{\beta^2}{\alpha^2 |h_2|^2 \frac{1}{\gamma_l} + \frac{1}{\gamma_v}} + \frac{1}{\Omega_1}} \right] d\theta.
\end{aligned}
\tag{14}
$$

Considering the pdf of $|h_2|^2$ (i.e., t in the derivation), and according to the definition of expectation, we have,

$$
\begin{aligned}
& P_b(\mathcal{E}) \\
= {} & \frac{1}{\Omega_1} \frac{c_1}{\pi} \int_0^{\pi/2} \int_0^\infty \exp\left(-\frac{c_2}{2\sin^2\theta} \cdot \frac{\alpha^2 t}{\alpha^2 t \frac{1}{\gamma_l} + \frac{1}{\gamma_v}} \right) \frac{1}{\frac{c_2}{2\sin^2\theta} \cdot \frac{\beta^2}{\alpha^2 t \frac{1}{\gamma_l} + \frac{1}{\gamma_v}} + \frac{1}{\Omega_1}} \cdot \frac{1}{\Omega_2} e^{-\frac{t}{\Omega_2}} dt d\theta \\
= {} & \frac{1}{\Omega_1} \frac{c_1}{\pi} \int_0^\infty \frac{1}{\Omega_2} e^{-\frac{t}{\Omega_2}} \cdot \int_0^{\pi/2} \exp\left(-\frac{c_2}{2\sin^2\theta} \cdot \frac{\alpha^2 t}{\alpha^2 t \frac{1}{\gamma_l} + \frac{1}{\gamma_v}} \right) \frac{1}{\frac{c_2}{2\sin^2\theta} \cdot \frac{\beta^2}{\alpha^2 t \frac{1}{\gamma_l} + \frac{1}{\gamma_v}} + \frac{1}{\Omega_1}} \cdot d\theta \cdot dt
\end{aligned}
\tag{15}
$$

By using the variable substitution of θ in (15), partial fraction and the special functions, we can derive the unconditional probability $P_b(\mathcal{E})$ as stated in the following proposition.

Theorem 4. *The averaged BER performance of the proposed one-relay Soft-Decode-and-Forward distributed Alamouti's code system, with Gaussian approximation parameters γ_l,*

channel statistics γ_v, $\boldsymbol{\Omega} = [\Omega_1, \Omega_2]$ *and the modulation parameters* c_1 *and* c_2, *is given as*

$$P_b(\gamma_l, \gamma_v, \boldsymbol{\Omega}, c_1, c_2)$$
$$= \frac{c_1}{2\Omega_2} \int_0^\infty \left\{ [1 - \Phi(\sqrt{P})] \exp\left(-\frac{t}{\Omega_2}\right) \right.$$
$$\left. - \frac{1}{\sqrt{S}} [1 - \Phi(\sqrt{PS})] \exp\left(PS - P - \frac{t}{\Omega_2}\right) \right\} dt \tag{16}$$

where $P = \frac{c_2\alpha^2 t}{2\alpha^2 t \frac{1}{\gamma_l} + \frac{2}{\gamma_v}}$, $S = \frac{2}{c_2\gamma_v\beta^2\Omega_1} + \frac{2t\alpha^2}{c_2\gamma_l\beta^2\Omega_1} + 1$ *and* $\Phi(x) = erf(x) = \frac{2}{\sqrt{\pi}} \int_0^x e^{-t^2} dt$ *is the error function.*

Proof: See appendix 7.5.

6.3.2   Averaged BER for Soft-relaying without STC

Consider the soft-relaying system without STC as the reference system. The difference from the one-relay SDF & DSTBC system exists in the second time phase. In the reference one-relay SDF system, the relay obtains the normalized LLR for vertical parity bits l_i, simply multiplies it with a constant η and forwards to the destination. The receiver observations y_i^{ref} is given by

$$y_i^{ref} = \eta h_2 l_i + v_i, \quad i \in [1, (n-k) \times k] \tag{17}$$

where v_i is the Gaussian noise at the destination node with $v_i \sim \mathcal{CN}(0, \sigma_v^2)$.

Substituting l_i from (2), the received signals are:

$$y_i^{ref} = \eta h_2(\sqrt{E_s}x_i + n_i) + v_i \tag{18}$$

The SNR at the receiver can be written as

$$\gamma_T = \frac{\eta^2|h_2|^2}{\eta^2|h_2|^2\frac{1}{\gamma_l} + \frac{1}{\gamma_v}}. \tag{19}$$

The averaged BER can further be obtained by averaging over the random variable h_2.

$$
\begin{aligned}
P_b(\mathcal{E}) &= E_{h_2}\left[c_1 Q\left(\sqrt{c_2 \gamma_T}\right) \right] \\
&= E_{h_2}\left[\frac{c_1}{\pi} \int_0^{\pi/2} \exp\left(-\frac{c_2 \gamma_T}{2\sin^2\theta} \right) d\theta \right] \\
&= \frac{c_1}{\pi} \int_0^{\pi/2} E_{h_2}\left[\exp\left(-\frac{c_2}{2\sin^2\theta} \cdot \frac{\eta^2 |h_2|^2}{\eta^2 |h_2|^2 \frac{1}{\gamma_l} + \frac{1}{\gamma_v}} \right) \right] d\theta.
\end{aligned} \tag{20}
$$

By considering the variable substitution of θ in (20), we can derive the unconditional probability $P_b(\mathcal{E})$, as stated in the following proposition.

Theorem 5. *The averaged BER performance of the reference SDF system, with Gaussian approximation parameters γ_l and channel statistics γ_v, Ω_2 and the modulation parameters c_1 and c_2, is given as*

$$
P_b(\gamma_l, \gamma_v, \Omega_2, c_1, c_2) = \frac{c_1}{2\Omega_2} \int_0^\infty e^{-\frac{t}{\Omega_2}} \cdot [1 - \Phi(\sqrt{W})] dt \tag{21}
$$

where $W = \frac{c_2}{2} \frac{\eta^2 t}{\eta^2 t \frac{1}{\gamma_l} + \frac{1}{\gamma_v}}$ and $\Phi(x) = erf(x)$ is the error function.

Proof: See appendix 7.5.

Considering both propositions, we further have

Corollary 1. *When $\alpha = \eta$ and $\beta = 0$, the performance of the proposed one-relay SDF & DSTBC system shown in (16) reduces to the performance of the reference SDF system shown in (21).*

Proof: Marcum Q-Function can be represented by error function as

$$
Q(x) = \frac{1}{2} - \frac{1}{2}\Phi(\frac{x}{\sqrt{2}}). \tag{22}
$$

Chernoff bound of Q function is

$$
Q(x) \leq \frac{1}{2}\exp(-\frac{x^2}{2}), \quad x > 0. \tag{23}
$$

When $\beta \to 0$, $S \to +\infty$. From (22) and (23), we have

$$
\begin{aligned}
&\lim_{S \to \infty} \frac{1}{\sqrt{S}}[1 - \Phi(\sqrt{PS})]\exp(PS - P - \frac{t}{\Omega_2}) \\
={} &\lim_{S \to \infty} \frac{1}{\sqrt{S}} 2Q(\sqrt{2PS})\exp(PS - P - \frac{t}{\Omega_2}) \\
\leq{} &\lim_{S \to \infty} \frac{1}{\sqrt{S}}\exp(-PS)\exp(PS - P - \frac{t}{\Omega_2}) \\
={} &\lim_{S \to \infty} \frac{1}{\sqrt{S}}\exp(-P - \frac{t}{\Omega_2}) = 0
\end{aligned}
\tag{24}
$$

Since $P > 0$ and $S > 0$,

$$
\frac{1}{\sqrt{S}}[1 - \Phi(\sqrt{PS})]\exp(PS - P - \frac{t}{\Omega_2}) \geq 0.
\tag{25}
$$

From (24) and (25), we have

$$
\lim_{S \to \infty} \frac{1}{\sqrt{S}}[1 - \Phi(\sqrt{PS})]\exp(PS - P - \frac{t}{\Omega_2}) = 0.
\tag{26}
$$

When $\alpha = \eta, P = W$. By substituting (26), (16) is equal to (21), when $\alpha = \eta$ and $\beta = 0$. $\qquad \square$

From the above derivation and the results in the two propositions, the proposed system with DSTBC can be regarded as the generalization of the SDF system.

6.3.3 Line model

To evaluate the BER performance at the receiver of the proposed one-relay SDF & DSTBC and reference one-relay SDF system in (16) and (21), respectively, we use the line simulation model[60,15] which assumes that the relay is located on the line connecting the source with the destination as in Fig. 6.3. This model is more practical in real systems where the relay is usually located somewhere between the two terminals. We set the distance between source and relay as unit 1 and that between relay and destination as λ. When the relay moves from the source to the destination, λ changes from 1 to 0.
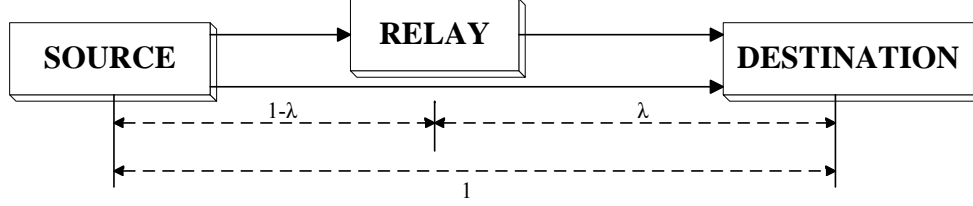
Figure 6.3. Line model

In addition to Rayleigh fading, large path-loss model with path loss exponent $n = 2$ is also considered to calculate the average SNR at the relay and destination nodes in different time phases. That is, the SNR values in two systems are related as

$$\Omega_2 = \Omega_1 \cdot \frac{1}{\lambda^2} \tag{27}$$

6.3.4 2nd-Time-Phase Power Allocation and Optimization

Power Allocation between the Source and the Relay in the second time phase

In subsection 6.3.2, we discussed the differences between two systems in the second time phase. We use E to represent the total power used in two systems. E is the sum of E_1 and E_2 which are the power in the first and second time phase respectively. In the first time phase, the power spent in both systems are the same. In order to make the total power between the reference one-relay SDF and the proposed one-relay SDF & DSTBC systems equal, the power used in the second time phase, which are E_2^{ref} and E_2^{prop}, should be equal.

For the reference system, the relay decodes the received stream horizontally and further gets the LLR of $P_v(l)$. It then forwards l to the destination. The average energy of transmitted signal at the relay can be calculated as

$$\begin{aligned} E[|l|^2] &= E[|\sqrt{E_s}x + n|^2] \\ &= E_s|x|^2 + 2\sqrt{E_s}E[x]E[n^*] + \sigma_n^2. \end{aligned} \tag{28}$$

73

Since $E[n] = E[n^*] = 0$, then we have,

$$E[|l|^2] = E_s + \sigma_l^2/\mu_l^2$$

In order to normalize the transmission energy per symbol in the second phase to E_s, we transmit the received signal with a coefficient η, where

$$\eta = \frac{\sqrt{E_s}}{\sqrt{E[|l|^2]}} = \frac{1}{\sqrt{1 + \frac{1}{\gamma_l}}}. \tag{29}$$

For the proposed one-relay SDF & DSTBC system when DSTBC is used, the relay and source cooperatively transmit signal to the destination. The transmission factors at the relay and source are α and β respectively. In order to make a fair comparison between the two systems, we need to equal the total energy.

$$\begin{aligned} E_2^{prop} &= E[|\alpha l|^2] + E[|\beta\sqrt{E_s}x|^2] \\ &= \alpha^2 E[|l|^2] + \beta^2 E_s \\ &= \alpha^2(E_s + \sigma_l^2/\mu_l^2) + \beta^2 E_s = E_2^{ref} = E_s \end{aligned} \tag{30}$$

Then we have

$$\alpha^2 = \frac{(1-\beta^2)E_s}{(E_s + \sigma_l^2/\mu_l^2)} = \frac{1-\beta^2}{1 + \frac{1}{\gamma_l}}, \quad \beta \in [0,1].$$

Power Optimization

Substituting the relationship between α and β in Proposition 1, it provides a way to optimally allocate the power between the relay node and source node in the 2nd time phase. For any given channel scenario, (16) is a function of only one parameter β. The optimal β value can be obtained by setting the 1st derivative to be zero. However, by observing

Figure 6.4. BER performance of proposed one-relay SDF & DSTBC system by changing γ_l when $\lambda = 0.3$, $\Omega_1 = 10dB$, $\gamma_v = 1$

(16), it is much involved to find a closed-form equation of this derivative. At this point, a simple numerical method is introduced to find the value of β where the optimal Space-Time decoded performance is achieved. We simply divide β from 0 to 1 into n small steps. For the ith small step, we denote the variation of BER performance as ΔBER_i. Then the optimal power ratio β_{opt} is located at the ith step where $\Delta BER_i \approx 0$. By this method, β_{opt} is easy to obtain.

6.3.5   Numerical Results for DSTBC Decoding

We evaluate the BER performance for DSTBC decoding of the proposed one-relay SDF & DSTBC system by changing γ_l and λ where Figs. 6.4 and 6.5 show their averaged BER respectively. The results illustrate that STBC outperforms traditional soft relaying ($\beta = 0$) for most of the cases which is due to the diversity gained reaped with DSTBC.

Fig. 6.4 contains the theoretical BER and simulation results when power allocation is used in line model. The relay locates between the source and the destination where $\lambda = 0.3$ and we fix the direct link SNR to 10dB. These results clearly show the close match between
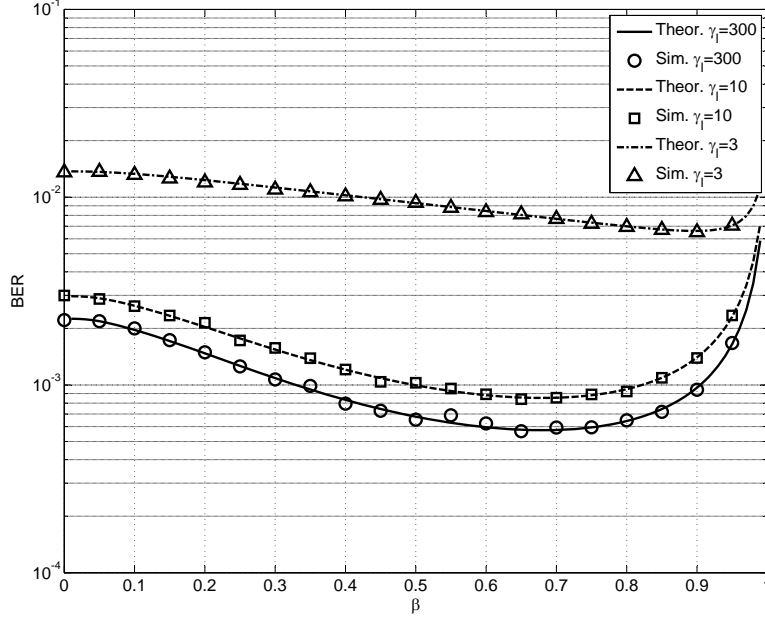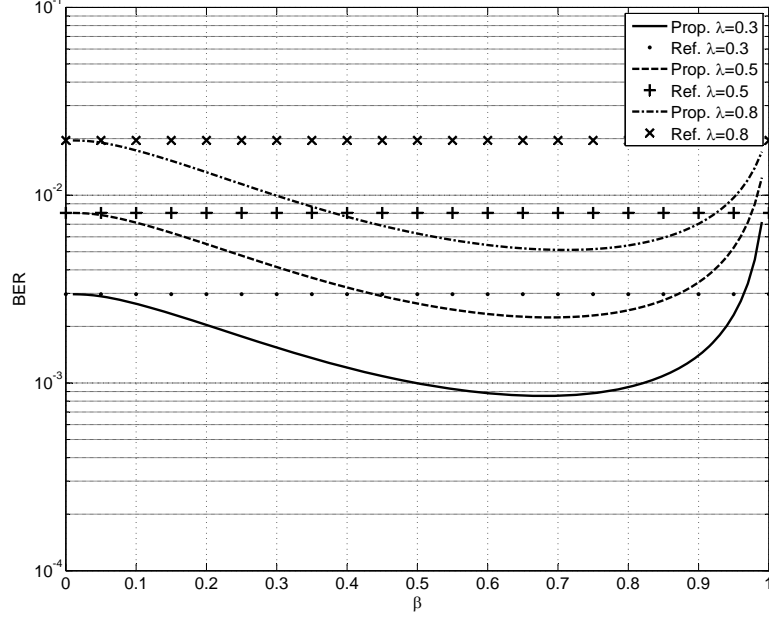
Figure 6.5. BER performance of proposed one-relay SDF & DSTBC system by changing λ when $\gamma_l = 10$, $\Omega_1 = 10dB$, $\gamma_v = 1$

that theoretical and simulation BER performance and hence validates our analytic work.

Numerical power optimization method illustrated in the last subsection is introduced to calculate the maximal power allocation ratio β_{opt} under different channel conditions. Table 6.3 shows the numerical results of power optimization. These results of β_{opt} are consistent with the three curves in Fig. 6.4 with the same system conditions.

Table 6.3. Optimal power ratio β_{opt} in different channel conditions.

γ_l	λ	Ω	β_{opt}
300	0.3	10dB	0.68
10	0.3	10dB	0.68
3	0.3	10dB	0.90

We can consider the reference one-relay SDF system as a special case of proposed one-relay SDF & DSTBC system when $\beta = 0$. To verify this extreme case, we evaluate the reference one-relay SDF and proposed one-relay SDF & DSTBC system performance when the relay locates where $\lambda = 0.3$, 0.5, and 0.8 and the direct link SNR is fixed to 10dB as well. Fig. 6.5 shows the results and confirm that when $\beta = 0$, the proposed one-relay SDF & DSTBC system recedes to reference one-relay SDF system. On the other hand, we can

76
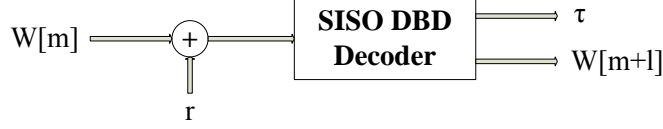
Figure 6.6. Modified one stage SISO TPC decoder

see that it is not alway superior to use DSTBC instead of SDF alone. When $\beta > 0.96$ for $\lambda = 0.3$, the reference system outperforms. Intuitively, these are the cases where the function of relay is not fully utilized due to the very small amplifying factor α. In fact, by comparing results in Propositions 1 and 2, it is always possible to determine when to use DSTBC and when to reduce it to SDF alone.

6.4 Turbo Decoding and Simulation Results

6.4.1 Turbo decoding

The destination receives the two parts of the TPC matrix $\{S, P_h\}$ and P_v via the direct and relay Rayleigh channels over different SNRs. Then it constructs a complete TPC by arranging the received data matrices S, P_h and P_v as in Fig. 6.1 in order to start rows and columns iterative decoding.

Similarly to the soft-decoding performed at the relay, the SISO decoder at the destination uses Chase II algorithm[16] to find the decision codeword $\tau = \{\tau_1, \tau_2, \ldots, \tau_n\}$, $\tau_j \in \{-1, +1\}$, for each decoded row or column. The confidence value ϕ of the decision codeword C will be evaluated using:

$$\phi_i = f\left(\sum_{j \in \left\{ j | (y_i^j - d_i^j).d_i^j < 0 \right\}} (y_i^j - d_i^j)^2 \right), 1 \leq i \leq k. \tag{31}$$

The final normalized log extrinsic soft output for the jth bit $(1 \leq j \leq n)$ of the decoded codeword is given by[56]:

$$w_j = \tau_j \left(\frac{\sigma^2}{2} \ln\left(\frac{\phi + \exp(2r_j\tau_j/\sigma^2)}{1 - \phi} \right) - r_j\tau_j, \right) \tag{32}$$

77

where w_j is the normalized log extrinsic information output, τ_j is the element of the decision codeword, r_j is the soft input bit to the decoder. The value of soft output also depends on variance σ^2 of the channel. We assume that the two values of σ^2 for the two received parts at the destination are provided at the input of the decoder. In rows decoding of the TPC matrix, the value of σ^2 for the first k rows is equal to σ_w^2/Ω_1 of the direct channel in the first time phase, whereas this value is set to $1/\gamma_T$ for the remaining $n - k$ rows of the TPC matrix shown in Fig. 6.1.

Fig. 6.6 shows the SISO decoder implementation for the cooperative based decoder. The diagram represents one stage of decoding along the rows (columns) where m denotes the mth decoding stage; τ is the hard-decoded output and r is the channel output. The input bit to the decoder is the summation of the channel output and the normalized log extrinsic information of the previous decoding stage. For the first decoding stage, w_j $(1 \leq j \leq n)$ is set to zero for all the decoded rows.

6.4.2 Simulation and Results

In this part, we show the simulation results obtained from the proposed one-relay Space-Time coded distributed Turbo Product Code(STBC-DTPC) system using SDF relaying protocol at the relay. We compare its performance with the original distributed Turbo Product Code[75]. The two component codes used in the DTPC simulations have the same parameters, where $n = 64$, $k = 51$ and $\delta = 6$.

The simulations are carried over 0.1 steps of λ from 0 up to 1 using the line model, and for every step the system is tested against different values of γ_w to obtain the system performance in terms of the BER. The performance of original DTPC and STBC-DTPC systems are shown in Fig. 6.7 where the thick solid line is for STBC-DTPC system. The γ_w which represents the SNR of the direct link (from source to relay) of both systems are selected as 4dB, 5dB, 6dB, 7dB, and 8dB respectively. The results show that the overall decoding output at destination turns better when the direct link situation becomes better.
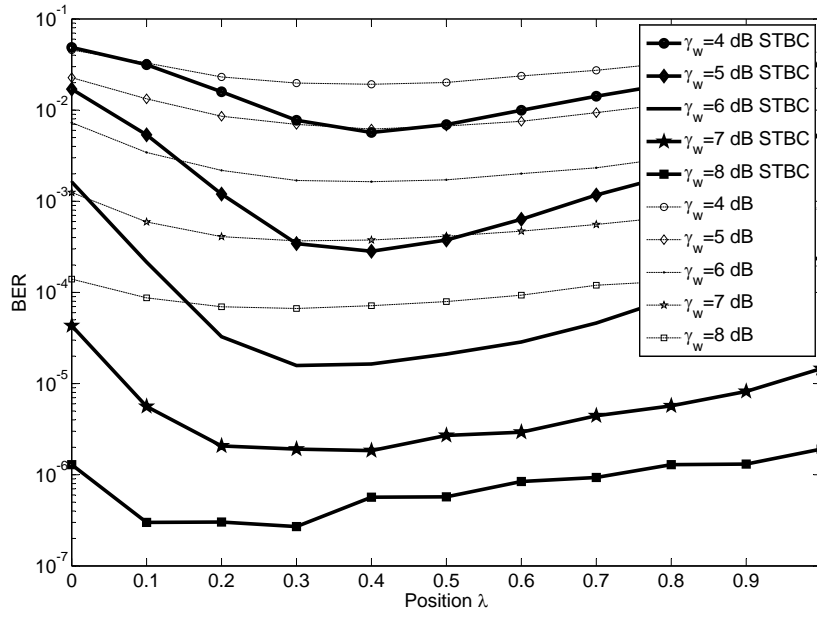
Figure 6.7. The BER performance of STBC-DTPC in Rayleigh fading channel by fixing γ_w to 4,5,6,7,8dB
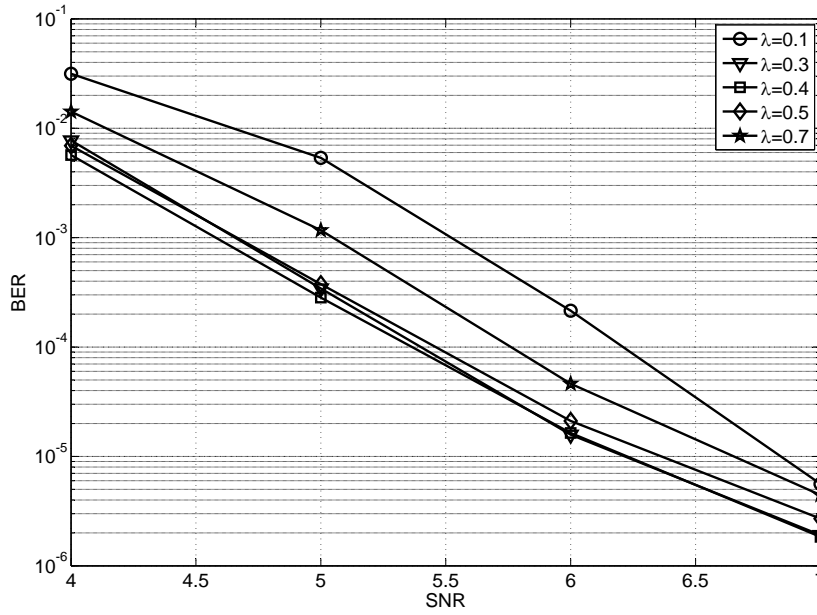
Figure 6.8. The BER performance of STBC-DTPC in Rayleigh fading channel compared to SDF-DTPC by fixing λ to 0.1,0.3,0.4,0.5,0.7

Furthermore, Fig. 6.7 shows the difference between the two systems in performance expands when the channel condition raises.

Fig. 6.8 shows the performance of STBC-DTPC system in another scenario. λ (the relay location between the source and the destination) is fixed to 0.1, 0.3, 0.4, 0.5 and 0.7 respectively. At each relay location, we raise the source to destination channel condition from 4dB to 7dB to get the overall BER performance at destination after turbo decoding. The results show that STBC-DTPC system reach its best performance when the λ equals 0.3 or 0.4 which indicates that the relay moves to the middle of the source-destination line.

6.4.3   Power Allocation and Optimization

Power Allocation for two time phases

In subsection 6.4.3, we presented the power allocation method between the source and the relay in the second time phase. We use E to represent the total power and E_1 and E_2 represent the power in the first and second time phase respectively. Furthermore, E_{21} and E_{22} are used to define the power at the source and the relay in the second time phase. In the method in subsection 6.4.3, we assumed the power spent in two time phases are the same ($E_1 = E_2 = E_{21} + E_{22} = 1$). However, there is a question regarding this power allocation method: if we unevenly allocate power between two time phases ($E_1 \neq E_2$), could we get a better overall performance than the previous equal allocation method?

In order to make the total power between the proposed method and the 2nd-time-phase method equal, the total power used in the two time phases should be 2, which is

$$E = E_1 + E_2 = E_1 = E_1 + E_{21} + E_{22} = 2. \tag{33}$$

The proposed algorithm can be implemented in the following steps:

1. Take values of E_1 from 0 to 2 with an arbitrary interval.

2. In the first time phase, the source sends information stream to both the relay and destination using power E_1. We can approximate the SNR of the output signal at the relay (γ_l) by Monte-Carlo simulation.

3. The averaged BER performance of the one-relay SDF distributed Alamouti's code system can be evaluated by (4) after γ_l is obtained. The problem of getting the optimal power ratio between the relay and the source can be seen as a 2nd-Time-Phase Power Allocation and Optimization problem and β_{opt} can be obtained by following the method in Section 6.4.3.

4. Based on E_1, E_2 and β, we can get the overall system performance from Monte-Carlo simulations.

5. Choose the optimal system performance from the results based on different E_1.

We can also represent the steps of this proposed algorithm with a flowchart shown in Fig 6.9.

Simulation results

Same as previous sections, we test our proposed algorithm in the line model as shown in Fig. 6.10. The relay locates near to the source where $\lambda = 0.8$ and the SNR between the source and destination (i.e., SNR_{sd}) is 10dB.

By giving different values of E_1 from 0 to 2 with an arbitrary interval of 0.05, as illustrated in step 2, we approximate the SNR of the output signal at the relay by Monte-Carlo simulation. Fig 6.11 shows the Gaussian approximation of LLR values when $E_1 = 0.3$. "x" marks show the pdf of LLR at the relay and the solid line is the approximated Gaussian pdf by using GA method. The pdf of LLR matches the Gaussian well which indicates that LLR values can be approximated by Gaussian distributed random variable.

For a certain value of E_1, the value of E_2 can be calculated by (33). The problem of getting the optimal power ratio between the relay and the source can be seen as a 2nd-Time-
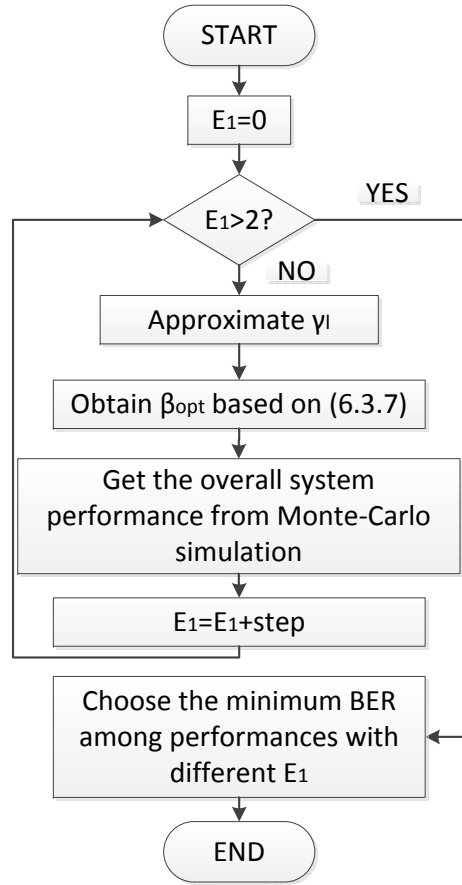
Figure 6.9. The flowchart of proposed power allocation algorithm.
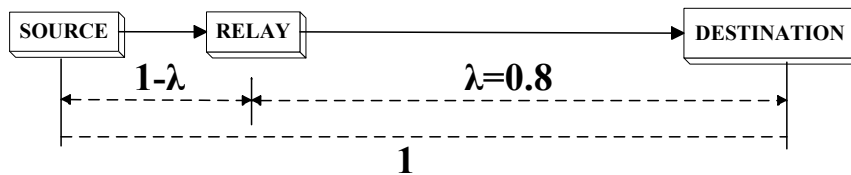
Figure 6.10. Line model.
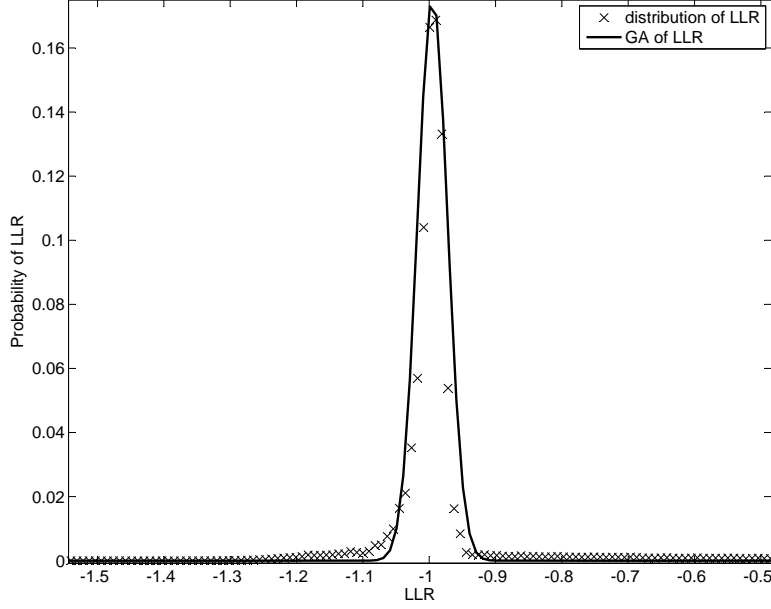
Figure 6.11. Gaussian approximation of LLR values when $E_1 = 0.3$.

Phase Power Allocation and Optimization problem. We obtain the optimal value of β (β_{opt}) by the method stated in Section 6.4.3. Thus, when $E_1 = 0.05, 0.1, 0.2$ and 0.3, the β_{opt} is shown in Fig. 6.12 and Table 6.4.

Table 6.4. Optimal power ratio β_{opt} for different E_1.

E_1	σ_l	γ_l	β_{opt}
0.05	0.409	6	0.73
0.1	0.2323	18	0.70
0.2	0.0734	186	0.70
0.3	0.0227	1941	0.70

Based on E_1, E_2 and β, we get the overall system performance after turbo decoding from Monte-Carlo simulation as shown in Fig. 6.13.

In the 2nd-Time-Phase Power Allocation and Optimization method in Section 6.4.3, we have $E_1 = E_2 = 1$. It is a special case of our proposed method when $E_1 = 1$ in Fig. 6.13. It shows that the performance when $E_1 = 1$ is not optimal in our scenario. When $E_1 = 1.55$, the whole system obtains the overall optimal power allocation and the BER after turbo decoding reaches 1.3×10^{-4}.
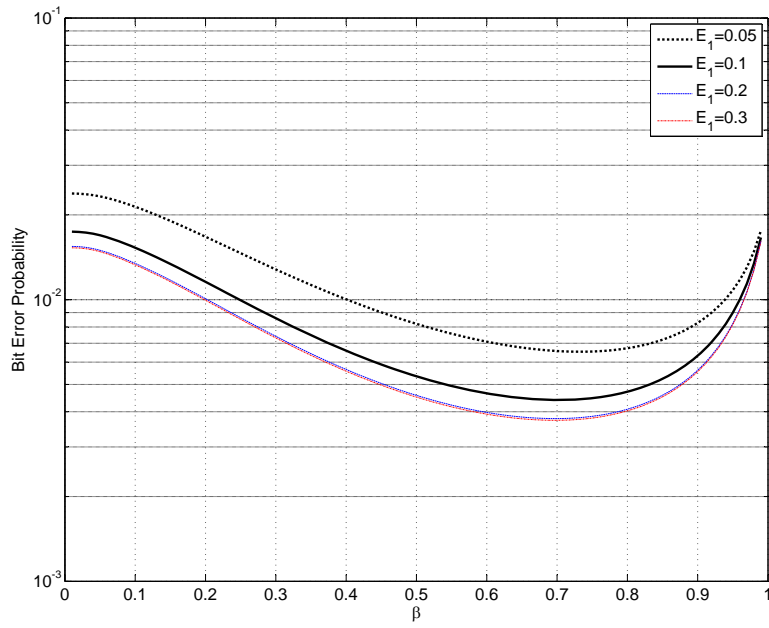
Figure 6.12. Optimal power ratio β_{opt} for different E_1.
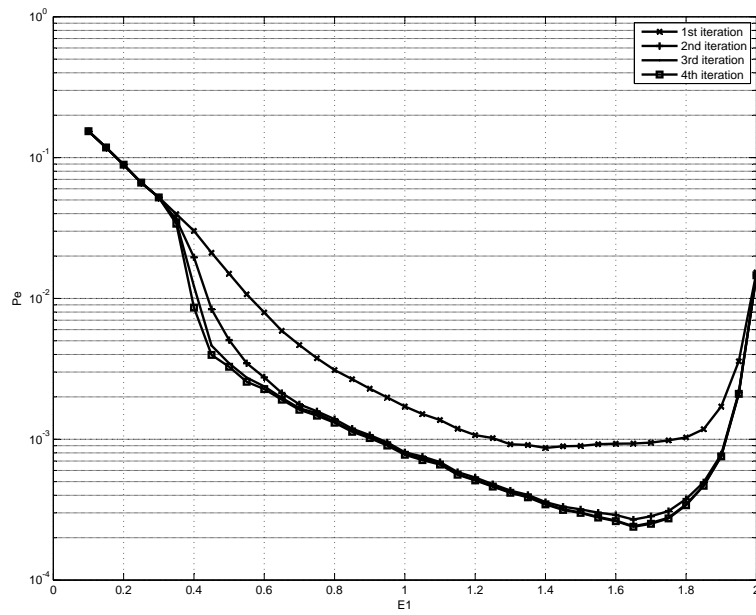
Figure 6.13. The overall system performance in line model when $\lambda = 0.8$ and $SRN_{sd} = 10$dB.

Chapter 7
DISTRIBUTED SPACE-TIME CODE ENHANCED SOFT DECODE-AND-FORWARD (SDF) RELAYING SYSTEM WITH TWO RELAYS

7.1 System Model
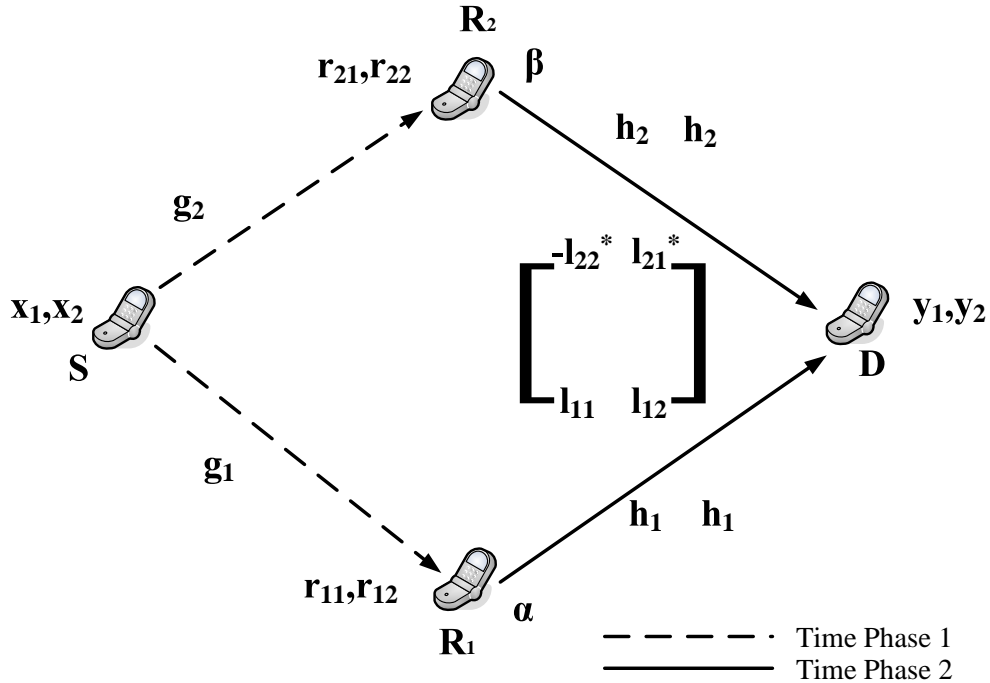
Figure 7.1. The system model of two-relay SDF & DSTBC.

We consider a four-node-network consisting of one source 'S', one destination 'D' and two relays 'R_1' and 'R_2' as shown in Fig. 7.1. All channels (i.e., g_1, g_2, h_1, h_2) are assumed to be mutually independent Rayleigh fading channels. Additive Gaussian noise is assumed at the Relay nodes and the destination node. The relays demodulate and decode the received data stream and generate the reliability values of the source, i.e., the log-likelihood ratio

(LLR) values. This soft information is then coordinately sent to the destination using the Alamouti's code as shown in the solid lines.

The modern decoding algorithms for channel codes, including the sum-product algorithm for low-density parity-check (LDPC) codes and the maximum *a-posteriori* probability (MAP) algorithm for turbo codes, all use the belief propagation and can be collectively called the message-passing algorithms. The soft output of the decoder, represented as the LLR values, can be seen as the result of the sum effect of independent random variables. By the central limit theorem (CLT), these values approach to a Gaussian distribution. This feature is captured in the Gaussian Approximation (GA) in[22]. The solid statistical justification for the GA on why and how well the assumption holds can be found in[22,9,30]. The LLR messages from decoders of message passing algorithms can be approximated by GA. This has been detailed illustrated from Chapter 5. Therefore, the soft value in node $R_i(i = 1, 2)$ for a source bit x_j, after a simple normalization, can be represented as

$$l_{ij} = x_j + n_{ij}, \tag{1}$$

where $n_{ij} \sim \mathcal{CN}(0, \sigma_i^2/\mu_i^2); j = 1, \ldots, N$ are complex normal distributed random variables and N is the number of bits in the source packet. μ_i and σ_i are the mean and variance of the Gaussian approximation. In practice, these values can be obtained from simulation by using all ones (or zeros) as the input bits. As a result, the signal-to-noise-ratio (SNR) of the output signal at ith relay is

$$\gamma_i = \frac{\mu_i^2}{\sigma_i^2}. \tag{2}$$

7.1.1 Space-Time Encoding at Relays

The outputs of relay decoders are rearranged into two signal streams as shown in Table 7.1 and radiated to the destination. α and β are amplifying factors in R_1 and R_2, which can be used to adjust the total transmission power and the power allocation.

After distributed space-time coding, the received data at the destination are

$$\begin{bmatrix} y_1 \\ y_2^* \end{bmatrix} = \begin{bmatrix} \alpha l_{11} & -\beta l_{22}^* \\ \alpha l_{12} & \beta l_{21}^* \end{bmatrix} \begin{bmatrix} h_1 \\ h_2 \end{bmatrix} + \begin{bmatrix} v_1 \\ v_2 \end{bmatrix}$$

where $v_i \sim \mathcal{CN}(0, \sigma_v^2)$ $(i = 1, 2)$ and let $\gamma_v = E_s/\sigma_v^2$. Here E_s is the average power for the signal transmitted from the source. Substituting l_{ij} from (1), the received signals are

$$Y = HX + N + V \qquad (3)$$

where $Y = [y_1, y_2^*]^T$ ("T" represents transpose), $X = [x_1, x_2^*]^T$, $V = [v_1, v_2^*]^T$, $H = \begin{bmatrix} \alpha h_1 & -\beta h_2 \\ \beta h_2^* & \alpha h_1^* \end{bmatrix}$

and $N = \begin{bmatrix} \alpha h_1 n_{11} - \beta h_2 n_{22}^* \\ \alpha h_1^* n_{12}^* + \beta h_2^* n_{21} \end{bmatrix}$.

7.1.2 Space-Time Decoding at Destination

At the destination, the classical space-time decoding algorithm is adopted to estimate the transmitted data, which multiplies the received data with $H^+ = (H^H H)^{-1} H^H$ where H^H is the Hermitian of H. It can be found that

$$H^+ = \frac{1}{\alpha^2 |h_1|^2 + \beta^2 |h_2|^2} \begin{bmatrix} \alpha h_1^* & \beta h_2 \\ -\beta h_2^* & \alpha h_1 \end{bmatrix}$$

Table 7.1. Symbols transmitted at antennas

	time$_1$	time$_2$	time$_3$	time$_4$	...
Antenna at R_2	$-\beta l_{22}^*$	βl_{21}^*	$-\beta l_{24}^*$	βl_{23}^*	...
Antenna at R_1	αl_{11}	αl_{12}	αl_{13}	αl_{14}	...

87

and the estimates of the transmitted symbols $[\hat{x}_1, \hat{x}_2^*]^T$ are

$$
\begin{bmatrix} \hat{x}_1 \\ \hat{x}_2^* \end{bmatrix} = \begin{bmatrix} x_1 \\ x_2^* \end{bmatrix} + H^+ \begin{bmatrix} \alpha h_1 n_{11} - \beta h_2 n_{22}^* \\ \alpha h_1^* n_{12}^* + \beta h_2^* n_{21} \end{bmatrix} + H^+ \begin{bmatrix} v_1 \\ v_2^* \end{bmatrix}.
$$

Since $n_{ij} \sim \mathcal{CN}(0, 1/\gamma_i)$ and $v_i \sim \mathcal{CN}(0, E_s/\gamma_v)$, the SNR of $\hat{x}_i, i = 1, 2$, is found as

$$
\gamma_T = \frac{\alpha^2 |h_1|^2 + \beta^2 |h_2|^2}{\alpha^2 |h_1|^2/\gamma_1 + \beta^2 |h_2|^2/\gamma_2 + 1/\gamma_v}. \tag{4}
$$

7.2 Performance of DSTBC Decoding

7.2.1 Average BER for Decoding of DSTBC

The system average BER performance is based on the distribution of γ_T (i.e., energy per symbol over noise). Given a fixed value γ_T, the BER P_b for coherent binary signals is[83] $P_b(\gamma_T) \approx c_1 Q\left(\sqrt{c_2 \gamma_T}\right)$ where c_1, c_2 are modulation parameters, such as $c_1 = 1, c_2 = 2$ for BPSK. Considering the probability distribution of γ_T, the averaged BER can be obtained as[83]

$$
P_b(\mathcal{E}) = \frac{c_1}{\pi} \int_0^{\pi/2} \mathcal{M}\gamma_T \left(-\frac{c_2}{2 \sin^2 \theta}\right) d\theta \tag{5}
$$

where $\mathcal{M}\gamma_T(\cdot)$ is the moment generating function (MGF) of γ_T. By observing (4), we can see that γ_T is in the form of a function $T = \frac{X+Y}{aX+bY+c}$ with positive constants of a, b and c. Without the loss of generality (WLOG), we assume $a \leq b$ hereafter. Since h_i in γ_T follows $h_i \sim \mathcal{CN}(0, \Omega_i)$, $|h_i|^2$ is exponentially distributed random variable (RV) with parameter $\frac{1}{\Omega_i}$ for $i = 1, 2$. Therefore, we can set X and Y in T as exponential RVs with parameter λ_1 and

λ_2. By comparing γ_T and T, we have the parameters in T as

$$\lambda_1 = \frac{1}{\alpha^2 \Omega_1}, \quad \lambda_2 = \frac{1}{\beta^2 \Omega_2}$$
$$a = 1/\gamma_1, \quad b = 1/\gamma_2, \quad c = 1/\gamma_v \tag{6}$$

In order to solve (5), we need to find the MGF of T first and then tackle the integral in (5) afterwards. We first present the following Lemma.

Lemma 2. *Assume X, Y are exponential random variables with parameter λ_1, λ_2 and $0 < a \le b$, $0 < c$. The MGF $\mathcal{M}_T(s; \lambda_1, \lambda_2)$ of the function $T = \frac{X+Y}{aX+bY+c}$ is given as*

$$\mathcal{M}_T(s; \lambda_1, \lambda_2) = 1 + \int_0^{1/a} s \frac{\exp\left(st - \frac{\lambda_1 ct}{1-at}\right)}{\frac{\lambda_1}{\lambda_2}\frac{bt-1}{1-at}+1} dt$$
$$+ \int_0^{1/b} s\left(1 - \frac{1}{\frac{\lambda_1}{\lambda_2}\frac{bt-1}{1-at}+1}\right) \exp\left(st - \frac{\lambda_2 ct}{1-bt}\right) dt \tag{7}$$

Proof: See Appendix A. $\qquad\qquad\square$

Based on (7), we can further obtain the system average BER as follows.

Theorem 6. *For the system with two relays and soft information forwarding with distributed STBC, given the parameters γ_i ($i = 1, 2$ and $\gamma_1 \ge \gamma_2$) in the Gaussian approximation, the channel statistics $\Omega_i(i = 1, 2)$ and γ_v, the power amplifying factors α and β and the modulation parameters c_1 and c_2, the average BER performance is*

$$P_b(\mathcal{E}) = \frac{c_1}{2} - \frac{c_1\sqrt{c_2}}{2\sqrt{2\pi}}\left[\int_0^{\gamma_1} \frac{\exp\left(-\frac{c_2 t}{2} - \frac{1}{\alpha^2\Omega_1}\frac{t/\gamma_v}{1-t/\gamma_1}\right)}{\sqrt{t}\left(\frac{\beta^2\Omega_2}{\alpha^2\Omega_1}\frac{t/\gamma_2-1}{1-t/\gamma_1}+1\right)} dt\right.$$
$$\left. + \int_0^{\gamma_2}\left(1 - \frac{1}{\frac{\beta^2\Omega_2}{\alpha^2\Omega_1}\frac{t/\gamma_2-1}{1-t/\gamma_1}+1}\right)\frac{\exp\left(-\frac{c_2 t}{2} - \frac{1}{\beta^2\Omega_2}\frac{t/\gamma_v}{1-t/\gamma_2}\right)}{\sqrt{t}} dt\right] \tag{8}$$

Proof: See Appendix B. $\qquad\qquad\square$

This one-integral formula, considering all necessary parameters in the system and channels, can be numerically calculated very easily and thus provides an accurate and quick evaluation of the system performance for various conditions.

7.2.2 Line model

To evaluate the BER performance at the receiver of the proposed two-relay SDF & DSTBC system in (8), we use the line simulation model[60,15] which assumes that the relay is located on the line connecting the source with the destination as in Fig. 6.3. This model is more practical in real systems where the relay is usually located somewhere between the two terminals. We set the distance between source and relay as unit 1 and that between relay and destination as λ. When the relay moves from the source to the destination, λ changes from 1 to 0.

In addition to Rayleigh fading, large path-loss model with path loss exponent $n = 2$ is also considered to calculate the average SNR at the relay and destination nodes in different time phases. That is, the SNR values in two systems are related as

$$\Omega_2 = \Omega_1 = \Omega \cdot \frac{1}{\lambda^2} \tag{9}$$

7.2.3 Power Allocation and Optimization

Power Allocation between the Source and the Relay

In subsection 7.2.1, we discussed the DSTBC decoding performance for our proposed two-relay SDF & DSTBC system in the second time phase. For the convenience of further comparison between one-relay and two-relay system, we use the same notation and method for power allocation in this proposed two-relay system. We use E to represent the total power. E is the sum of E_1 and E_2 which are the power in the first and second time phase respectively. In the first time phase, the power spent in both systems are the same. In order to make the total power between the one-relay and the two-relay systems equal, the power used in the second time phase, which are $E_2^{1-relay}$ and $E_2^{2-relay}$, should be equal to E_s.

For the proposed two-relay system when DSTBC is used, the two relays cooperatively transmit signal to the destination. The transmission factors at the two relays are α and β

respectively. In order to make a fair comparison between the two systems, we need to equal the total energy.

$$
\begin{aligned}
E_2^{2-relay} &= E[|\alpha l_{11}|^2] + E[|\beta l_{21}|^2] \\
&= \alpha^2 E[|\sqrt{E_s}x_1 + n_{11})|^2] + \beta^2 E[|\sqrt{E_s}x_1 + n_{21}^2|^2] \\
&= \alpha^2 (E_s + \sigma_1^2/\mu_1^2) + \beta^2 (E_s + \sigma_2^2/\mu_2^2) = E_s
\end{aligned}
\tag{10}
$$

Then we have

$$
\alpha^2 = \frac{E_s - \beta^2(E_s + \sigma_2^2/\mu_2^2)}{E_s + \sigma_1^2/\mu_1^2} = \frac{1 - \beta^2(1 + 1/\gamma_2)}{1 + 1/\gamma_1}, \quad \beta \in [0,1].
$$

Power Optimization

Substituting the relationship between α and β in Theorem 6, it provides a way to optimally allocate the power between the two relay nodes in the 2nd time phase. For any given channel scenario, (8) is a function of only one parameter β. The optimal β value can be obtained by setting the 1st derivative to be zero. However, by observing (8), it is much involved to find a closed-form equation of this derivative. At this point, a simple numerical method is introduced to find the value of β where the optimal Space-Time decoded performance is achieved. We simply divide β from 0 to 1 into n small steps. For the ith small step, we denote the variation of BER performance as ΔBER_i. Then the optimal power ratio β_{opt} is located at the ith step where $\Delta BER_i \approx 0$. By this method, β_{opt} is easy to obtain.

7.2.4 Numerical and Simulation Results for DSTBC Decoding

We validate the exact BER expression in (8) with Monte-Carlo simulation results. In the reported results here, we choose $\Omega_1 = \Omega_2 = 1$ and $c_1 = 1$, $c_2 = 2$ (i.e., BPSK modulation). First, we unevenly allocate the power at two relays with $\alpha = \sqrt{2/3}, \beta = \sqrt{1/3}$. We also
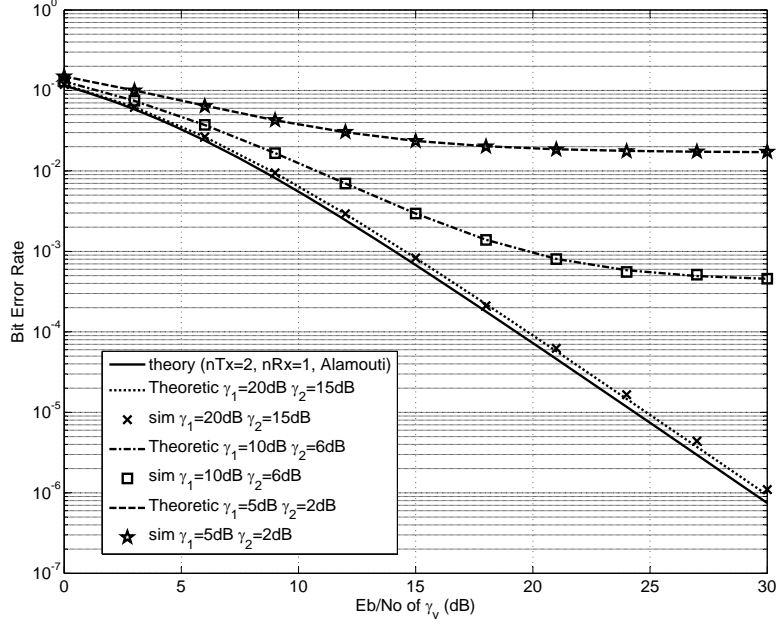
Figure 7.2. Average system BER, $\alpha = \sqrt{\frac{2}{3}}$, $\beta = \sqrt{\frac{1}{3}}$.

pick arbitrary values for SNRs pairs at relays (γ_1 and γ_2) and change the channel condition of the relay link (γ_v) from 0dB to 30dB to evaluate the BER performance. It can be found in Fig. 7.2 that, for all five pairs of SNRs at two relays, the analytic and simulation results match perfectly. The curve of "theory (nTx=2, nRx=1, Alamouti)" shows the well known BER results of the classic Alamouti's code with 2 transmitters and 1 receiver. We can see that when the virtual Gaussian channel SNRs are high ($\gamma_1 = 20dB$ and $\gamma_2 = 15dB$), the system performance with 2 relays approaches to the performance of classic Alamouti's code as expected. Second, we divide power at two relays evenly with $\alpha = \beta = \sqrt{1/2}$. We pick arbitrary γ_v, and for each γ_v and increase the SNRs at both relays from 0dB to 10dB. As shown in Fig. 7.3, the simulation and analytic results again match to each other perfectly.

We also compare the two-relay case with the one-relay case. For the one-relay system, the transmit power is the sum of two-relay case for the fair comparison. As shown in Fig. 7.3, the two-relay system outperforms in both tested scenarios at $\gamma_v = 10$ and 20 dB. These outperforming results show that, for the two-relay scheme, the diversity gain is obtained at
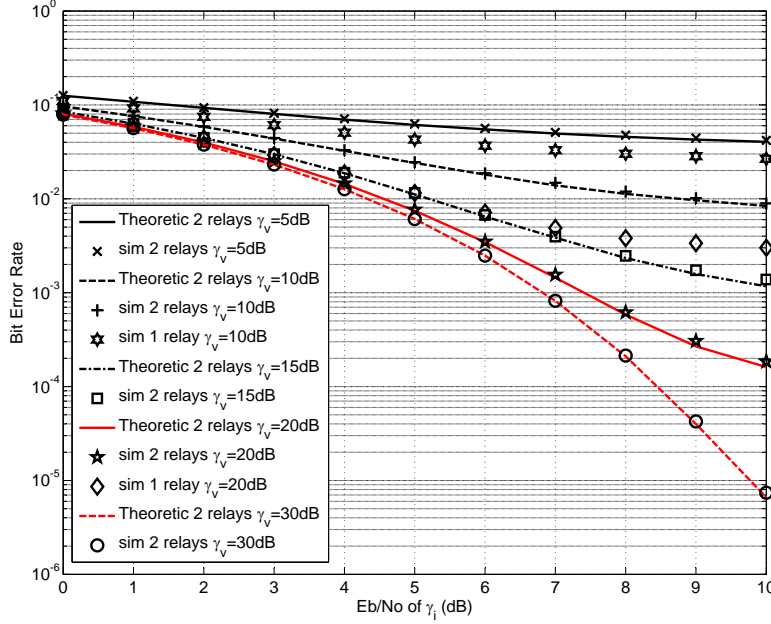
Figure 7.3. Average system BER, $\alpha = \beta = \sqrt{\frac{1}{2}}$.

the receiver by using the distributed STBC.

The result in this section clearly has other potential applications. For example, for given channel conditions and the total power of the relays, (8) may serve as the objective function so that α and β can be optimally selected to minimize the system BER.

7.2.5 Comparison of One-Relay and Two-Relay Systems

We evaluate the BER performance comparison for DSTBC decoding of the one-relay and two-relay systems by changing γ_l, γ_1, γ_2, β and λ where Figs. 7.4 and 7.5 show their averaged BER respectively. The results illustrate that STBC outperforms traditional soft relaying ($\beta = 0$) for most of the cases which is due to the diversity gained reaped with DSTBC. They also show that if the Gaussian approximation SNRs γ_l, γ_1, γ_2 are high (10 dB), the two-relay system outperforms.

Fig. 7.5 contains the theoretical BER when power allocation is used in line model. The relays locates between the source and the destination where $\lambda = 0.3$, $\lambda = 0.5$, $\lambda = 0.8$ and we fix the direct link SNR to 10dB. We compare the BER of three systems: one-relay

93

Figure 7.4. BER performance of proposed two-relay SDF & DSTBC system by changing γ_l when $\lambda = 0.3$, $\Omega_1 = 10dB$, $\gamma_v = 1$

Figure 7.5. BER performance of proposed two-relay SDF & DSTBC system by changing λ when $\gamma_l = 10$, $\Omega_1 = 10dB$, $\gamma_v = 1$

soft information relaying system (without DSTBC), one-relay DSTBC system with source and relay cooperation in the second time phase, and two-relay DSTBC system with two relays cooperation in the second time phase. These results clearly show that when the GA SNR is high (10 dB), two-relay system outperforms one-relay systems due to the channel coding gain obtained at the relays from the soft decoder. We can consi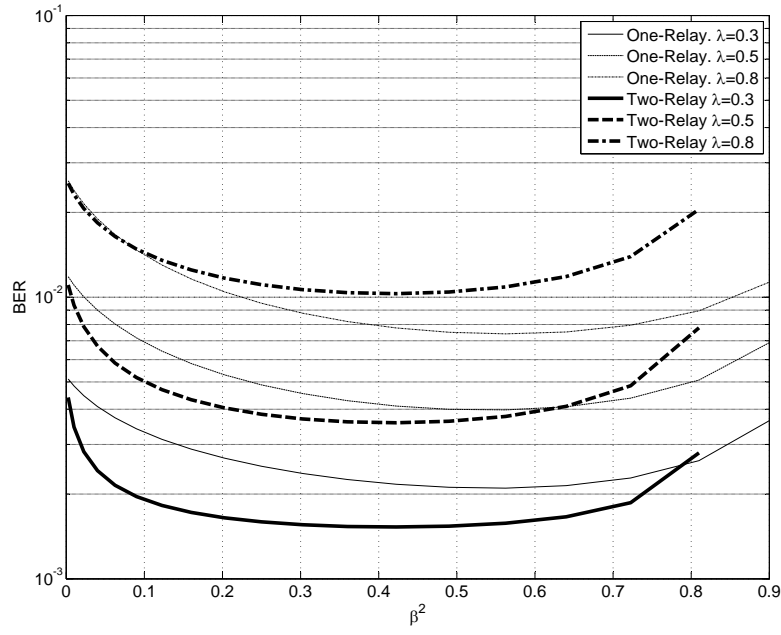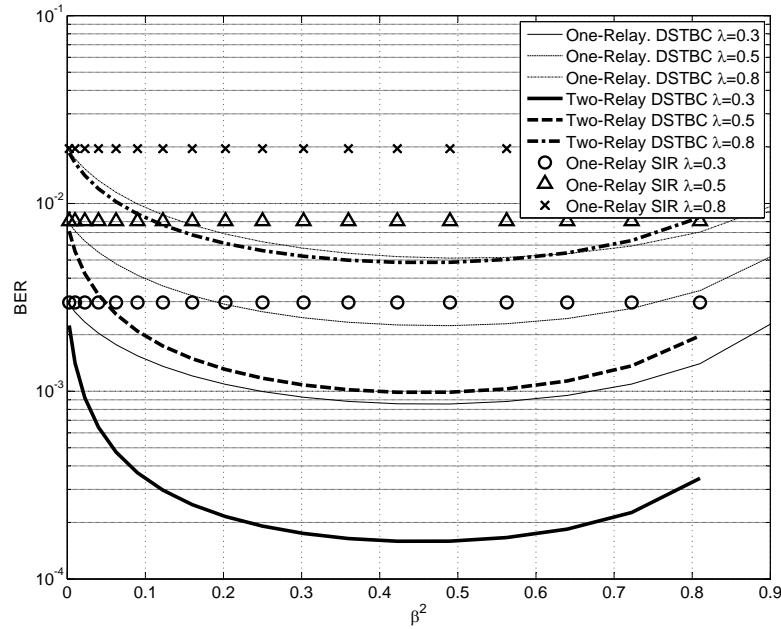der the one-relay soft information relaying system (without DSTBC) as a special case of the one-relay DSTBC system when $\beta = 0$. To verify this extreme case, we evaluate one-relay SIR and one-relay DSTBC system performance when the relay locates where $\lambda = 0.3$, 0.5, and 0.8 and the direct link SNR is fixed to 10dB as well. Fig. 7.5 shows the results and confirm that when $\beta = 0$, the one-relay DSTBC system recedes to one-relay SIR system.

However, the two-relay DSTBC system is not always superior to one-relay DSTBC system, especially when the GA SNR is low (5 dB). Fig. 7.4 shows the comparison of these two systems when the relays cannot obtain good decoding results. With the same system conditions as in the last experiment, the relays locate between the source and the destination where $\lambda = 0.3$, $\lambda = 0.5$, $\lambda = 0.8$ and we fix the direct link SNR to 10dB. For the one-relay system, we change β^2 to allocate different power between the source and the relay. For the one-relay system, changing β^2 makes different power allocation between the two relays. By observing three pairs of curves in Fig. 7.4, when β^2 are small, the two-relay system has better performance while, when β^2 are large, the one-relay system outperforms. It clearly shows the tradeoff on the power allocation between the source and the relays. The source locates farther than the relays to the receiver, however, it transmits clean set of information. There exists a certain point that when the power allocated on the source is large enough, e.g. $\beta^2 > 0.6$ when relays locate at $\lambda = 0.5$, the one-relay system outperforms due to the significant effect of error-free signal transmitted by the source.
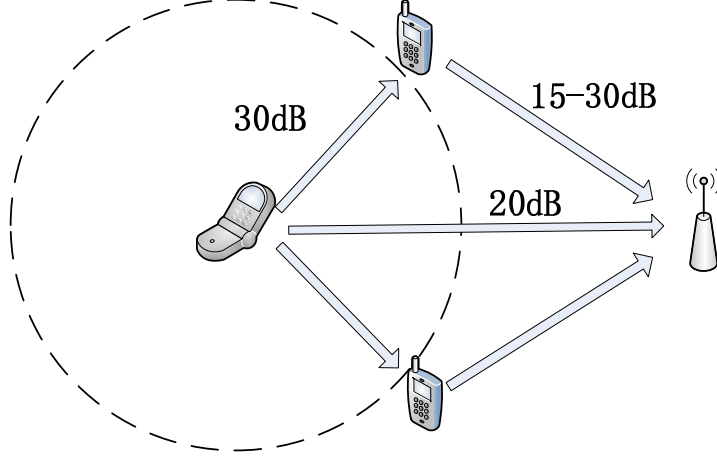
Figure 7.6. Test scenario for two-relay DSTBC system.

7.3   Turbo Decoding and Simulation Results

The destination receives TPC matrix $\{S, P_h\}$ in the first time phase via direct link from the source. Both relays will coordinately forward the TPC matrix P_v using Alamouti's code via two relay paths over different SNRs. Then the destination constructs a complete TPC by arranging the received data matrices S, P_h and P_v in order to start rows and columns iterative decoding.

We test the overall system decoding performance in a 2-dimensional scenario. As shown in Fig. 7.6, two relays can move around the source at fixed distances. We assume the SNR for direct channel is 15dB and SNRs for inter-user channels are fixed to 20dB. Since the distances between the relays and destination are varying, the SNRs for relay channels can be changed from 10dB to 25dB.

Fig. 7.7 shows the overall turbo decoding BER under this scenario. It shows that as the improvement of the relay link condition, the overall decoding performance increases. We can also see an error floor occurs at high SNR_{rd}. This is becuase the direct link condition is fixed, no matter how we increase the relay link condition, the overall performance improvement is limited.
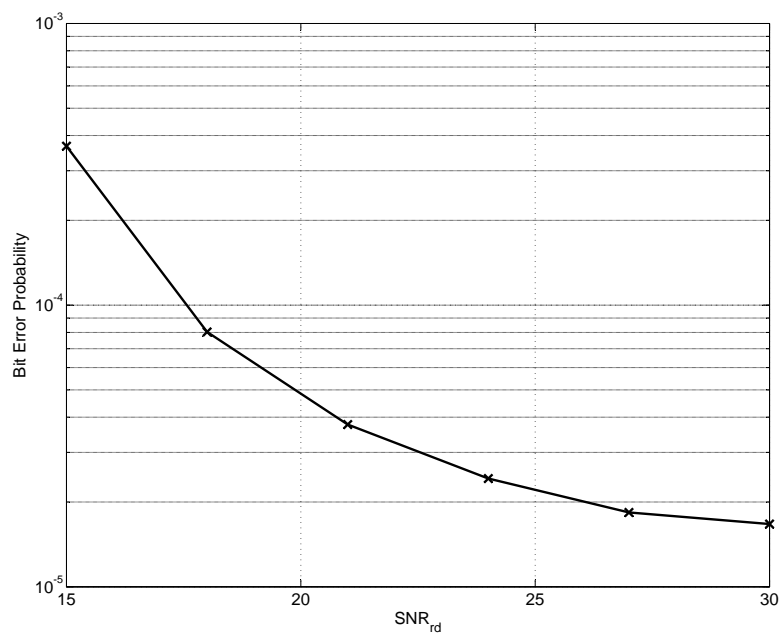
Figure 7.7. Overall performance of the two-relay DSTBC system where $SNR_{sd} = 20$dB and $SNR_{sr} = 30$dB.

Bibliography

Bibliography

1. 3G MIMO. `http://en.wikipedia.org/wiki/3G_MIMO`.

2. S. Abdelkader, C. Pietsch, and J. Lindner. Receive signal processing for space-time coded transmissions in the presence of channel estimation errors. In *Personal, Indoor and Mobile Radio Communications, 2005. PIMRC 2005. IEEE 16th International Symposium on*, volume 1, pages 26 –30, sept. 2005. doi: 10.1109/PIMRC.2005.1651392.

3. J. Abouei, H. Bagheri, and A. Khandani. An efficient adaptive distributed space-time coding scheme for cooperative relaying. *IEEE Trans. Wireless Commun.*, 8(10):4957 – 4962, October 2009.

4. Kyung Seung Ahn and R.W. Heath. Performance analysis of maximum ratio combining with imperfect channel estimation in the presence of cochannel interferences. *IEEE Trans. Wireless Commun.*, 8(3):1080 –1085, march 2009. ISSN 1536-1276. doi: 10. 1109/TWC.2009.080114.

5. N. Al-Dhahir. Single-carrier frequency-domain equalization for space-time block-coded transmissions over frequency-selective fading channels. *Communications Letters, IEEE*, 5(7):304 –306, jul 2001. ISSN 1089-7798. doi: 10.1109/4234.935750.

6. S.M. Alamouti. A simple transmit diversity technique for wireless communications. *IEEE Journal on Selected Areas in Communications*, 16(8):1451 – 1458, 1998.

7. P.A. Anghel and M. Kaveh. On the performance of distributed space-time coding systems with one and two non-regenerative relays. *IEEE Trans. Wireless Commun.*, 5 (3):682 – 692, March 2006.

8. P.A. Anghel, G. Leus, and M. Kaveh. Distributed Space-Time Cooperative Systems with Regenerative Relays. *IEEE Trans. Wireless Commun.*, 5(11):3130 – 3141, November 2006.

9. Xingkai Bao and Jing Li. Efficient message relaying for wireless user cooperation: Decode-amplify-forward (DAF) and hybrid daf and coded-cooperation. *IEEE Trans. Wireless Commun.*, 6(11):3975 – 3984, Nov. 2007.

10. Xingkai Bao and Jing Li. Adaptive network coded cooperation (ANCC) for wireless relay networks: matching code-on-graph with network-on-graph. *IEEE Trans. Wireless Commun.*, 7(2):574 – 583, Feb. 2008.

11. K. Ben Letaief and Wei Zhang. Cooperative communications for cognitive radio networks. *Proceedings of the IEEE*, 97(5):878 –893, may 2009. ISSN 0018-9219. doi: 10.1109/JPROC.2009.2015716.

12. A. Bletsas, A. Khisti, D.P. Reed, and A. Lippman. A simple cooperative diversity method based on network path selection. *Selected Areas in Communications, IEEE Journal on*, 24(3):659 – 672, march 2006. ISSN 0733-8716. doi: 10.1109/JSAC.2005. 862417.

13. A. Bletsas, A.G. Dimitriou, and J.N. Sahalos. Interference-limited opportunistic relaying with reactive sensing. *IEEE Trans. Wireless Commun.*, 9(1):14 –20, january 2010. ISSN 1536-1276. doi: 10.1109/TWC.2010.01.081128.

14. P. O. Borjesson and C.-E. W. Sundberg. Simple approximations of the error function Q(x) for communications applications. *IEEE Trans. Commun.*, COM-27(3):639–643, Mar. 1979.

15. A. Chakrabarti, A. de Baynast, A. Sabharwal, and B. Aazhang. Low density parity check codes for the relay channel. *Selected Areas in Communications, IEEE Journal on*, 25(2):280 –291, february 2007. ISSN 0733-8716. doi: 10.1109/JSAC.2007.070205.

16. D. Chase. Class of algorithms for decoding block codes with channel measurement information. *IEEE Trans. Inf. Theory*, 18(1):170–182, 1972. ISSN 0018-9448.

17. C.-J. Chen and Li-Chun Wang. A unified capacity analysis for wireless systems with joint multiuser scheduling and antenna diversity in nakagami fading channels. *IEEE Trans. Commun.*, 54(3):469 – 478, march 2006. ISSN 0090-6778. doi: 10.1109/TCOMM.2005.863778.

18. Yung-Fang Chen and Chia-Shu Wang. Adaptive antenna arrays for interference cancellation in ofdm communication systems with virtual carriers. *IEEE Trans. Vehi. Tech.*, 56(4):1837 –1844, july 2007. ISSN 0018-9545. doi: 10.1109/TVT.2007.897653.

19. M. Chiani, D. Dardari, and M. K. Simon. New exponential bounds and approximations for the computation of error probability in fading channels. *IEEE Trans. Wireless Commun.*, 2(4):840–845, July 2003.

20. N. Chiurtu, B. Rimoldi, and E. Telatar. On the capacity of multi-antenna gaussian channels. In *Information Theory, 2001. Proceedings. 2001 IEEE International Symposium on*, page 53, 2001. doi: 10.1109/ISIT.2001.935916.

21. Jinho Choi. Opportunistic beamforming with single beamforming matrix for virtual antenna arrays. *IEEE Trans. Vehi. Tech.*, 60(3):872 –881, march 2011. ISSN 0018-9545. doi: 10.1109/TVT.2011.2113197.

22. Sae-Young Chung, T.J. Richardson, and R.L. Urbanke. Analysis of sum-product decoding of low-density parity-check codes using a Gaussian approximation. *IEEE Trans. Inf. Theory*, 47(2):657 – 670, Feb. 2001.

23. A. Coskun and C. Candan. Transmit precoding for flat-fading mimo multiuser systems with maximum ratio combining receivers. *IEEE Trans. Vehi. Tech.*, 60(2):710 –716, feb. 2011. ISSN 0018-9545. doi: 10.1109/TVT.2010.2096484.

24. D.B. da Costa and S. Aissa. Performance of Cooperative Diversity Networks: Analysis of Amplify-and-Forward Relaying under Equal-Gain and Maximal-Ratio Combining. In *IEEE International Conference on Communications, 2009.*, pages 1 – 5, August 2009.

25. Lin Dai and K. Letaief. Throughput maximization of ad-hoc wireless networks using adaptive cooperative diversity and truncated arq. *IEEE Trans. Commun.*, 56(11):1907 –1918, november 2008. ISSN 0090-6778. doi: 10.1109/TCOMM.2008.041164.

26. P.A. Dighe, R.K. Mallik, and S.S. Jamuar. Analysis of transmit-receive diversity in rayleigh fading. *IEEE Trans. Commun.*, 51(4):694 – 703, april 2003. ISSN 0090-6778. doi: 10.1109/TCOMM.2003.810871.

27. M. Dohler, M. Hussain, A. Desai, and H. Aghvami. Performance of distributed space-time block codes. In *Vehicular Technology Conference, 2004. VTC 2004-Spring. 2004 IEEE 59th*, volume 2, pages 742 – 746 Vol.2, may 2004. doi: 10.1109/VETECS.2004. 1388927.

28. H. El Gamal and Jr. Hammons, A.R. Analyzing the turbo decoder using the gaussian approximation. *Information Theory, IEEE Transactions on*, 47(2):671 –686, feb 2001. ISSN 0018-9448. doi: 10.1109/18.910581.

29. S.E. El-Khamy, E.E. Sourour, and T.A. Kadous. Analysis of incoherent pre-rake td-d/dpsk/cdma wireless portable communications. In *Radio Science Conference, 1998. NRSC '98. Proceedings of the Fifteenth National*, pages C13/1 –C13/8, feb 1998. doi: 10.1109/NRSC.1998.711474.

30. M. Fu. Stochastic analysis of turbo decoding. *IEEE Trans. Inf. Theory*, 51(1):81 – 100, Jan. 2005.

31. Andrea Goldsmith. *Wireless Communications*. Cambridge University Press, August 2005.

32. I. S. Gradshteyn and I. M. Ryzhik. *Table of Integrals, Series and Products*. Academic Press, San Diego, CA, 7th edition, 2007.

33. Quansheng Guan, F.R. Yu, Shengming Jiang, and V.C.M. Leung. Capacity-optimized topology control for manets with cooperative communications. *IEEE Trans. Wireless Commun.*, 10(7):2162 –2170, july 2011. ISSN 1536-1276. doi: 10.1109/TWC.2011. 060711.100702.

34. P. Gupta and P.R. Kumar. The capacity of wireless networks. *IEEE Trans. Inf. Theory*, 46(2):388 –404, mar 2000. ISSN 0018-9448. doi: 10.1109/18.825799.

35. J. Hagenauer, E. Offer, and L. Papke. Iterative decoding of binary block and convolutional codes. *Trans. Inf. Theory*, 42(2):429–445, Mar 1996. ISSN 0018-9448. doi: 10.1109/18.485714.

36. L. Hanzo, T.H. Liew, and B.L. Yeap. *Turbo coding, turbo equalisation and space-time coding for transmission over fading channels.* Wiley-IEEE Press, 2002.

37. Lajos L. Hanzo, T. H. Liew, and B. L. Yeap. *Turbo Coding, Turbo Equalisation and Space-Time Coding for Transmission over Fading Channels.* Wiley-IEEE Press, 1st edition, 2002.

38. M.O. Hasna and M.-S. Alouini. Performance analysis of two-hop relayed transmissions over Rayleigh fading channels. In *Vehicular Technology Conference, 2002.*, volume 4, pages 1992 – 1996, December 2002.

39. M.O. Hasna and M.-S. Alouini. A performance study of dual-hop transmissions with fixed gain relays. *IEEE Trans. Wireless Commun.*, 3(6):1536–1276, January 2005.

40. Y-W. Hong, W.-J. Huang, F-H. Chiu, and C.-C.J. Kuo. Cooperative communications in resource-constrained wireless networks. *Signal Processing Magazine, IEEE*, 24(3):47 –57, may 2007. ISSN 1053-5888. doi: 10.1109/MSP.2007.361601.

41. R. Hoshyar and R. Tafazolli. Soft decode and forward of MQAM modulations for cooperative relay channels. In *IEEE Vehicular Technology Conference*, pages 639 – 643, May 2008.

42. Yao Hua, Qian Zhang, and Zhisheng Niu. A cooperative mac protocol with virtual-antenna array support in a multi-ap wlan system. *IEEE Trans. Wireless Commun.*, 8 (9):4806 –4814, september 2009. ISSN 1536-1276. doi: 10.1109/TWC.2009.081505.

43. Hon Tat Hui. The performance of the maximum ratio combining method in correlated rician-fading channels for antenna-diversity signal combining. *Antennas and Propagation, IEEE Transactions on*, 53(3):958 – 964, march 2005. ISSN 0018-926X. doi: 10.1109/TAP.2004.842649.

44. T.E. Hunter, S. Sanayei, and A. Nosratinia. Outage analysis of coded cooperation. *IEEE Trans. Inf. Theory*, 52(2):375 – 391, feb. 2006. ISSN 0018-9448. doi: 10.1109/ TIT.2005.862084.

45. Peng Huo and Lei Cao. Error performance of cooperative diversity with distributed Space-Time code. In *International Conference on Computing, Networking and Communications, Wireless Communications Symposium (ICNC'12 - WC)*, Maui, Hawaii, USA, January 2012.

46. S.S. Ikki and M.H. Ahmed. Performance Analysis of Generalized Selection Combining for Amplify-and-Forward Cooperative-Diversity Networks. In *IEEE International Conference on Communications, 2009.*, pages 1 – 6, June 2009.

47. M. Janani, A. Hedayat, T.E. Hunter, and A. Nosratinia. Coded cooperation in wireless communications: space-time transmission and iterative decoding. *IEEE Transactions on Signal Processing*, 52(2):362 – 371, Feb. 2004.

48. Yindi Jing and H. Jafarkhani. Relay Power Allocation in Distributed Space-Time Coded Networks with Channel Statistical Information. *IEEE Trans. Wireless Commun.*, 10(2):443 – 449, February 2011.

49. Minchul Ju, Hyoung-Kyu Song, and Il-Min Kim;. Exact BER analysis of distributed alamouti's code for cooperative diversity networks. *IEEE Trans. Commun.*, 57(8):2380 – 2390, Aug. 2009.

50. G. K. Karagiannidis and A. S. Lioumpas. An improved approximation for the Gaussian Q-function. *IEEE Commun. Lett*, 11(8):644–646, Aug. 2007.

51. Y.G. Kim and N.C. Beaulieu. Exact closed-form solutions for the bep of decode-and-forward cooperative systems in nakagami-m fading channels. *IEEE Trans. Commun.*, 59(9):2355 –2361, september 2011. ISSN 0090-6778. doi: 10.1109/TCOMM.2011. 062311.100040.

52. I. Krikidis, J. Thompson, S. Mclaughlin, and N. Goertz. Max-min relay selection for legacy amplify-and-forward systems with interference. *IEEE Trans. Wireless Commun.*, 8(6):3016 –3027, june 2009. ISSN 1536-1276. doi: 10.1109/TWC.2009.080383.

53. J.N. Laneman and G.W. Wornell. Distributed space-time-coded protocols for exploiting cooperative diversity in wireless networks. *IEEE Trans. Inf. Theory*, 49(10):2415 – 2425, Oct. 2003.

54. J.N. Laneman, D.N.C. Tse, and G.W. Wornell. Cooperative diversity in wireless networks: Efficient protocols and outage behavior. *IEEE Trans. Inf. Theory*, 50(12):3062 – 3080, Dec. 2004.

55. Erik G. Larsson and Petre Stoica. *Space-Time Block Coding for Wireless Communications*. Cambridge University Press, 2003.

56. N. Le, A.R. Soleymani, and Y.R. Shayan. Distance-based-decoding of block turbo codes. *Communications Letters, IEEE*, 9(11):1006–1008, Nov. 2005. ISSN 1089-7798. doi: 10.1109/LCOMM.2005.11014.

57. I.E. Lee, M.L. Sim, and F.W.L. Kung. Performance enhancement of outdoor visible-light communication system using selective combining receiver. *Optoelectronics, IET*, 3(1):30 –39, february 2009. ISSN 1751-8768. doi: 10.1049/iet-opt:20070014.

58. In-Ho Lee and Dongwoo Kim. End-to-end BER analysis for dual-hop ostbc transmissions over Rayleigh fading channels. *IEEE Trans. Commun.*, 56(3):347 – 351, March 2008.

59. Yinman Lee and Ming-Hung Tsai. Performance of decode-and-forward cooperative communications over nakagami-m fading channels. *IEEE Trans. Vehi. Tech.*, 58(3): 1218 –1228, march 2009. ISSN 0018-9545. doi: 10.1109/TVT.2008.928907.

60. Chuxiang Li, Guosen Yue, M.A. Khojastepour, Xiaodong Wang, and M. Madihian. Ldpc-coded cooperative relay systems: performance analysis and code design. *Communications, IEEE Transactions on*, 56(3):485 –496, march 2008. ISSN 0090-6778. doi: 10.1109/TCOMM.2008.060032.

61. Y. Li, B. Vucetic, T. F. Wong, and M. Dohler. Distributed turbo coding with soft information relaying in multihop relay networks. 24(11):2040–2050, 2006. ISSN 0733-8716. doi: 10.1109/JSAC.2006.881630.

62. Y. Li, B. Vucetic, T.F. Wong, and M. Dohler. Distributed turbo coding with soft information relaying in multihop relay networks. *Selected Areas in Communications, IEEE Journal on*, 24(11):2040–2050, Nov. 2006. ISSN 0733-8716. doi: 10.1109/JSAC. 2006.881630.

63. Yabo Li, Wei Zhang, and Xiang-Gen Xia. Distributive high-rate space frequency codes achieving full cooperative and multipath diversities for asynchronous cooperative communications. *IEEE Trans. Vehi. Tech.*, 58(1):207 –217, jan. 2009. ISSN 0018-9545. doi: 10.1109/TVT.2008.923678.

64. Pei Liu, Zhifeng Tao, Zinan Lin, E. Erkip, and S. Panwar. Cooperative wireless communications: a cross-layer approach. *Wireless Communications, IEEE*, 13(4):84 –92, aug. 2006. ISSN 1536-1284. doi: 10.1109/MWC.2006.1678169.

65. T.K.Y. Lo. Maximum ratio transmission. *IEEE Trans. Commun.*, 47(10):1458 –1461, oct 1999. ISSN 0090-6778. doi: 10.1109/26.795811.

66. P. Loskot and N. C. Beaulieu. Prony and polynomial approximations for evaluation of the average probability of error over slow-fading channels. *IEEE Trans. Veh. Tech.*, 58 (3):1269–1280, Mar. 2009.

67. M.A. Maddah-Ali and A.K. Khandani. A new non-orthogonal space-time code with low decoding complexity. *IEEE Trans. Wireless Commun.*, 5(5):1115 – 1121, may 2006. ISSN 1536-1276. doi: 10.1109/TWC.2006.1633364.

68. Y. Mao and M. Wu. Tracing malicious relays in cooperative wireless communications. *Information Forensics and Security, IEEE Transactions on*, 2(2):198 –212, june 2007. ISSN 1556-6013. doi: 10.1109/TIFS.2007.897242.

69. H. Mheidat, M. Uysal, and N. Al-Dhahir. Equalization techniques for distributed space-time block codes with amplify-and-forward relaying. *Signal Processing, IEEE Transactions on*, 55(5):1839 –1852, may 2007. ISSN 1053-587X. doi: 10.1109/TSP. 2006.889974.

70. P. Mitran, H. Ochiai, and V. Tarokh. Space-time diversity enhancements using collaborative communications. *IEEE Trans. Inf. Theory*, 51(6):2041 – 2057, june 2005. ISSN 0018-9448. doi: 10.1109/TIT.2005.847731.

71. A. Muller and J. Speidel. Exact symbol error probability of m-psk for multihop transmission with regenerative relays. *Communications Letters, IEEE*, 11(12):952 –954, december 2007. ISSN 1089-7798. doi: 10.1109/LCOMM.2007.070820.

72. P. Murphy and A. Sabharwal. Design, implementation, and characterization of a cooperative communications system. *IEEE Trans. Vehi. Tech.*, 60(6):2534 –2544, july 2011. ISSN 0018-9545. doi: 10.1109/TVT.2011.2158461.

73. R.U. Nabar, H. Bolcskei, and F.W. Kneubuhler. Fading relay channels: performance limits and space-time signal design. *Selected Areas in Communications, IEEE Journal on*, 22(6):1099 – 1109, aug. 2004. ISSN 0733-8716. doi: 10.1109/JSAC.2004.830922.

74. E. Obiedat, G. Chen, and L. Cao. Distributed turbo product codes over multiple relays. *7th IEEE Consumer Communications and Networking Conference, 2010. CCNC 2010*, 2010.

75. E.A. Obiedat, Wei Xiang, J. Leis, and Lei Cao. Soft incremental redundancy for distributed turbo product codes. In *Consumer Communications and Networking Conference*, pages 1–5, Las Vegas, NV, Jan 2010.

76. Esam A. Obiedat and Lei Cao. Joint Distributed Space-Time Block Coding with Distributed Turbo Product Code (DSTBC-DTPC). In *Global Telecommunications Conference, 2011. GLOBECOM '11. IEEE*, Dec. 2011.

77. Sheldon M. Ross. *Introduction to Probability Models*. Academic Press, eighth edition, 2003.

78. A.K. Sadek, Weifeng Su, and K.J.R. Liu. Performance analysis for multi-node decode-and-forward relaying in cooperative wireless networks. In *Acoustics, Speech, and Signal Processing, 2005. Proceedings. (ICASSP '05). IEEE International Conference on*, volume 3, pages iii/521 – iii/524 Vol. 3, march 2005. doi: 10.1109/ICASSP.2005.1415761.

79. A.K. Sadek, Weifeng Su, and K.J.R. Liu. Multinode cooperative communications in wireless networks. *Signal Processing, IEEE Transactions on*, 55(1):341 –355, jan. 2007. ISSN 1053-587X. doi: 10.1109/TSP.2006.885773.

80. S. Savazzi and U. Spagnolini. Cooperative space-time coded transmissions in nakagami-m fading channels. In *Global Telecommunications Conference, 2007. GLOBECOM '07. IEEE*, pages 4334 –4338, nov. 2007. doi: 10.1109/GLOCOM.2007.824.

81. G. Scutari and S. Barbarossa. Distributed space-time coding for regenerative relay networks. *IEEE Trans. Wireless Commun.*, 4(5):2387 – 2399, Sept. 2005.

82. A. Sendonaris, E. Erkip, and B. Aazhang. User cooperation diversity. part ii. implementation aspects and performance analysis. *IEEE Trans. Commun.*, 51(11):1939 – 1948, nov. 2003. ISSN 0090-6778. doi: 10.1109/TCOMM.2003.819238.

83. Marvin K. Simon and Mohamed-Slim Alouini. *Digital Communication over Fading Channels: A Unified Approach to Performance Analysis*. Wiley-Interscience, 1st edition, 2000.

84. M.K. Simon and M.-S. Alouini. A unified performance analysis of digital communication with dual selective combining diversity over correlated rayleigh and nakagami-m fading channels. *IEEE Trans. Commun.*, 47(1):33 –43, jan 1999. ISSN 0090-6778. doi: 10.1109/26.747811.

85. M.A. Smadi, V.K. Prabhu, and A.K.S. Al-Bayati. Performance analysis of optimum diversity combining for partially coherent frequency-selective fading channel with intersymbol interference. *IEEE Trans. Vehi. Tech.*, 57(6):3589 –3597, nov. 2008. ISSN 0018-9545. doi: 10.1109/TVT.2008.921614.

86. H. Sneesens and L. Vandendorpe. Soft decode and forward improves cooperative communications. In *Computational Advances in Multi-Sensor Adaptive Processing, 2005 1st IEEE International Workshop on*, pages 157–160, 2005.

87. Harold H. Sneessens and Luc Vandendorpe. Soft decode and forward improves cooperative communications. In *IEE International Conference on 3G and Beyond*, pages 1 – 4, Nov. 2005.

88. M.P. Sousa, R.F. Lopes, A. Kumar, W.T.A. Lopes, and M.S. Alencar. Cooperative stbc with fuzzy election applied to surveillance wireless video sensor networks. In *GLOBECOM Workshops (GC Wkshps), 2010 IEEE*, pages 241 –245, dec. 2010. doi: 10.1109/GLOCOMW.2010.5700318.

89. Weifeng Su. Performance analysis for a suboptimum ml receiver in decode-and-forward communications. In *Global Telecommunications Conference, 2007. GLOBECOM '07. IEEE*, pages 2962 –2966, nov. 2007. doi: 10.1109/GLOCOM.2007.561.

90. Weifeng Su, A.K. Sadek, and K.J.R. Liu. Ser performance analysis and optimum power allocation for decode-and-forward cooperation protocol in wireless networks. In *Wireless Communications and Networking Conference, 2005 IEEE*, volume 2, pages 984 – 989 Vol. 2, march 2005. doi: 10.1109/WCNC.2005.1424642.

91. Li Sun, Taiyi Zhang, Long Lu, and Hao Niu. Cooperative communications with relay selection in wireless sensor networks. *Consumer Electronics, IEEE Transactions on*, 55(2):513 –517, may 2009. ISSN 0098-3063. doi: 10.1109/TCE.2009.5174415.

92. H.A. Suraweera, D.S. Michalopoulos, and G.K. Karagiannidis. Performance of Distributed Diversity Systems with a Single Amplify-and-Forward Relay. *IEEE Trans. Vehi. Tech.*, 58(5):2603 – 2608, June 2009.

93. Beng Soon Tan, Kwok Hung Li, and Kah Chan Teh. Performance analysis of LD-PC codes with maximum-ratio combining cascaded with selection combining over nakagami-m fading. *IEEE Trans. Wireless Commun.*, 10(6):1886 –1894, June 2011. ISSN 1536-1276. doi: 10.1109/TWC.2011.040511.101226.

94. V. Tarokh, N. Seshadri, and A.R. Calderbank. Space-time codes for high data rate wireless communication: performance criterion and code construction. *IEEE Trans. Inf. Theory*, 44(2):744 –765, mar 1998. ISSN 0018-9448. doi: 10.1109/18.661517.

95. V. Tarokh, H. Jafarkhani, and A.R. Calderbank. Space-time block coding for wireless communications: performance results. *IEEE Journal on Selected Areas in Communications*, 17(3):451 – 460, Mar. 1999.

96. V. Tarokh, H. Jafarkhani, and A.R. Calderbank. Space-time block codes from orthogonal designs. *IEEE Trans. Inf. Theory*, 45(5):1456 –1467, jul 1999. ISSN 0018-9448. doi: 10.1109/18.771146.

97. S. Thoen, L. Van der Perre, B. Gyselinckx, and M. Engels. Performance analysis of combined transmit-sc/receive-mrc. *IEEE Trans. Commun.*, 49(1):5 –8, jan 2001. ISSN 0090-6778. doi: 10.1109/26.898241.

98. K. Tourki, M.-S. Alouini, and L. Deneire. Blind Cooperative Diversity using Distributed Space-Time Coding in Block Fading Channels. *IEEE Trans. Commun.*, 58(8):2447 – 2456, August 2010.

99. K. Vardhe, Chi Zhou, and D. Reynolds. Energy efficiency analysis of multistage cooperation in sensor networks. In *GLOBECOM 2010, 2010 IEEE Global Telecommunications Conference*, pages 1 –5, dec. 2010. doi: 10.1109/GLOCOM.2010.5684156.

100. A. Vosoughi and Yupeng Jia. Maximizing throughput in cooperative networks via cross-layer adaptive designs. In *Sarnoff Symposium, 2010 IEEE*, pages 1 –6, april 2010. doi: 10.1109/SARNOF.2010.5469737.

101. K. Woradit, T.Q.S. Quek, and Z.Z. Lei. Cooperative multicell arq in mimo cellular systems. In *Signal Processing Advances in Wireless Communications (SPAWC), 2010 IEEE Eleventh International Workshop on*, pages 1 –5, june 2010. doi: 10.1109/SPAWC.2010.5670997.

102. J. Yackoski, L. Zhang, C.-C. Shen, L. Cimini, and B. Gui. Networking with cooperative communications: Holistic design and realistic evaluation. *Communications Magazine, IEEE*, 47(8):113 –119, august 2009. ISSN 0163-6804. doi: 10.1109/MCOM.2009.5181901.

103. Lie-Liang Yang and Hsiao-Hwa Chen. Error probability of digital communications using relay diversity over nakagami-m fading channels. *IEEE Trans. Wireless Commun.*, 7 (5):1806 –1811, may 2008. ISSN 1536-1276. doi: 10.1109/TWC.2008.061086.

104. Zhihang Yi and Il-Min Kim. Diversity order analysis of the decode-and-forward co-operative networks with relay selection. *IEEE Trans. Wireless Commun.*, 7(5):1792 –1799, may 2008. ISSN 1536-1276. doi: 10.1109/TWC.2008.061041.

105. Qi Zhang and A. Nallanathan. Transmitted-reference impulse radio systems based on selective combining. *IEEE Trans. Wireless Commun.*, 7(11):4105 –4109, november 2008. ISSN 1536-1276. doi: 10.1109/T-WC.2008.070587.

106. Qinqing Zhang and S.A. Kassam. Hybrid arq with selective combining for fading channels. *Selected Areas in Communications, IEEE Journal on*, 17(5):867 –880, may 1999. ISSN 0733-8716. doi: 10.1109/49.768201.

107. Shunqing Zhang and V.K.N. Lau. Multi-relay selection design and analysis for multi-stream cooperative communications. *IEEE Trans. Wireless Commun.*, 10(4):1082 –1089, april 2011. ISSN 1536-1276. doi: 10.1109/TWC.2011.020111.090520.

108. Lizhong Zheng and D.N.C. Tse. Diversity and multiplexing: a fundamental tradeoff in multiple-antenna channels. *IEEE Trans. Inf. Theory*, 49(5):1073 – 1096, may 2003. ISSN 0018-9448. doi: 10.1109/TIT.2003.810646.

109. Y. Zhou, S. Rondineau, D. Popovic, A. Sayeed, and Z. Popovic. Virtual channel space time processing with dual-polarization discrete lens antenna arrays. *Antennas and Propagation, IEEE Transactions on*, 53(8):2444 – 2455, aug. 2005. ISSN 0018-926X. doi: 10.1109/TAP.2005.852518.

110. Yong Zhou, Ju Liu, Chao Zhai, and L. Zheng. Two-transmitter two-receiver cooperative mac protocol: Cross-layer design and performance analysis. *IEEE Trans. Vehi. Tech.*, 59(8):4116 –4127, oct. 2010. ISSN 0018-9545. doi: 10.1109/TVT.2010.2060216.

LIST OF APPENDICES

APPENDIX:A

THE DERIVATION OF AN ERROR PROBABILITY $P_b(\boldsymbol{\gamma}, \boldsymbol{\Omega}, c_1, c_2)$

IN A ONE-INTEGRAL FORM

Since h_2 is circularly symmetric complex Gaussian variable, i.e., $h_2 \sim \mathcal{CN}(0, \Omega_2)$, the PDF of $|h_2|^2$, $f_{h_2}(t)$, is an exponential function with parameter $\frac{1}{\Omega_2}$. By including this PDF according to the definition of expectation and settting $Z = \frac{c_2/2}{\frac{\alpha^2 t}{\gamma_n} + \frac{1}{\gamma_v}}$, (18) becomes

$$
\begin{aligned}
P_b(\mathcal{E}) &= \frac{c_1}{\pi} \int_0^{\pi/2} \int_0^{\infty} \frac{1}{1 + \frac{c_2}{2\sin^2\theta}\gamma_w\Omega_1} \cdot \frac{1}{1 + \frac{1}{\sin^2\theta}Z\beta^2\Omega_1} \cdot \frac{1}{1 + \frac{1}{\sin^2\theta}Z\alpha^2 t\Omega} \cdot \frac{1}{\Omega_2}e^{-\frac{t}{\Omega_2}}\,dt\,d\theta \\
&= \frac{c_1}{\pi} \int_0^{\infty} \frac{1}{\Omega_2}\exp\left(-\frac{t}{\Omega_2}\right) \cdot \int_0^{\pi/2} \frac{1}{1 + \frac{c_2}{2\sin^2\theta}\gamma_w\Omega_1} \\
&\quad \cdot \frac{1}{1 + \frac{1}{\sin^2\theta}Z\beta^2\Omega_1} \cdot \frac{1}{1 + \frac{1}{\sin^2\theta}Z\alpha^2 t\Omega} \cdot d\theta \cdot dt
\end{aligned}
\tag{11}
$$

Set $u = \frac{1}{\tan\theta}$, then we have $1 + u^2 = \frac{1}{\sin^2\theta}$, $du = \frac{-1}{\sin^2\theta}d\theta$, $d\theta = -\sin^2\theta\,du = -\frac{1}{1+u^2}du$.

$$
\begin{aligned}
P_b(\mathcal{E}) &= \frac{c_1}{\pi} \int_0^{\infty} \frac{1}{\Omega_2}\exp\left(-\frac{t}{\Omega_2}\right) \cdot \int_0^{+\infty} \frac{1}{1 + \frac{1}{2}(1+u^2)c_2\gamma_w\Omega_1} \cdot \\
&\quad \frac{1}{1 + (1+u^2)Z\beta^2\Omega_1} \cdot \frac{1}{1 + (1+u^2)Z\alpha^2 t\Omega} \cdot \frac{1}{1+u^2}du \cdot dt.
\end{aligned}
\tag{12}
$$

Set $A = Z\beta^2\Omega_1$, $B = Z\alpha^2 t\Omega$, $C = \frac{1}{2}c_2\gamma_w\Omega_1$, and the integration of u as $P_b^{(u)}(\boldsymbol{\gamma}, \boldsymbol{\Omega}, c_1, c_2)$

So,

$$P_b^{(u)}(\boldsymbol{\gamma}, \boldsymbol{\Omega}, c_1, c_2)$$

$$= \int_0^{+\infty} \frac{1}{Au^2 + A + 1} \cdot \frac{1}{Bu^2 + B + 1} \cdot \frac{1}{Cu^2 + C + 1} \cdot \frac{1}{u^2 + 1} du$$

$$= \int_0^{+\infty} [\frac{1}{u^2 + 1} - \frac{A^3}{(A-B)(A-C)} \frac{1}{Au^2 + A + 1} + \frac{B^3}{(A-B)(B-C)} \frac{1}{Bu^2 + B + 1}$$

$$+ \frac{C^3}{(A-C)(C-B)} \frac{1}{Cu^2 + C + 1}] du$$

$$= \int_0^{+\infty} \frac{1}{u^2 + 1} du - \frac{A^3}{(A-B)(A-C)} \int_0^{+\infty} \frac{1}{Au^2 + A + 1} du + \frac{B^3}{(A-B)(B-C)}$$

$$\int_0^{+\infty} \frac{1}{Bu^2 + B + 1} du + \frac{C^3}{(A-C)(C-B)} \int_0^{+\infty} \frac{1}{Cu^2 + C + 1} du \qquad (13)$$

From [32], it is known that

$$\int \frac{1}{a + bx^2} dx = \frac{1}{\sqrt{ab}} \arctan x\sqrt{\frac{b}{a}} \qquad if \quad [ab > 0].$$

Then,

$$P_b^{(u)}(\boldsymbol{\gamma}, \boldsymbol{\Omega}, c_1, c_2)$$

$$= \arctan u|_0^{+\infty} - \frac{A^3}{(A-B)(A-C)} \frac{1}{\sqrt{A(A+1)}} \arctan \left(u\sqrt{\frac{A}{A+1}} \right) \Big|_0^{+\infty}$$

$$+ \frac{B^3}{(A-B)(B-C)} \frac{1}{\sqrt{B(B+1)}} \arctan \left(u\sqrt{\frac{B}{B+1}} \right) \Big|_0^{+\infty}$$

$$+ \frac{C^3}{(A-C)(C-B)} \frac{1}{\sqrt{C(C+1)}} \arctan \left(u\sqrt{\frac{C}{C+1}} \right) \Big|_0^{+\infty}$$

$$= \frac{\pi}{2} \Big[1 - \frac{A^3}{(A-B)(A-C)} \frac{1}{\sqrt{A(A+1)}}$$

$$+ \frac{B^3}{(A-B)(B-C)} \frac{1}{\sqrt{B(B+1)}} + \frac{C^3}{(A-C)(C-B)} \frac{1}{\sqrt{C(C+1)}} \Big] \qquad (14)$$

Therefore, we have obtained the exact one-integral form of BER performance of the distributed Alamouti's code for proposed cooperative diversity system as stated in (19) in Theorem 2.

APPENDIX:B

THE DERIVATION OF $W(\rho_i, c_2, \boldsymbol{\gamma}, \boldsymbol{\Omega})$ USING APPROXIMATION METHODS

Since,

$$
\begin{aligned}
W(\rho_i, c_2, \boldsymbol{\gamma}, \boldsymbol{\Omega}) &= E_{h_{11}, h_{12}, h, h_2}[\exp(-\rho_i c_2 \gamma_T)] \\
&= E_{h_2}[E_{h_{11}, h_{12}, h}[\exp(-\rho_i c_2 (\gamma_w |h_{11}|^2 + \mu \beta^2 |h_{12}|^2 + \mu \alpha^2 |h_2|^2 |h|^2)) |h_2]],
\end{aligned}
$$

by substituting μ with $\frac{1}{\frac{\alpha^2 |h_2|^2}{\gamma_n} + \frac{1}{\gamma_v}}$, and following Lemma 1 in section 2, we can transform it to

$$
W(\rho_i, c_2, \boldsymbol{\gamma}, \boldsymbol{\Omega}) = E_{h_2}\left[\frac{1}{1 + \rho_i c_2 \gamma_w \Omega_{11}} \frac{1}{1 + \rho_i c_2 \frac{1}{\frac{\alpha^2 |h_2|^2}{\gamma_n} + \frac{1}{\gamma_v}} \beta^2 \Omega_1} \frac{1}{1 + \rho_i c_2 \frac{1}{\frac{\alpha^2 |h_2|^2}{\gamma_n} + \frac{1}{\gamma_v}} \alpha^2 |h_2|^2 \Omega}\right]. \quad (15)
$$

We continue to derive the above equation by the definition of expectation and set $t = |h_2|^2$. Since Rayleigh fading is assumed, $|h|^2$, $|h_{11}|^2$, $|h_{12}|^2$, $|h_2|^2$ are exponentially distributed with parameters $\frac{1}{\Omega}$, $\frac{1}{\Omega_1}$, $\frac{1}{\Omega_1}$, $\frac{1}{\Omega_2}$, respectively. Averaging over h_2, we have

$$
\begin{aligned}
&W(\rho_i, c_2, \boldsymbol{\gamma}, \boldsymbol{\Omega}) \\
&= \frac{1}{\Omega_2} \frac{1}{1 + \rho_i c_2 \gamma_w \Omega_1} \int_0^\infty \frac{1}{1 + \rho_i c_2 \frac{1}{\frac{\alpha^2 t}{\gamma_n} + \frac{1}{\gamma_v}} \beta^2 \Omega_1} \frac{1}{1 + \rho_i c_2 \frac{1}{\frac{\alpha^2 t}{\gamma_n} + \frac{1}{\gamma_v}} \alpha^2 t \Omega} \exp\left(-\frac{t}{\Omega_2}\right) dt \\
&= \frac{1}{\Omega_2} \cdot \frac{1}{1 + \rho_i c_2 \gamma_w \Omega_1} \cdot \frac{\frac{\alpha^2}{\gamma_n}}{\frac{\alpha^2}{\gamma_n} + \rho_i c_2 \alpha^2 \Omega} \\
&\quad \int_0^\infty \frac{t + \frac{1}{\gamma_v} \frac{\gamma_n}{\alpha^2}}{t + \frac{1}{\gamma_v} \frac{\gamma_n}{\alpha^2} + \rho_i c_2 \beta^2 \Omega_1 \frac{\gamma_n}{\alpha^2}} \cdot \frac{t + \frac{1}{\gamma_v} \frac{\gamma_n}{\alpha^2}}{t + \frac{1}{\gamma_v} \frac{1}{\frac{\alpha^2}{\gamma_n} + \rho_i c_2 \alpha^2 \Omega}} \exp\left(-\frac{t}{\Omega_2}\right) dt \quad (16)
\end{aligned}
$$

We set

$$
A' = \frac{\gamma_n}{\gamma_v \alpha^2}, \quad B' = \frac{1}{\gamma_v} \frac{\gamma_n}{\alpha^2} + \rho_i c_2 \beta^2 \Omega_1 \frac{\gamma_n}{\alpha^2}, \quad \text{and} \quad C' = \frac{1}{\gamma_v} \frac{1}{\frac{\alpha^2}{\gamma_n} + \rho_i c_2 \alpha^2 \Omega}. \quad (17)
$$

Then we have,

$$W(\rho_i, c_2, \boldsymbol{\gamma}, \boldsymbol{\Omega}) = \frac{1}{\Omega_2} \cdot \frac{1}{1 + \rho_i c_2 \gamma_w \Omega_1} \cdot \frac{\frac{\alpha^2}{\gamma_n}}{\frac{\alpha^2}{\gamma_n} + \rho_i c_2 \alpha^2 \Omega} \cdot$$
$$\int_0^\infty \frac{t + A'}{t + B'} \cdot \frac{t + A'}{t + C'} \cdot \exp\left(-\frac{t}{\Omega_2}\right) dt. \tag{18}$$

Partial fraction has been taken on the integrand, and $W(\rho_i, c_2, \boldsymbol{\gamma}, \boldsymbol{\Omega})$ can be solved as

$$W(\rho_i, c_2, \boldsymbol{\gamma}, \boldsymbol{\Omega})$$
$$= \frac{1}{\Omega_2} \frac{1}{1 + \rho_i c_2 \gamma_w \Omega_1} \frac{1}{1 + \rho_i c_2 \Omega \gamma_n} \left[\int_0^\infty \exp\left(-\frac{t}{\Omega_2}\right) dt + \frac{(A' - B')^2}{C' - B'} \int_0^\infty \frac{\exp(-\frac{t}{\Omega_2})}{B' + t} dt \right.$$
$$\left. + \frac{(A' - C')^2}{B' - C'} \int_0^\infty \frac{\exp(-\frac{t}{\Omega_2})}{C' + t} dt \right]. \tag{19}$$

By checking $(^{32}$,p 334, eqn(3.310)) and $(^{32}$,p 341, eqn(3.352-4)), it can be found that

$$\int_0^\infty \exp(-px)dx = \frac{1}{p}, \quad [\boldsymbol{Re} \quad p > 0]$$
$$\int_0^\infty \frac{\exp(-\mu x)}{x + \beta} dx = -\exp(\beta\mu)\boldsymbol{Ei}(-\mu\beta), \quad [|\arg\beta| < \pi, \boldsymbol{Re} \quad \mu > 0]. \tag{20}$$

Substituting (20) into (19) gives the final form of $W(\omega_i, c_2, \boldsymbol{\gamma}, \boldsymbol{\Omega})$.

$$W(\omega_i, c_2, \boldsymbol{\gamma}, \boldsymbol{\Omega})$$
$$= \frac{1}{\Omega_2} \frac{1}{1 + \rho_i c_2 \gamma_w \Omega_1} \frac{1}{1 + \rho_i c_2 \Omega \gamma_n} \cdot \left[\Omega_2 - \frac{(A' - B')^2}{C' - B'} \exp\left(\frac{B'}{\Omega_2}\right) \boldsymbol{Ei}\left(-\frac{B'}{\Omega_2}\right) \right.$$
$$\left. - \frac{(A' - C')^2}{B' - C'} \exp\left(\frac{C'}{\Omega_2}\right) \boldsymbol{Ei}\left(-\frac{C'}{\Omega_2}\right) \right]. \tag{21}$$

Finally, the approximation BER of the distribute Alamouti coding system can be obtained by using inequality (29) and (21), as stated in Theorem 3.

APPENDIX:C

THE DERIVATION OF AN AVERAGED ERROR PROBABILITY $P_b(\mathcal{E})$ FOR PROPOSED ONE-RELAY SDF & DSTBC SYSTEM

Considering the variable substitution of θ in (15), we set $u = \frac{1}{\tan\theta}$, then we have $1 + u^2 = \frac{1}{\sin^2\theta}$, $du = \frac{-1}{\sin^2\theta}d\theta$, $d\theta = -\sin^2\theta du = -\frac{1}{1+u^2}du$.

$$
P_b(\mathcal{E}) = \frac{c_1}{\pi}\int_0^\infty \frac{1}{\Omega_2}e^{-\frac{t}{\Omega_2}} \cdot \int_0^{+\infty}\exp\left[-\frac{c_2}{2}(1+u^2)\cdot\frac{\alpha^2 t}{\alpha^2 t\frac{1}{\gamma_l}+\frac{1}{\gamma_v}}\right]
$$
$$
\frac{1}{\frac{c_2}{2}(1+u^2)\cdot\frac{\beta^2}{\alpha^2 t\frac{1}{\gamma_l}+\frac{1}{\gamma_v}}+\frac{1}{\Omega_1}}\cdot\frac{1}{1+u^2}du\cdot dt. \tag{22}
$$

Then,

$$
P_b^{(u)}(\mathcal{E})
$$
$$
= \int_0^{+\infty}\exp\left[-\frac{c_2}{2}(1+u^2)\cdot\frac{\alpha^2 t}{\alpha^2 t\frac{1}{\gamma_l}+\frac{1}{\gamma_v}}\right]\frac{1}{\frac{c_2}{2}(1+u^2)\cdot\frac{\beta^2}{\alpha^2 t\frac{1}{\gamma_l}+\frac{1}{\gamma_v}}+\frac{1}{\Omega_1}}\cdot\frac{1}{1+u^2}du
$$
$$
= \exp\left[-\frac{c_2}{2}\frac{\alpha^2 t}{\alpha^2 t\frac{1}{\gamma_l}+\frac{1}{\gamma_v}}\right]\int_0^{+\infty}\exp\left[-u^2\frac{c_2\alpha^2 t}{2\alpha^2 t\frac{1}{\gamma_l}+\frac{2}{\gamma_v}}\right]\left[\frac{1}{\frac{c_2}{2}(1+u^2)\cdot\frac{\beta^2}{\alpha^2 t\frac{1}{\gamma_l}+\frac{1}{\gamma_v}}+\frac{1}{\Omega_1}}\cdot\frac{1}{1+u^2}\right]du
$$
$$
= \exp\left[-\frac{c_2}{2}\frac{\alpha^2 t}{\alpha^2 t\frac{1}{\gamma_l}+\frac{1}{\gamma_v}}\right]\int_0^{+\infty}\exp\left[-u^2\frac{c_2\alpha^2 t}{2\alpha^2 t\frac{1}{\gamma_l}+\frac{2}{\gamma_v}}\right]
$$
$$
\left[\frac{\Omega_1}{1+u^2}-\frac{c_2\gamma_l\gamma_v\beta^2\Omega_1^2}{2\gamma_n+2t\gamma_v\alpha^2+c_2\gamma_l\gamma_v\beta^2\Omega_1+c_2\gamma_l\gamma_v\beta^2\Omega_1 u^2}\right]du
$$
$$
= \Omega_1\exp\left[-\frac{c_2\alpha^2 t}{2\alpha^2 t\frac{1}{\gamma_l}+\frac{2}{\gamma_v}}\right]\left\{\int_0^{+\infty}\exp\left[-u^2\frac{c_2\alpha^2 t}{2\alpha^2 t\frac{1}{\gamma_l}+\frac{2}{\gamma_v}}\right]\frac{1}{1+u^2}du\right.
$$
$$
\left.-\int_0^{+\infty}\exp\left[-u^2\frac{c_2\alpha^2 t}{2\alpha^2 t\frac{1}{\gamma_l}+\frac{2}{\gamma_v}}\right]\frac{1}{\frac{2}{c_2\gamma_v\beta^2\Omega_1}+\frac{2t\alpha^2}{c_2\gamma_l\beta^2\Omega_1}+1+u^2}du\right\} \tag{23}
$$

By setting $P = \frac{c_2\alpha^2 t}{2\alpha^2 t\frac{1}{\gamma_l}+\frac{2}{\gamma_v}}, Q = \frac{2}{c_2\gamma_v\beta^2\Omega_1} + \frac{2t\alpha^2}{c_2\gamma_l\beta^2\Omega_1} + 1$

$$
\begin{aligned}
P_b^{(u)}(\mathcal{E}) &= \Omega_1 \exp\left[-P\right]\left\{ \int\limits_0^{+\infty} \exp\left[-u^2 P\right]\frac{1}{1+u^2}du \right. \\
&\quad \left. - \int\limits_0^{+\infty} \exp\left[-u^2 P\right]\frac{1}{Q+u^2}du \right\}
\end{aligned}
\tag{24}
$$

With the help of the following equation in $[^{32}$ p367 3.466-1$]$,

$$
\int_0^\infty \frac{e^{-\omega^2 x^2}}{x^2 + \xi^2}dx = [1 - \Phi(\xi\omega)]\frac{\pi}{2\xi}e^{\xi^2\omega^2}, \qquad [\boldsymbol{Re}\,\xi > 0, |\arg\omega| < \frac{\pi}{4}], \tag{25}
$$

the first items becomes,

$$
\int\limits_0^{+\infty} \exp\left[-u^2 P\right]\frac{1}{1+u^2}du = \left[1 - \Phi\left(\sqrt{P}\right)\right]\frac{\pi}{2}\exp(P),
$$

and the second items changes to,

$$
\int\limits_0^{+\infty} \exp\left[-u^2 P\right]\frac{1}{Q+u^2}du = \left[1 - \Phi(\sqrt{PQ})\right]\frac{\pi}{2\sqrt{Q}}\exp(PQ).
$$

By substituting the above two results into (24), (22) becomes,

$$
\begin{aligned}
& P_b(\mathcal{E}) \\
&= \frac{c_1}{\pi}\int\limits_0^\infty \frac{1}{\Omega_2}e^{-\frac{t}{\Omega_2}} \cdot \Omega_1 \exp\left(-P\right)\left\{ \left[1 - \Phi\left(\sqrt{P}\right)\right]\frac{\pi}{2}\exp(P) \right. \\
&\quad \left. - \left[1 - \Phi\left(\sqrt{PQ}\right)\right]\frac{\pi}{2\sqrt{Q}}\exp(PQ) \right\}dt
\end{aligned}
\tag{26}
$$

From eqn. (26), we can easily get the averaged BER performance of the proposed Soft-Decode-and-Forward distributed Alamouti's code system as stated in (16) in Theorem 4.

APPENDIX:D

THE DERIVATION OF AN AVERAGED ERROR PROBABILITY $P_b(\mathcal{E})$ FOR REFERENCE ONE-RELAY SDF SYSTEM WITHOUT DSTBC

By setting $t = |h_2|^2$,

$$
\begin{aligned}
&P_b(\mathcal{E}) \\
&= \frac{c_1}{\pi} \int_0^{\pi/2} \int_0^\infty \exp\left[-\frac{c_2}{2\sin^2\theta} \cdot \frac{\eta^2 t}{\eta^2 t \frac{1}{\gamma_l} + \frac{1}{\gamma_v}}\right] \cdot \frac{1}{\Omega_2} e^{-\frac{t}{\Omega_2}} \cdot dt d\theta \\
&= \frac{c_1}{\pi} \int_0^\infty \frac{1}{\Omega_2} e^{-\frac{t}{\Omega_2}} \cdot \int_0^\infty \exp\left[-\frac{c_2}{2}(1 + u^2) \cdot \frac{\eta^2 t}{\eta^2 t \frac{1}{\gamma_l} + \frac{1}{\gamma_v}}\right] \cdot \frac{1}{1 + u^2} du \cdot dt.
\end{aligned}
$$

And we have,

$$
\begin{aligned}
&P_b^{(u)}(\mathcal{E}) \\
&= \int_0^\infty \exp\left[-\frac{c_2}{2}(1 + u^2) \cdot \frac{\eta^2 t}{\eta^2 t \frac{1}{\gamma_l} + \frac{1}{\gamma_v}}\right] \cdot \frac{1}{1 + u^2} du \\
&= \int_0^\infty \exp\left[-\frac{c_2}{2} \frac{\eta^2 t}{\eta^2 t \frac{1}{\gamma_l} + \frac{1}{\gamma_v}} - \frac{c_2}{2} u^2 \cdot \frac{\eta^2 t}{\eta^2 t \frac{1}{\gamma_l} + \frac{1}{\gamma_v}}\right] \cdot \frac{1}{1 + u^2} du \\
&= \exp\left[-\frac{c_2}{2} \frac{\eta^2 t}{\eta^2 t \frac{1}{\gamma_l} + \frac{1}{\gamma_v}}\right] \cdot \int_0^\infty \exp\left[-u^2 \cdot \frac{c_2}{2} \frac{\eta^2 t}{\eta^2 t \frac{1}{\gamma_l} + \frac{1}{\gamma_v}}\right] \cdot \frac{1}{1 + u^2} du. \quad (27)
\end{aligned}
$$

By setting $W = \frac{c_2}{2} \frac{\eta^2 t}{\eta^2 t \frac{1}{\gamma_l} + \frac{1}{\gamma_v}}$, then

$$
P_b^{(u)}(\mathcal{E}) = \exp(-W) \cdot \int_0^\infty \exp\left[-u^2 \cdot W\right] \cdot \frac{1}{1 + u^2} du.
$$

With the help of (25), $P_b^{(u)}(\mathcal{E})$ becomes,

$$\begin{aligned}
P_b^{(u)}(\mathcal{E}) &= \exp(-W) \cdot [1 - \Phi(\sqrt{W})]\frac{\pi}{2}\exp(W) \\
&= [1 - \Phi(\sqrt{W})]\frac{\pi}{2}. \tag{28}
\end{aligned}$$

By substituting (28) into (27), we get the averaged BER performance of the reference Soft-Decode-and-Forward system as stated in (21) in Theorem 5.

APPENDIX:E

THE DERIVATION OF MGF OF FUNCTION $T = \frac{X+Y}{aX+bY+c}$

The cumulative distribution function (CDF) of T can be calculated by the definition of CDF

$$
\begin{aligned}
F_T(t) &= P\{T \le t\} \\
&= P\left\{\frac{X+Y}{aX+bY+c} \le t\right\} \\
&= P\{X+Y \le aXt + bYt + ct\} \\
&= P\{(1-at)X \le (bt-1)Y + ct\}
\end{aligned}
\tag{29}
$$

Since a and b are symetric, suppose $0 \le a \le b$, then $0 \le 1/b \le 1/a$.

1. If $t \ge 1/a$, then $1 - at \le 0$ and $bt - 1 > 0$. In this case, $F_T(t) = 1$.

2. If $1/b \le t < 1/a$, then $1 - at > 0$ and $bt - 1 \ge 0$.

$$
\begin{aligned}
F_T(t) &= P\{(1-at)X \le (bt-1)Y + ct\} \\
&= P\left\{X \le \frac{bt-1}{1-at}Y + \frac{ct}{(1-at)}\right\} \\
&= \int_0^\infty \left[1 - \exp\left(-\lambda_1\left(\frac{bt-1}{1-at}y + \frac{ct}{1-at}\right)\right)\right]\lambda_2 \exp(-\lambda_2 y)dy \\
&= 1 - \lambda_2 \int_0^\infty \exp\left(-\lambda_1\left(\frac{bt-1}{1-at}y + \frac{ct}{1-at}\right) - \lambda_2 y\right)dy \\
&= 1 - \lambda_2 \exp\left(\lambda_1\frac{ct}{1-at}\right)\int_0^\infty \exp\left(\left[-\lambda_1\frac{bt-1}{1-at} - \lambda_2\right]y\right)dy \\
&= 1 - \frac{\exp\left(-\lambda_1\frac{ct}{1-at}\right)}{\frac{\lambda_1}{\lambda_2}\frac{bt-1}{1-at} + 1}
\end{aligned}
\tag{30}
$$

3. If $0 \le t < 1/b$, then $1 - at > 0$ and $bt - 1 < 0$. $F_T(t) \ge 0$ holds only when

$\frac{bt-1}{1-at}Y + \frac{ct}{1-at} \geq 0$ which is $Y \leq \frac{ct}{1-bt}$.

$$
\begin{aligned}
F_T(t) &= \int_0^{\frac{ct}{1-bt}} \left[1 - \exp\left(-\lambda_1 \frac{bt-1}{1-at} y - \lambda_1 \frac{ct}{1-at} \right) \right] \lambda_2 \exp(-\lambda_2 y) dy \\
&= 1 - \frac{\exp\left(-\lambda_1 \frac{ct}{1-at} \right)}{\frac{\lambda_1}{\lambda_2} \frac{bt-1}{1-at} + 1} - \left(1 - \frac{1}{\frac{\lambda_1}{\lambda_2} \frac{bt-1}{1-at} + 1} \right) \exp\left(-\lambda_2 \frac{ct}{1-bt} \right) \quad (31)
\end{aligned}
$$

Based on the discussion above,

$$
F_T(t) = \begin{cases}
1 - \dfrac{\exp\left(-\lambda_1 \frac{ct}{1-at} \right)}{\frac{\lambda_1}{\lambda_2} \frac{bt-1}{1-at} + 1} - \left(1 - \dfrac{1}{\frac{\lambda_1}{\lambda_2} \frac{(bt-1)}{(1-at)} + 1} \right) \\
\qquad \exp\left(-\lambda_2 \frac{ct}{1-bt} \right), \quad 0 \leq t < 1/b, \\[2mm]
1 - \dfrac{\exp\left(-\lambda_1 \frac{ct}{1-at} \right)}{\frac{\lambda_1}{\lambda_2} \frac{bt-1}{1-at} + 1}, \quad 1/b \leq t < 1/a \\[2mm]
1, \quad t \geq 1/a
\end{cases}
$$

Then the MGF can be derived as

$$
\begin{aligned}
&\mathcal{M}_T(s, \lambda_1, \lambda_2) \\
&= \int_0^\infty \exp(st) dF_T(t) \\
&= \int_0^{1/b} \exp(st) dF_T(t) + \int_{1/b}^{1/a} \exp(st) dF_T(t) \\
&= \exp(st) F_T(t) |_0^{1/b} - \int_0^{1/b} s F_T(t) \exp(st) dt \\
&\quad + \exp(st) F_T(t) |_{1/b}^{1/a} - s \int_{1/b}^{1/a} F_T(t) \exp(st) dt \quad (32)
\end{aligned}
$$

The first term in (32) can be derived as

$$
\exp(st) F_T(t) |_{t=0}^{1/b} = \exp(s/b) \left[1 - \exp\left(-\lambda_1 \frac{c/b}{1 - a/b} \right) \right] \quad (33)
$$

The third term in (32) can be derived as

$$
\begin{aligned}
&\exp(st)F_T(t)\big|_{1/b}^{1/a} \\
&= \ \exp(s/a) - \exp(s/b)\left[1 - \exp\left(-\lambda_1 \frac{c/b}{1 - a/b}\right)\right]
\end{aligned}
\tag{34}
$$

By substituting (33) and (34) into (32), we can easily get the MGF of function T as stated in (7) in Lemma 2.

APPENDIX:F

THE DERIVATION OF AN AVERAGED ERROR PROBABILITY $P_b(\mathcal{E})$ FOR THE PROPOSED TWO-RELAY SDF & DSTBC SYSTEM

We substitute the MGF in (7) into (5) to derive the BER performance of the proposed system.

$$
\begin{aligned}
P_b(\mathcal{E}) &= \frac{c_1}{\pi} \int_0^{\pi/2} \mathcal{M}\gamma_T(s)\, d\theta\Big|_{s=-\frac{c_2}{2\sin^2\theta}} \\
&= \frac{c_1}{\pi} \int_0^{\pi/2} d\theta + \frac{c_1}{\pi} \int_0^{\pi/2} \int_0^{1/a} s\frac{\exp\left(st - \lambda_1 \frac{ct}{1-at}\right)}{\frac{\lambda_1}{\lambda_2}\frac{bt-1}{1-at} + 1}\, dt\, d\theta \\
&\quad + \frac{c_1}{\pi} \int_0^{\pi/2} \int_0^{1/b} s\exp\left(st - \lambda_2 \frac{ct}{1-bt}\right) dt\, d\theta \\
&\quad - \frac{c_1}{\pi} \int_0^{\pi/2} \int_0^{1/b} s\frac{\exp\left(st - \lambda_2 \frac{ct}{1-bt}\right)}{\frac{\lambda_1}{\lambda_2}\frac{bt-1}{1-at} + 1}\, dt\, d\theta\Big|_{s=-\frac{c_2}{2\sin^2\theta}} \\
&= \frac{c_1}{2} + \frac{c_1}{\pi}\left[\int_0^{1/a} \frac{1}{\frac{\lambda_1}{\lambda_2}\frac{bt-1}{1-at}+1}\exp\left(-\lambda_1 \frac{ct}{1-at}\right)\Phi(\theta)dt \right. \\
&\quad + \int_0^{1/b} \exp\left(-\lambda_2 \frac{ct}{1-bt}\right)\Phi(\theta)dt \\
&\quad \left. - \int_0^{1/b} \frac{1}{\frac{\lambda_1}{\lambda_2}\frac{bt-1}{1-at}+1}\exp\left(-\lambda_2 \frac{ct}{1-bt}\right)\Phi(\theta)dt \right]
\end{aligned}
\tag{35}
$$

where $\Phi(\theta) = \int_0^{\pi/2}(-\frac{c_2}{2\sin^2\theta})\exp(-\frac{c_2}{2\sin^2\theta}t)d\theta$. By setting $u = \frac{1}{\tan\theta}$, then we have $1 + u^2 = \frac{1}{\sin^2\theta}$, $du = \frac{-1}{\sin^2\theta}d\theta$, $d\theta = -\sin^2\theta du = -\frac{1}{1+u^2}du$.

We substitute θ into u, and then $\Phi(\theta)$ becomes

$$
\begin{aligned}
\Phi(\theta) &= -\frac{c_2}{2}\int_0^\infty (1+u^2)\exp\left(-\frac{c_2 t}{2}(1+u^2)\right)\left(-\frac{1}{1+u^2}\right)du \\
&= \frac{c_2}{2}\int_0^\infty \exp\left(-\frac{c_2 t}{2}(1+u^2)\right)du \\
&= \frac{c_2}{2}\exp\left(-\frac{c_2 t}{2}\right)\int_0^\infty \exp\left(-\frac{c_2 t}{2}u^2\right)du
\end{aligned}
\tag{36}
$$

129

By checking (3.321-3) on p336 in [32], which is

$$\int_0^\infty \exp(-q^2 x^2)dx = \frac{\sqrt{\pi}}{2q}, [q > 0],$$

and by substituting (36) into (35), we obtain BER as

$$P_b(\mathcal{E}) = \frac{c_1}{2} - \frac{c_1\sqrt{c_2}}{2\sqrt{2\pi}} \left[\int_0^{1/a} \frac{\exp\left(-\frac{c_2 t}{2} - \lambda_1\frac{ct}{1-at}\right)}{\sqrt{t}\left(\frac{\lambda_1}{\lambda_2}\frac{bt-1}{1-at} + 1\right)}dt \right. $$
$$\left. + \int_0^{1/b} \left(1 - \frac{1}{\frac{\lambda_1}{\lambda_2}\frac{bt-1}{1-at} + 1}\right)\frac{\exp\left(-\frac{c_2 t}{2} - \lambda_2\frac{ct}{1-bt}\right)}{\sqrt{t}}dt \right] \tag{37}$$

By substituting parameters in (6) into (37), the final form of BER of the proposed Space-Time enhanced SIR system is stated in (8) in Theorem 6.

Vita

Born in Wuhan, China in 1981, Peng Huo received the B.S. degree in communications engineering from Wuhan University of Technology, Wuhan, China in July, 2003 and the M.S. degree from Wuhan University (WHU), Wuhan, China in July, 2006. He is currently working towards the Ph.D. degree in electrical engineering at The University of Mississippi, University, MS. During his Ph.D. program, he worked as a graduate assistant for the Department of Electrical Engineering as well as the National Center for Physical Acoustics. Currently, he is working as a patent agent for China Science Patent Trademark Agents Ltd. (CSPTAL), one of the leading Intellectual Property firms in China.